Quality documentation of MFASIS coeffcients production for RTTOV v14

Pascal Raisig[1], Leonhard Scheck[1,2], Christina Stumpf[1], and Christina Köpken-Watts[1]

[1]DWD
[2]Hans-Ertel-Zentrum/LMU München

Thursday 30th January, 2025

Contents

1 Introduction **2**

2 Uncertainty tables **3**

3 Uncertainty figures **20**

List of Figures **76**

1 Introduction

This document gives an overview on the quality of reflectance simulations with MFASIS in its neural network (NN) version as utilized in RTTOV v14 using the available MFASIS coefficients.

The uncertainties of the reflectances simulated with MFASIS are quantified with respect to reflectances simulated with the RTTOV Discrete Ordinates Method (DOM) (see Hocking, 2016). As reference for the simulation input the NWP model profile dataset, provided by the NWP SAF, is used to cover a wide range of atmospheric cloud simulations. For each channel of an instrument a specific neuronal network definition is available as RTTOV coefficient. This neural network definition is optimized to achieve high accuracy and speed.
Section 2 summarizes the results as overview tables per instrument. Each table contains the neuronal network definition (NN def column) in terms of number of layers (L) and neurons per layer (N), as well as, the uncertainties from the reflectance simulations with MFASIS for three explicit albedos: 0, 0.5 and 1.0. Listed in the tables are the mean error (me), mean absolute error (mae), root mean square error (rmse) and the 99th percentile (p99).
Section 3 provides additionally more detailed figures for each instrument and channel. Depicted are the differences between the simulated MFASIS and DOM reflectances (MFASIS - DOM) as function of the cloud optical depth τ as one-dimensional probability density functions.

For more detailed information about MFASIS please see the RTTOV science and validation report for RTTOV v14.

2 Uncertainty tables

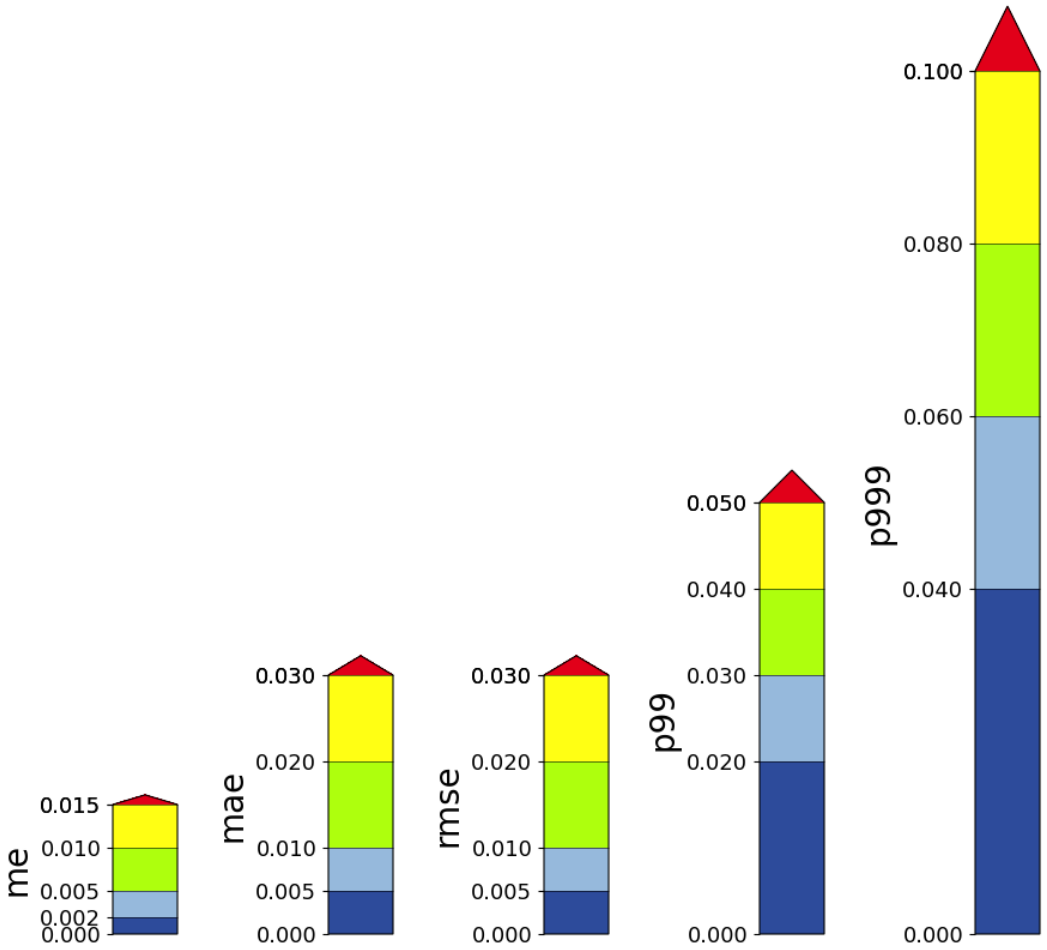

Figure 1: Color coding for the different uncertainty values in the tables for the instruments.

dscovr 1 epic

Channel	Wavelength [µm]	NN def	Albedo	me	mae	rmse	p99
1	0.442	L8N15	0.00	0.0004	0.0041	0.0066	0.0231
			0.50	-0.0002	0.0036	0.0061	0.0211
			1.00	-0.0005	0.0042	0.0069	0.0237
2	0.551	L8N15	0.00	0.0025	0.0046	0.0066	0.0217
			0.50	0.0025	0.0041	0.0062	0.0204
			1.00	0.002	0.0039	0.0057	0.0181
3	0.68	L8N15	0.00	0.0017	0.0035	0.0057	0.0202
			0.50	0.0018	0.0038	0.0056	0.0192
			1.00	0.0024	0.0047	0.0063	0.0196
6	0.779	L8N15	0.00	0.0009	0.0045	0.0074	0.0264
			0.50	-0.0003	0.0038	0.0062	0.0226
			1.00	-0.0024	0.0046	0.0066	0.0223

Figure 2: MFASIS uncertainties for the instrument: DSCOVR 1 EPIC

eos 1 modis

Channel	Wavelength [µm]	NN def	Albedo	me	mae	rmse	p99
1	0.645	L8N25	0.00	0.0039	0.0048	0.0077	0.0268
			0.50	0.004	0.0049	0.0079	0.0272
			1.00	0.0036	0.005	0.0077	0.026
2	0.856	L8N25	0.00	0.0011	0.004	0.0065	0.0227
			0.50	0.0023	0.0043	0.0066	0.0226
			1.00	0.0027	0.005	0.0073	0.0235
3	0.466	L8N15	0.00	0.0009	0.0048	0.0077	0.026
			0.50	0.0002	0.0044	0.0073	0.0259
			1.00	-0.0021	0.005	0.0084	0.0336
4	0.554	L8N15	0.00	0.0032	0.005	0.0077	0.0269
			0.50	0.0032	0.0051	0.0076	0.026
			1.00	0.002	0.0053	0.0079	0.0278
5	1.242	L8N25	0.00	0.0016	0.0047	0.0083	0.0328
			0.50	0.0025	0.0053	0.0085	0.0325
			1.00	0.0044	0.0072	0.0098	0.0289
6	1.629	L8N25	0.00	-0.002	0.0045	0.0086	0.0304
			0.50	-0.0001	0.0065	0.0096	0.0308
			1.00	-0.0004	0.0083	0.0113	0.0317
8	0.412	L8N15	0.00	-0.0009	0.004	0.0066	0.023
			0.50	0.0001	0.0034	0.0059	0.0214
			1.00	-0.0004	0.0041	0.0065	0.0216
9	0.442	L8N15	0.00	0.0005	0.0033	0.0057	0.0182
			0.50	0.0004	0.0032	0.0057	0.0185
			1.00	0.0004	0.0042	0.0066	0.02
10	0.487	L8N15	0.00	0.0012	0.0041	0.0062	0.02
			0.50	0.0008	0.0033	0.0056	0.019
			1.00	0.001	0.0033	0.0056	0.0189
11	0.53	L8N15	0.00	0.0013	0.0041	0.0064	0.0213
			0.50	0.0021	0.004	0.0063	0.0213
			1.00	0.0011	0.0042	0.0066	0.025
12	0.547	L8N15	0.00	0.0019	0.0054	0.0075	0.0225
			0.50	0.0019	0.0047	0.0069	0.0221
			1.00	0.0016	0.0046	0.0066	0.0212
13	0.666	L8N15	0.00	0.0037	0.0048	0.007	0.0229
			0.50	0.0019	0.0042	0.0062	0.0205
			1.00	0.0002	0.0047	0.0068	0.0229
14	0.677	L8N15	0.00	-0.0001	0.0038	0.0061	0.0213
			0.50	0.0005	0.0039	0.006	0.0212
			1.00	-0.0004	0.0044	0.0065	0.0226
15	0.747	L8N15	0.00	0.0011	0.0048	0.0074	0.0269
			0.50	0.0019	0.0049	0.0072	0.0256
			1.00	0.0025	0.0067	0.0089	0.0268
16	0.866	L8N15	0.00	-0.0008	0.0041	0.0064	0.0226
			0.50	0.0008	0.0043	0.0065	0.0226
			1.00	0.0011	0.0058	0.0083	0.0261

Figure 3: MFASIS uncertainties for the instrument: EOS 1 MODIS

eos 2 modis

Channel	Wavelength [µm]	NN def	Albedo	me	mae	rmse	p99
1	0.645	L8N15	0.00	0.0027	0.005	0.0081	0.0276
			0.50	0.0023	0.0055	0.0083	0.0276
			1.00	0.0028	0.0064	0.0087	0.027
2	0.856	L8N25	0.00	0.0007	0.0032	0.0057	0.0208
			0.50	0.0024	0.0043	0.0063	0.0213
			1.00	0.0041	0.0058	0.0078	0.0219
3	0.466	L8N15	0.00	0.0026	0.0043	0.0066	0.0209
			0.50	0.0008	0.0036	0.0059	0.0179
			1.00	-0.001	0.0041	0.0062	0.0172
4	0.554	L8N15	0.00	0.0023	0.0054	0.0079	0.025
			0.50	0.0027	0.005	0.0074	0.0246
			1.00	0.0016	0.0052	0.0076	0.0273
5	1.241	L8N25	0.00	0.0013	0.0038	0.007	0.0273
			0.50	0.0044	0.0064	0.0091	0.0298
			1.00	0.0069	0.0092	0.0128	0.0423
6	1.628	L8N25	0.00	-0.0013	0.0045	0.0085	0.0286
			0.50	-0.001	0.0054	0.0088	0.0286
			1.00	-0.0024	0.007	0.01	0.0296
8	0.412	L8N15	0.00	0.0	0.0041	0.0067	0.0226
			0.50	-0.0008	0.0044	0.0069	0.0238
			1.00	-0.0008	0.0047	0.0072	0.0225
9	0.442	L8N15	0.00	0.0017	0.0048	0.0075	0.0247
			0.50	-0.0002	0.0055	0.0079	0.0259
			1.00	-0.0027	0.0063	0.0091	0.0275
10	0.487	L8N15	0.00	0.0017	0.0045	0.007	0.0222
			0.50	0.0015	0.0041	0.0069	0.0229
			1.00	0.0004	0.0043	0.007	0.0227
11	0.53	L8N15	0.00	-0.0015	0.0052	0.0071	0.0211
			0.50	0.001	0.0041	0.0062	0.0204
			1.00	0.0017	0.0045	0.0065	0.02
12	0.547	L8N15	0.00	0.0006	0.0054	0.0077	0.0241
			0.50	-0.0006	0.0062	0.0084	0.0249
			1.00	-0.0022	0.0068	0.0088	0.0236
13	0.666	L8N15	0.00	-0.0004	0.0041	0.0062	0.0207
			0.50	-0.0015	0.0049	0.0068	0.0199
			1.00	-0.0026	0.006	0.0082	0.0229
14	0.678	L8N15	0.00	0.002	0.004	0.0062	0.0217
			0.50	0.0012	0.0033	0.0057	0.0214
			1.00	-0.0018	0.0053	0.0073	0.0226
15	0.747	L8N15	0.00	-0.0009	0.0051	0.0074	0.0256
			0.50	-0.0003	0.0047	0.0069	0.0233
			1.00	0.0007	0.0058	0.0081	0.0242
16	0.867	L8N15	0.00	-0.0005	0.0042	0.007	0.0256
			0.50	0.0	0.0044	0.0069	0.0247
			1.00	0.001	0.0061	0.0083	0.0254

Figure 4: MFASIS uncertainties for the instrument: EOS 2 MODIS

fy3 3 virr

Channel	Wavelength [µm]	NN def	Albedo	me	mae	rmse	p99
1	0.46	L8N15	0.00	0.0015	0.0039	0.0067	0.0231
			0.50	0.0006	0.0035	0.0062	0.0225
			1.00	-0.0004	0.0037	0.0063	0.0213
2	0.501	L8N15	0.00	0.002	0.0042	0.0065	0.0217
			0.50	0.0015	0.0039	0.0062	0.0207
			1.00	0.0014	0.0041	0.0064	0.0204
3	0.543	L8N15	0.00	0.0027	0.0052	0.0075	0.0245
			0.50	0.0017	0.005	0.0073	0.0235
			1.00	0.0011	0.0055	0.0075	0.0233
4	0.635	L8N25	0.00	0.001	0.0049	0.0076	0.0264
			0.50	0.0027	0.0043	0.0073	0.026
			1.00	0.0048	0.006	0.0084	0.025
7	1.593	L8N25	0.00	-0.0013	0.0048	0.0087	0.0309
			0.50	0.0013	0.0071	0.0099	0.0313
			1.00	0.0036	0.0101	0.0129	0.0363

Figure 5: MFASIS uncertainties for the instrument: FY3 3 VIRR

fy3 4 mersi2

Channel	Wavelength [µm]	NN def	Albedo	me	mae	rmse	p99
1	0.412	L8N15	0.00	0.0022	0.0042	0.0068	0.0237
			0.50	0.0001	0.0039	0.0062	0.0212
			1.00	-0.0004	0.0038	0.0063	0.0228
2	0.444	L8N15	0.00	0.0004	0.0034	0.0057	0.0208
			0.50	0.0001	0.003	0.0052	0.0198
			1.00	-0.001	0.0035	0.0057	0.0202
3	0.469	L8N15	0.00	0.0007	0.0044	0.0069	0.0255
			0.50	-0.0016	0.0046	0.0073	0.0275
			1.00	-0.0031	0.0055	0.0084	0.0303
4	0.491	L8N15	0.00	0.0005	0.0028	0.0049	0.0173
			0.50	0.0002	0.0029	0.0049	0.0171
			1.00	-0.0009	0.0032	0.0051	0.0171
5	0.553	L8N15	0.00	0.0022	0.006	0.0086	0.0274
			0.50	0.0016	0.006	0.0084	0.0265
			1.00	-0.0	0.0059	0.008	0.0241
6	0.556	L8N15	0.00	0.0016	0.004	0.0063	0.0207
			0.50	0.0017	0.004	0.0061	0.0206
			1.00	0.0019	0.0045	0.0062	0.0189
7	0.653	L8N15	0.00	0.0043	0.006	0.0091	0.029
			0.50	0.0043	0.0062	0.0091	0.0293
			1.00	0.004	0.0068	0.0094	0.0288
8	0.67	L8N15	0.00	-0.0007	0.0036	0.0057	0.0198
			0.50	0.0018	0.0042	0.006	0.0184
			1.00	0.0035	0.0066	0.0087	0.0243
10	0.746	L8N25	0.00	0.0032	0.0063	0.0102	0.0356
			0.50	0.0052	0.0065	0.0103	0.036
			1.00	0.006	0.0076	0.0108	0.0338
11	0.865	L8N15	0.00	0.0001	0.0047	0.0079	0.0286
			0.50	0.0015	0.0062	0.0087	0.0292
			1.00	0.0005	0.0076	0.0104	0.0343
12	0.868	L8N25	0.00	0.0017	0.0045	0.0077	0.0275
			0.50	0.0005	0.005	0.0078	0.0283
			1.00	0.0002	0.0058	0.0083	0.0267
16	1.03	L8N15	0.00	0.0029	0.0049	0.0083	0.0289
			0.50	0.0037	0.0062	0.0087	0.0278
			1.00	0.0018	0.0063	0.0096	0.0356
18	1.644	L8N25	0.00	-0.0011	0.0058	0.0093	0.0305
			0.50	0.001	0.0066	0.0093	0.0302
			1.00	0.0026	0.0086	0.0111	0.0303

Figure 6: MFASIS uncertainties for the instrument: FY3 4 MERSI2

fy4 1 agri

Channel	Wavelength [µm]	NN def	Albedo	me	mae	rmse	p99
1	0.469	L8N15	0.00	0.0012	0.0037	0.0061	0.0198
			0.50	0.002	0.0037	0.006	0.0193
			1.00	0.0016	0.0041	0.0065	0.0202
5	1.607	L8N25	0.00	-0.0015	0.0047	0.0086	0.0305
			0.50	-0.0019	0.005	0.0089	0.0315
			1.00	-0.0016	0.0061	0.0096	0.0326

Figure 7: MFASIS uncertainties for the instrument: FY4 1 AGRI

fy4 2 agri

Channel	Wavelength [µm]	NN def	Albedo	me	mae	rmse	p99
1	0.47	L8N15	0.00	0.0014	0.0043	0.0067	0.0232
			0.50	0.0019	0.0046	0.0072	0.0262
			1.00	0.0007	0.005	0.0074	0.0269
2	0.628	L8N15	0.00	0.0043	0.0063	0.0103	0.0376
			0.50	0.0028	0.0068	0.0106	0.0382
			1.00	0.0023	0.0088	0.012	0.0375
5	1.611	L8N25	0.00	-0.0006	0.0051	0.0091	0.0311
			0.50	0.0011	0.0069	0.0099	0.0313
			1.00	0.0023	0.0094	0.0126	0.0384

Figure 8: MFASIS uncertainties for the instrument: FY4 2 AGRI

gkompsat2 1 ami

Channel	Wavelength [µm]	NN def	Albedo	me	mae	rmse	p99
1	0.47	L8N15	0.00	-0.0008	0.0039	0.0062	0.02
			0.50	0.0009	0.0038	0.0062	0.02
			1.00	0.0014	0.0043	0.0069	0.0223
2	0.509	L8N15	0.00	-0.0004	0.0039	0.0061	0.0198
			0.50	0.0008	0.0041	0.0063	0.0209
			1.00	0.0011	0.0047	0.0071	0.0237
3	0.639	L8N15	0.00	0.0031	0.0061	0.009	0.0286
			0.50	0.0048	0.0065	0.0087	0.0276
			1.00	0.0052	0.0074	0.0095	0.0263
4	0.863	L8N15	0.00	-0.0005	0.0041	0.0071	0.025
			0.50	0.0013	0.0053	0.0077	0.0247
			1.00	0.0014	0.0067	0.0092	0.0275
6	1.609	L8N25	0.00	-0.0012	0.0042	0.0081	0.0288
			0.50	-0.0025	0.0055	0.0086	0.0293
			1.00	-0.0039	0.0071	0.0099	0.0299

Figure 9: MFASIS uncertainties for the instrument: GKOMPSAT2 1 AMI

goes 13 imager

Channel	Wavelength [µm]	NN def	Albedo	me	mae	rmse	p99
1	0.623	L8N25	0.00	0.0025	0.0045	0.0081	0.0294
			0.50	0.0033	0.005	0.0082	0.0299
			1.00	0.0035	0.0051	0.0079	0.0286

Figure 10: MFASIS uncertainties for the instrument: GOES 13 IMAGER

goes 14 imager

Channel	Wavelength [µm]	NN def	Albedo	me	mae	rmse	p99
1	0.621	L8N25	0.00	0.0028	0.0045	0.0079	0.0291
			0.50	0.0031	0.0044	0.0079	0.0296
			1.00	0.0034	0.0045	0.0076	0.0282

Figure 11: MFASIS uncertainties for the instrument: GOES 14 IMAGER

goes 15 imager

Channel	Wavelength [µm]	NN def	Albedo	me	mae	rmse	p99
1	0.621	L8N25	0.00	0.0031	0.0048	0.0084	0.0301
			0.50	0.0029	0.0048	0.0084	0.0305
			1.00	0.0025	0.005	0.0082	0.0293

Figure 12: MFASIS uncertainties for the instrument: GOES 15 IMAGER

goes 16 abi

Channel	Wavelength [µm]	NN def	Albedo	me	mae	rmse	p99
1	0.47	L8N15	0.00	0.0001	0.0032	0.0058	0.0203
			0.50	0.0	0.0034	0.0058	0.0199
			1.00	-0.0011	0.0036	0.0063	0.0224
2	0.636	L8N15	0.00	0.0011	0.0053	0.0081	0.0274
			0.50	0.0016	0.0052	0.0082	0.0279
			1.00	0.001	0.0063	0.009	0.0282
3	0.864	L8N15	0.00	0.0001	0.0039	0.0067	0.0268
			0.50	0.0012	0.0047	0.007	0.0259
			1.00	0.0	0.0062	0.0086	0.0284
5	1.609	L8N25	0.00	-0.0013	0.0048	0.0085	0.0292
			0.50	-0.0018	0.0051	0.0086	0.0294
			1.00	-0.001	0.0064	0.0094	0.0295
6	2.242	L8N25	0.00	-0.0005	0.0046	0.0087	0.0318
			0.50	0.0013	0.0071	0.01	0.0318
			1.00	0.0032	0.0109	0.0142	0.04

Figure 13: MFASIS uncertainties for the instrument: GOES 16 ABI

goes 17 abi

Channel	Wavelength [µm]	NN def	Albedo	me	mae	rmse	p99
1	0.47	L8N15	0.00	0.0014	0.004	0.0066	0.0228
			0.50	0.0017	0.0041	0.0068	0.0236
			1.00	0.0005	0.0043	0.0072	0.0257
2	0.636	L8N15	0.00	0.0029	0.005	0.0078	0.0262
			0.50	0.0039	0.0056	0.0079	0.0258
			1.00	0.0047	0.0072	0.0093	0.0249
3	0.864	L8N15	0.00	-0.0	0.0049	0.0079	0.0281
			0.50	0.0024	0.0066	0.0095	0.0289
			1.00	0.0054	0.0109	0.0154	0.0498
5	1.608	L8N25	0.00	-0.0013	0.0045	0.0085	0.0304
			0.50	-0.0007	0.0058	0.0092	0.031
			1.00	-0.0008	0.0072	0.0104	0.0322
6	2.242	L8N25	0.00	-0.0019	0.005	0.009	0.0313
			0.50	-0.0023	0.0065	0.0097	0.0314
			1.00	-0.0022	0.0088	0.0119	0.0341

Figure 14: MFASIS uncertainties for the instrument: GOES 17 ABI

goes 18 abi

Channel	Wavelength [µm]	NN def	Albedo	me	mae	rmse	p99
1	0.47	L8N15	0.00	-0.002	0.0049	0.0071	0.0229
			0.50	-0.0004	0.0035	0.0061	0.0215
			1.00	0.0002	0.0045	0.007	0.0235
2	0.636	L8N15	0.00	0.0035	0.0057	0.009	0.0291
			0.50	0.0029	0.0058	0.0087	0.0285
			1.00	0.0029	0.0066	0.009	0.0278
3	0.863	L8N15	0.00	0.0019	0.0043	0.0071	0.0237
			0.50	0.0003	0.0048	0.007	0.0239
			1.00	-0.0009	0.0065	0.009	0.0297
5	1.608	L8N25	0.00	-0.0018	0.0047	0.0088	0.0318
			0.50	-0.001	0.0057	0.0091	0.0318
			1.00	-0.0013	0.0071	0.0101	0.0322
6	2.241	L8N25	0.00	-0.0002	0.0045	0.0085	0.0313
			0.50	0.0045	0.0091	0.0119	0.0322
			1.00	0.0102	0.0151	0.0196	0.0518

Figure 15: MFASIS uncertainties for the instrument: GOES 18 ABI

goes 19 abi

Channel	Wavelength [µm]	NN def	Albedo	me	mae	rmse	p99
1	0.47	L8N15	0.00	-0.0002	0.0044	0.0071	0.025
			0.50	-0.0015	0.0048	0.0074	0.0267
			1.00	-0.0022	0.0054	0.0083	0.0305
2	0.636	L8N15	0.00	0.0041	0.0053	0.0085	0.0285
			0.50	0.0031	0.0057	0.0085	0.0283
			1.00	0.0031	0.0059	0.0084	0.0271
3	0.863	L8N15	0.00	0.0019	0.0051	0.0082	0.0274
			0.50	0.0017	0.0059	0.0083	0.0264
			1.00	0.0011	0.0075	0.01	0.0293
5	1.608	L8N25	0.00	-0.0017	0.0045	0.0082	0.029
			0.50	0.0011	0.007	0.0096	0.0292
			1.00	0.0039	0.01	0.0123	0.0313
6	2.241	L8N25	0.00	0.0001	0.0056	0.0097	0.0327
			0.50	-0.0009	0.0069	0.0104	0.0327
			1.00	-0.003	0.0098	0.0131	0.0392

Figure 16: MFASIS uncertainties for the instrument: GOES 19 ABI

himawari 8 ahi

Channel	Wavelength [µm]	NN def	Albedo	me	mae	rmse	p99
1	0.47	L8N15	0.00	-0.0006	0.0039	0.0065	0.0246
			0.50	0.0003	0.0037	0.006	0.0208
			1.00	0.0004	0.0039	0.0063	0.0202
2	0.509	L8N15	0.00	0.0013	0.0043	0.0071	0.0255
			0.50	0.0017	0.0044	0.0068	0.0233
			1.00	0.0023	0.0054	0.0075	0.0234
3	0.636	L8N15	0.00	0.0026	0.006	0.0089	0.029
			0.50	0.0014	0.0059	0.0088	0.0296
			1.00	0.0006	0.0063	0.009	0.0307
4	0.856	L8N25	0.00	0.0008	0.003	0.0053	0.0194
			0.50	0.0011	0.0033	0.0054	0.0194
			1.00	0.0015	0.0036	0.0056	0.0187
5	1.61	L8N25	0.00	-0.0015	0.0045	0.0084	0.0297
			0.50	-0.0014	0.0051	0.0087	0.0302
			1.00	-0.0017	0.0064	0.0097	0.0308
6	2.256	L8N25	0.00	-0.0013	0.0048	0.0089	0.0332
			0.50	0.0006	0.0076	0.0108	0.0335
			1.00	0.0026	0.012	0.0162	0.0488

Figure 17: MFASIS uncertainties for the instrument: HIMAWARI 8 AHI

himawari 9 ahi

Channel	Wavelength [µm]	NN def	Albedo	me	mae	rmse	p99
1	0.47	L8N15	0.00	-0.0018	0.0047	0.0072	0.0249
			0.50	-0.0004	0.004	0.0064	0.0223
			1.00	0.0	0.0044	0.0068	0.0232
2	0.509	L8N15	0.00	0.0033	0.0042	0.0065	0.0218
			0.50	0.0014	0.004	0.006	0.02
			1.00	-0.0003	0.0045	0.0065	0.0197
3	0.637	L8N15	0.00	0.0034	0.0056	0.0086	0.0276
			0.50	0.004	0.0058	0.0086	0.0278
			1.00	0.0031	0.0059	0.0083	0.0266
4	0.856	L8N15	0.00	0.0023	0.0059	0.0089	0.0275
			0.50	0.0025	0.0063	0.0085	0.026
			1.00	0.0008	0.0081	0.0105	0.0305
5	1.606	L8N25	0.00	-0.0026	0.0048	0.0087	0.0293
			0.50	-0.0001	0.0089	0.0121	0.039
			1.00	0.0001	0.0138	0.0192	0.0624
6	2.257	L8N25	0.00	-0.0016	0.0052	0.0094	0.0337
			0.50	-0.0011	0.0062	0.0097	0.0338
			1.00	-0.0	0.0083	0.0117	0.0367

Figure 18: MFASIS uncertainties for the instrument: HIMAWARI 9 AHI

jpss 0 viirs

Channel	Wavelength [µm]	NN def	Albedo	me	mae	rmse	p99
1	0.635	L8N15	0.00	0.0027	0.0051	0.0081	0.0266
			0.50	0.0034	0.0058	0.0083	0.0268
			1.00	0.0041	0.0074	0.0096	0.0267
2	0.861	L8N25	0.00	0.0004	0.003	0.0053	0.0193
			0.50	-0.0004	0.0036	0.0055	0.0193
			1.00	0.0002	0.0037	0.0056	0.019
3	0.41	L8N15	0.00	-0.0018	0.0042	0.0066	0.0212
			0.50	-0.0004	0.0034	0.0059	0.0204
			1.00	-0.0	0.0035	0.0059	0.0202
4	0.443	L8N15	0.00	0.0022	0.0048	0.0073	0.0223
			0.50	0.0016	0.0042	0.0067	0.0209
			1.00	0.0021	0.0044	0.0071	0.0221
5	0.486	L8N15	0.00	-0.001	0.0041	0.0063	0.0208
			0.50	-0.0004	0.0035	0.006	0.0206
			1.00	-0.0006	0.0039	0.0063	0.0208
6	0.55	L8N15	0.00	-0.0004	0.0051	0.007	0.0224
			0.50	0.0006	0.0046	0.0068	0.0217
			1.00	0.0001	0.0047	0.0065	0.0203
7	0.671	L8N15	0.00	-0.0005	0.0039	0.0059	0.0203
			0.50	-0.0006	0.0043	0.0064	0.0208
			1.00	-0.0011	0.0047	0.007	0.0238
8	0.745	L8N15	0.00	0.001	0.0044	0.0072	0.0256
			0.50	0.0022	0.0054	0.0076	0.0248
			1.00	0.0035	0.0072	0.0096	0.0281
9	0.861	L8N25	0.00	0.0001	0.003	0.0051	0.0181
			0.50	0.0005	0.0031	0.0049	0.0173
			1.00	0.0002	0.0037	0.0053	0.0171
11	1.238	L8N25	0.00	0.0008	0.004	0.0073	0.0291
			0.50	0.001	0.0045	0.0074	0.0291
			1.00	-0.0002	0.0055	0.008	0.0257
13	1.601	L8N25	0.00	-0.0015	0.0045	0.0083	0.0296
			0.50	-0.0022	0.0054	0.0087	0.0299
			1.00	-0.0029	0.0066	0.0097	0.0303
14	1.601	L8N25	0.00	-0.0014	0.0045	0.0085	0.0297
			0.50	0.0002	0.0063	0.0095	0.0307
			1.00	0.0015	0.0082	0.0118	0.0392
15	2.257	L8N25	0.00	-0.0001	0.0047	0.0088	0.0318
			0.50	0.0018	0.0069	0.0101	0.032
			1.00	0.004	0.01	0.0133	0.0362

Figure 19: MFASIS uncertainties for the instrument: JPSS 0 VIIRS

metop 1 avhrr

Channel	Wavelength [µm]	NN def	Albedo	me	mae	rmse	p99
1	0.633	L8N15	0.00	0.0049	0.0059	0.0091	0.0299
			0.50	0.0064	0.0075	0.01	0.0301
			1.00	0.0055	0.0074	0.0098	0.0288
3	1.608	L8N25	0.00	-0.0015	0.0046	0.0086	0.0305
			0.50	-0.0035	0.0059	0.0091	0.0307
			1.00	-0.0057	0.0079	0.0106	0.0313

Figure 20: MFASIS uncertainties for the instrument: METOP 1 AVHRR

metop 2 avhrr

Channel	Wavelength [µm]	NN def	Albedo	me	mae	rmse	p99
1	0.631	L8N15	0.00	0.0039	0.0062	0.0091	0.0296
			0.50	0.004	0.0064	0.0091	0.0293
			1.00	0.0046	0.0079	0.0104	0.0309
3	1.606	L8N25	0.00	-0.0023	0.0051	0.0091	0.0302
			0.50	0.0002	0.0069	0.0098	0.031
			1.00	0.0012	0.0085	0.0113	0.0326

Figure 21: MFASIS uncertainties for the instrument: METOP 2 AVHRR

metop 3 avhrr

Channel	Wavelength [µm]	NN def	Albedo	me	mae	rmse	p99
1	0.627	L8N15	0.00	0.0018	0.006	0.0088	0.0295
			0.50	0.003	0.0056	0.0086	0.0299
			1.00	0.0021	0.0062	0.0089	0.029
3	1.607	L8N25	0.00	-0.0024	0.0043	0.0083	0.0301
			0.50	-0.0002	0.0063	0.0094	0.0305
			1.00	0.0008	0.0079	0.011	0.0366

Figure 22: MFASIS uncertainties for the instrument: METOP 3 AVHRR

metopsg 1 metimage

Channel	Wavelength [µm]	NN def	Albedo	me	mae	rmse	p99
1	0.443	L8N15	0.00	-0.0016	0.0039	0.0068	0.0262
			0.50	-0.0008	0.0034	0.0063	0.0253
			1.00	-0.0011	0.0039	0.0068	0.0273
2	0.556	L8N15	0.00	0.0018	0.0046	0.0071	0.0231
			0.50	0.0009	0.005	0.0074	0.0237
			1.00	-0.0	0.0053	0.0078	0.0258
3	0.669	L8N15	0.00	-0.0004	0.0036	0.0057	0.019
			0.50	0.001	0.0036	0.0057	0.0192
			1.00	0.002	0.0052	0.0077	0.0226
4	0.753	L8N15	0.00	-0.0004	0.0048	0.0068	0.0228
			0.50	-0.0004	0.0046	0.0069	0.0229
			1.00	-0.0013	0.0052	0.0075	0.0265
6	0.863	L8N15	0.00	0.0006	0.0055	0.0086	0.0296
			0.50	0.0011	0.0048	0.0074	0.0256
			1.00	0.001	0.0063	0.0089	0.0285
8	1.241	L8N25	0.00	0.0018	0.0042	0.0072	0.0266
			0.50	0.0023	0.0049	0.0074	0.0262
			1.00	0.0017	0.0059	0.008	0.0236
10	1.63	L8N25	0.00	-0.0012	0.005	0.0093	0.0308
			0.50	-0.0013	0.0055	0.0092	0.0304
			1.00	-0.0021	0.0062	0.0095	0.0304
11	2.25	L8N25	0.00	-0.0017	0.0048	0.0088	0.0329
			0.50	0.0001	0.007	0.01	0.0326
			1.00	0.0013	0.0095	0.0126	0.0359

Figure 23: MFASIS uncertainties for the instrument: METOPSG 1 METIMAGE

msg 1 seviri

Channel	Wavelength [µm]	NN def	Albedo	me	mae	rmse	p99
1	0.639	L8N15	0.00	0.0033	0.0055	0.0085	0.0276
			0.50	0.0026	0.0055	0.0083	0.0271
			1.00	0.002	0.0059	0.0082	0.0259
3	1.634	L8N25	0.00	-0.0012	0.0046	0.0086	0.0299
			0.50	0.0009	0.007	0.0097	0.0297
			1.00	0.0022	0.009	0.0118	0.0325

Figure 24: MFASIS uncertainties for the instrument: MSG 1 SEVIRI

msg 2 seviri

Channel	Wavelength [µm]	NN def	Albedo	me	mae	rmse	p99
1	0.639	L8N15	0.00	0.002	0.0046	0.0074	0.0257
			0.50	0.0013	0.0053	0.0078	0.026
			1.00	0.001	0.0063	0.0086	0.0259
3	1.637	L8N25	0.00	-0.0004	0.0044	0.0081	0.0282
			0.50	-0.0002	0.0053	0.0084	0.0281
			1.00	-0.0002	0.0066	0.0094	0.0287

Figure 25: MFASIS uncertainties for the instrument: MSG 2 SEVIRI

msg 3 seviri

Channel	Wavelength [µm]	NN def	Albedo	me	mae	rmse	p99
1	0.637	L8N15	0.00	0.0028	0.005	0.0077	0.0252
			0.50	0.0025	0.0049	0.0076	0.0253
			1.00	0.0034	0.006	0.008	0.0241
3	1.637	L8N25	0.00	-0.002	0.0045	0.0082	0.0274
			0.50	-0.0016	0.0053	0.0084	0.0275
			1.00	-0.0012	0.0068	0.0096	0.029

Figure 26: MFASIS uncertainties for the instrument: MSG 3 SEVIRI

msg 4 seviri

Channel	Wavelength [µm]	NN def	Albedo	me	mae	rmse	p99
1	0.637	L8N15	0.00	0.0014	0.0061	0.0086	0.0275
			0.50	0.003	0.0057	0.0085	0.0286
			1.00	0.0033	0.0069	0.0094	0.0303
3	1.636	L8N25	0.00	-0.0002	0.0048	0.0084	0.0289
			0.50	-0.0003	0.0057	0.0089	0.0291
			1.00	0.0007	0.0075	0.0104	0.0303

Figure 27: MFASIS uncertainties for the instrument: MSG 4 SEVIRI

mtg 1 fci

Channel	Wavelength [µm]	NN def	Albedo	me	mae	rmse	p99
1	0.444	L8N15	0.00	-0.0007	0.0037	0.0061	0.0208
			0.50	-0.0005	0.0033	0.0057	0.0198
			1.00	-0.0013	0.0036	0.006	0.0205
2	0.51	L8N15	0.00	0.001	0.0045	0.0075	0.0271
			0.50	0.001	0.0049	0.0073	0.0257
			1.00	0.0009	0.005	0.0077	0.0275
3	0.64	L8N25	0.00	0.0027	0.0044	0.0075	0.0265
			0.50	0.0032	0.0046	0.0076	0.0268
			1.00	0.003	0.0047	0.0073	0.0259
4	0.865	L8N25	0.00	0.0003	0.0029	0.0053	0.0196
			0.50	0.0017	0.0034	0.0055	0.0198
			1.00	0.0036	0.0049	0.0068	0.022
7	1.61	L8N25	0.00	-0.0004	0.0053	0.0093	0.0317
			0.50	0.0003	0.0062	0.0096	0.0326
			1.00	0.0013	0.0078	0.0109	0.0337
8	2.25	L8N25	0.00	-0.0011	0.0051	0.0094	0.0349
			0.50	0.0005	0.0065	0.01	0.0352
			1.00	0.0022	0.0092	0.0125	0.0362

Figure 28: MFASIS uncertainties for the instrument: MTG 1 FCI

noaa 14 avhrr

Channel	Wavelength [µm]	NN def	Albedo	me	mae	rmse	p99
1	0.636	L8N15	0.00	0.003	0.0059	0.01	0.0351
			0.50	0.003	0.0063	0.0101	0.0355
			1.00	0.004	0.0077	0.0107	0.0342

Figure 29: MFASIS uncertainties for the instrument: NOAA 14 AVHRR

noaa 20 viirs

Channel	Wavelength [µm]	NN def	Albedo	me	mae	rmse	p99
1	0.641	L8N15	0.00	0.002	0.005	0.0076	0.0254
			0.50	0.0001	0.0066	0.0087	0.0251
			1.00	-0.004	0.0103	0.013	0.0316
2	0.867	L8N15	0.00	0.0004	0.0044	0.0075	0.0289
			0.50	0.0002	0.0047	0.0075	0.0288
			1.00	-0.0003	0.0062	0.0088	0.0301
3	0.411	L8N15	0.00	0.0012	0.0038	0.0062	0.02
			0.50	0.0013	0.0036	0.006	0.0193
			1.00	0.001	0.0034	0.006	0.0194
4	0.444	L8N15	0.00	0.0006	0.0037	0.0065	0.0218
			0.50	0.0002	0.0038	0.0064	0.0205
			1.00	-0.0005	0.0043	0.0069	0.0209
5	0.489	L8N15	0.00	0.0005	0.0047	0.0074	0.0255
			0.50	0.0007	0.0039	0.0064	0.0226
			1.00	0.0014	0.0043	0.0064	0.0218
6	0.556	L8N15	0.00	0.0008	0.0042	0.0065	0.0218
			0.50	0.0013	0.004	0.0063	0.0219
			1.00	0.0009	0.004	0.0062	0.0206
7	0.667	L8N15	0.00	0.0003	0.0039	0.0066	0.0243
			0.50	0.0018	0.0044	0.0066	0.0227
			1.00	0.0022	0.0054	0.0078	0.0253
8	0.746	L8N15	0.00	0.0035	0.0063	0.0094	0.0291
			0.50	0.0029	0.0063	0.0087	0.0274
			1.00	0.0028	0.0075	0.0099	0.0297
9	0.867	L8N15	0.00	0.0011	0.0046	0.0076	0.0274
			0.50	-0.0008	0.0048	0.0076	0.0277
			1.00	0.0013	0.0069	0.0093	0.029
11	1.238	L8N25	0.00	0.001	0.004	0.0076	0.0311
			0.50	-0.0001	0.0049	0.008	0.031
			1.00	-0.0009	0.006	0.0085	0.0265
13	1.603	L8N25	0.00	-0.0015	0.0045	0.0084	0.0303
			0.50	-0.0023	0.006	0.0095	0.0308
			1.00	-0.0031	0.008	0.0118	0.0406
14	1.604	L8N25	0.00	-0.0017	0.0043	0.0082	0.0291
			0.50	-0.0014	0.0048	0.0084	0.0294
			1.00	-0.0025	0.0058	0.009	0.0295
15	2.258	L8N25	0.00	-0.0001	0.0051	0.0095	0.0342
			0.50	0.0026	0.0078	0.0111	0.0348
			1.00	0.0055	0.0113	0.0151	0.0452

Figure 30: MFASIS uncertainties for the instrument: NOAA 20 VIIRS

noaa 21 viirs

Channel	Wavelength [µm]	NN def	Albedo	me	mae	rmse	p99
1	0.64	L8N15	0.00	0.0035	0.0057	0.0087	0.0281
			0.50	0.0044	0.006	0.0087	0.0278
			1.00	0.004	0.0068	0.0091	0.0265
2	0.867	L8N15	0.00	-0.001	0.0046	0.0076	0.0288
			0.50	-0.0012	0.0054	0.0079	0.0279
			1.00	-0.0007	0.0077	0.0109	0.0367
3	0.411	L8N15	0.00	0.0011	0.0041	0.007	0.0243
			0.50	-0.0001	0.0041	0.0072	0.026
			1.00	-0.0009	0.0047	0.0077	0.0279
4	0.445	L8N15	0.00	0.0005	0.004	0.0068	0.0242
			0.50	0.0007	0.0039	0.0066	0.0234
			1.00	0.0005	0.0039	0.0065	0.023
5	0.488	L8N15	0.00	0.0001	0.004	0.0061	0.02
			0.50	0.0017	0.0039	0.0062	0.0211
			1.00	-0.0003	0.005	0.0074	0.0221
6	0.555	L8N15	0.00	0.0038	0.0055	0.0079	0.0249
			0.50	0.0019	0.0048	0.0072	0.0239
			1.00	0.0006	0.0049	0.007	0.0216
7	0.671	L8N15	0.00	0.0005	0.0036	0.0059	0.0202
			0.50	0.0014	0.0039	0.0058	0.0187
			1.00	0.0017	0.0045	0.0064	0.0192
8	0.747	L8N15	0.00	-0.0005	0.0042	0.0074	0.0286
			0.50	-0.0035	0.0065	0.0104	0.0389
			1.00	-0.0054	0.0089	0.0141	0.0566
9	0.868	L8N15	0.00	0.0011	0.0045	0.0073	0.0242
			0.50	0.003	0.0058	0.0081	0.0236
			1.00	0.0046	0.0093	0.0132	0.0411
11	1.241	L8N25	0.00	0.0013	0.0033	0.0062	0.024
			0.50	0.0018	0.0042	0.0065	0.024
			1.00	0.001	0.0047	0.0068	0.0224
13	1.613	L8N25	0.00	-0.0012	0.0048	0.0087	0.0303
			0.50	0.0001	0.0064	0.0094	0.0309
			1.00	0.0017	0.0088	0.0114	0.0319
14	1.613	L8N25	0.00	-0.0025	0.0051	0.0091	0.033
			0.50	-0.0033	0.0058	0.0094	0.0327
			1.00	-0.0036	0.007	0.0104	0.0332
15	2.251	L8N25	0.00	-0.0002	0.0051	0.0094	0.0344
			0.50	0.0	0.0065	0.0101	0.0354
			1.00	0.0013	0.0087	0.0128	0.0416

Figure 31: MFASIS uncertainties for the instrument: NOAA 21 VIIRS

3 Uncertainty figures

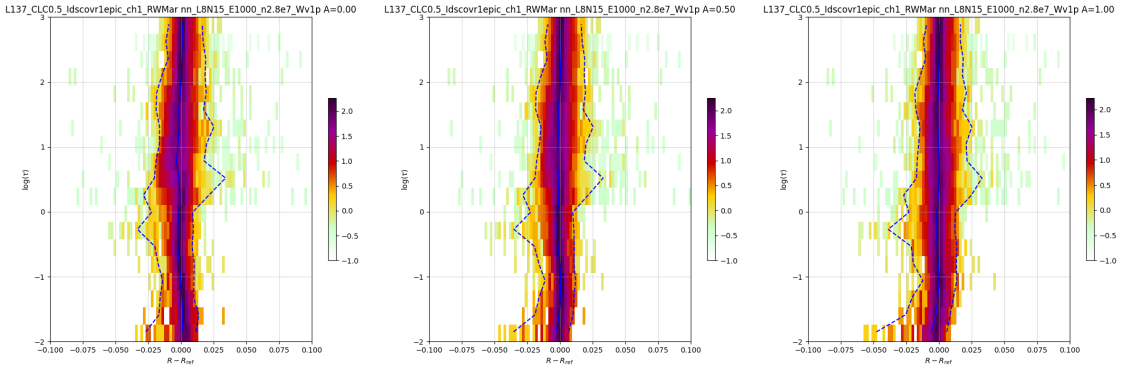

(a) (b) (c)

Figure 32: MFASIS $\Delta r_{\mathrm{MFASIS}-ref}$ as function of the cloud optical depth τ at albedo(s) of 0.00, 0.50, 1.00 (from left to right) for the instrument: DSCOVR 1 EPIC CH1

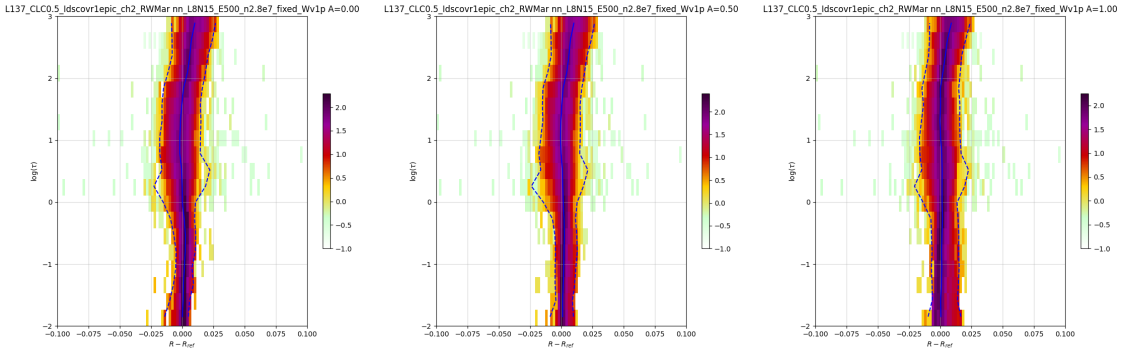

(a) (b) (c)

Figure 33: MFASIS $\Delta r_{\mathrm{MFASIS}-ref}$ as function of the cloud optical depth τ at albedo(s) of 0.00, 0.50, 1.00 (from left to right) for the instrument: DSCOVR 1 EPIC CH2

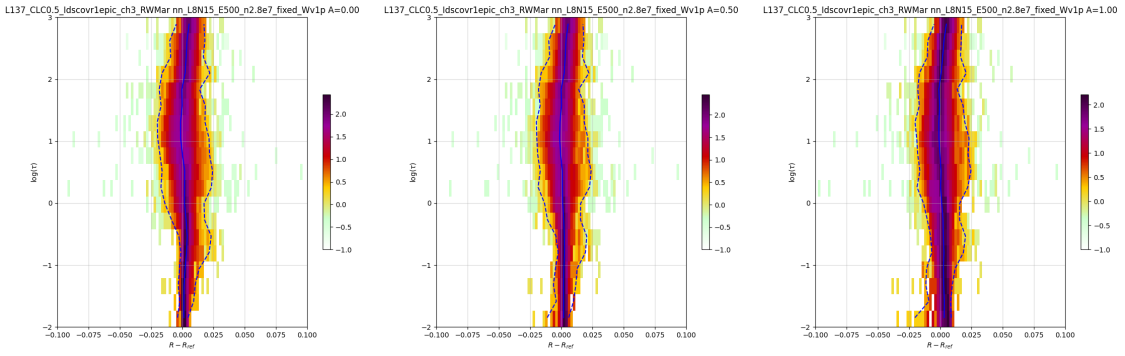

(a) (b) (c)

Figure 34: MFASIS $\Delta r_{\mathrm{MFASIS}-ref}$ as function of the cloud optical depth τ at albedo(s) of 0.00, 0.50, 1.00 (from left to right) for the instrument: DSCOVR 1 EPIC CH3

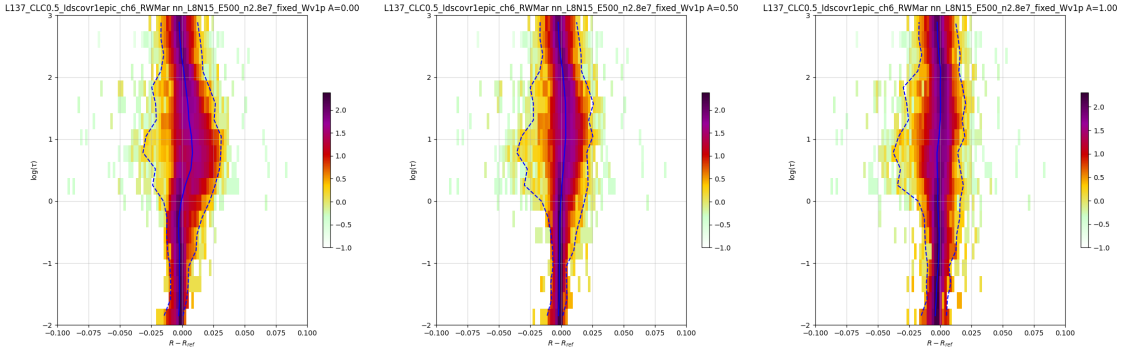

(a) (b) (c)

Figure 35: MFASIS $\Delta r_{\mathrm{MFASIS}-ref}$ as function of the cloud optical depth τ at albedo(s) of 0.00, 0.50, 1.00 (from left to right) for the instrument: DSCOVR 1 EPIC CH6

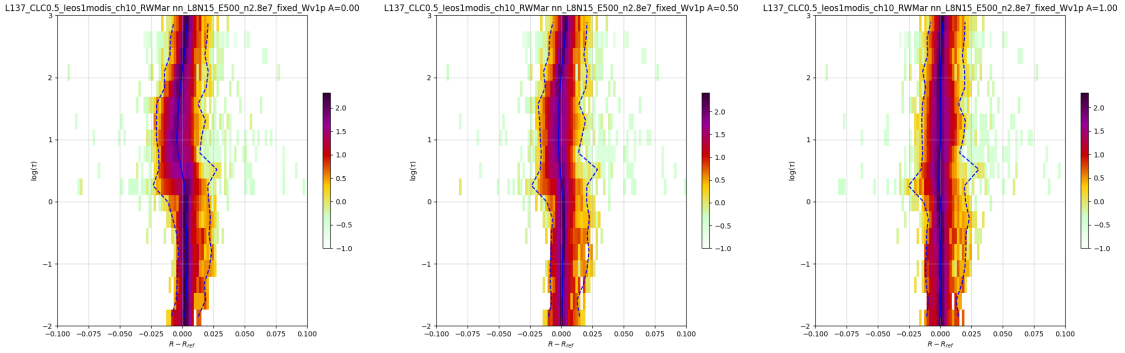

(a) (b) (c)

Figure 36: MFASIS $\Delta r_{\mathrm{MFASIS}-ref}$ as function of the cloud optical depth τ at albedo(s) of 0.00, 0.50, 1.00 (from left to right) for the instrument: EOS 1 MODIS CH10

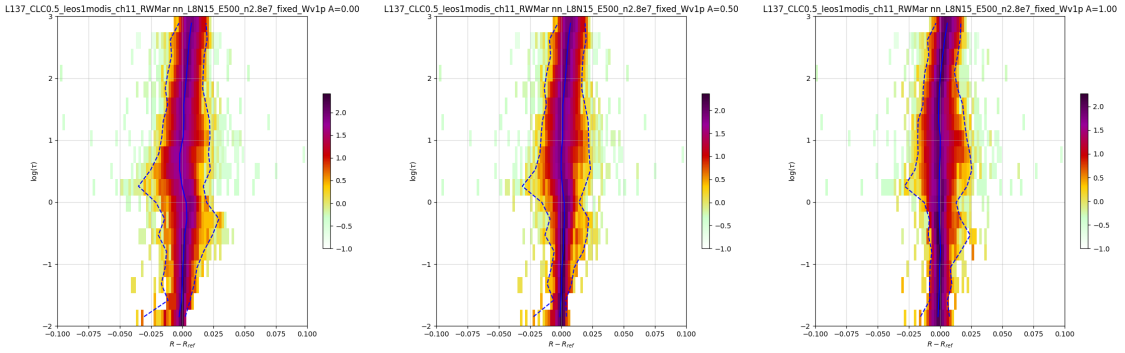

(a) (b) (c)

Figure 37: MFASIS $\Delta r_{\mathrm{MFASIS}-ref}$ as function of the cloud optical depth τ at albedo(s) of 0.00, 0.50, 1.00 (from left to right) for the instrument: EOS 1 MODIS CH11

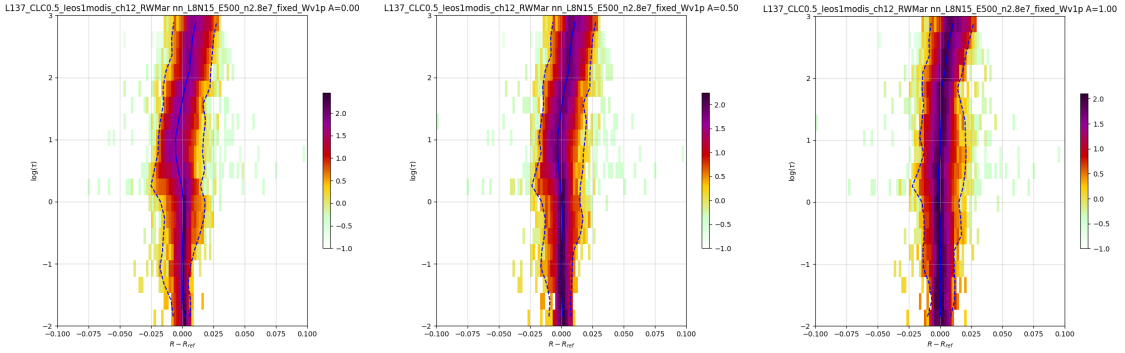

(a) (b) (c)

Figure 38: MFASIS $\Delta r_{\mathrm{MFASIS}-ref}$ as function of the cloud optical depth τ at albedo(s) of 0.00, 0.50, 1.00 (from left to right) for the instrument: EOS 1 MODIS CH12

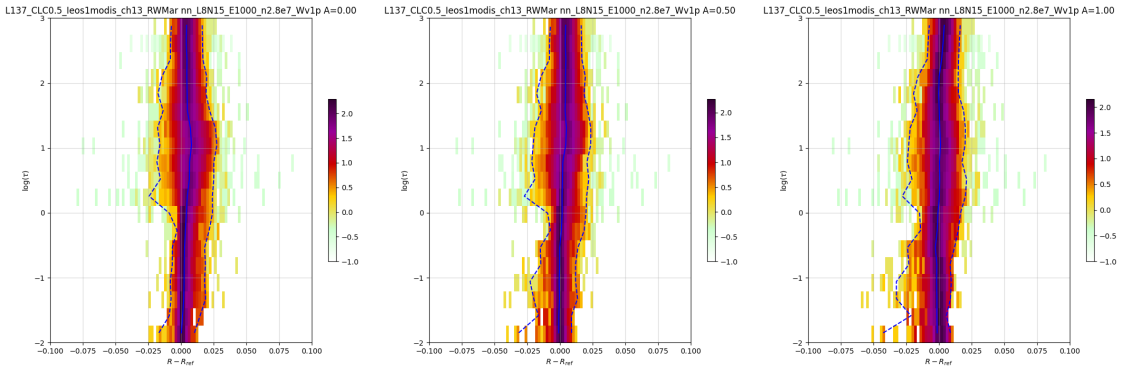

(a) (b) (c)

Figure 39: MFASIS $\Delta r_{\mathrm{MFASIS}-ref}$ as function of the cloud optical depth τ at albedo(s) of 0.00, 0.50, 1.00 (from left to right) for the instrument: EOS 1 MODIS CH13

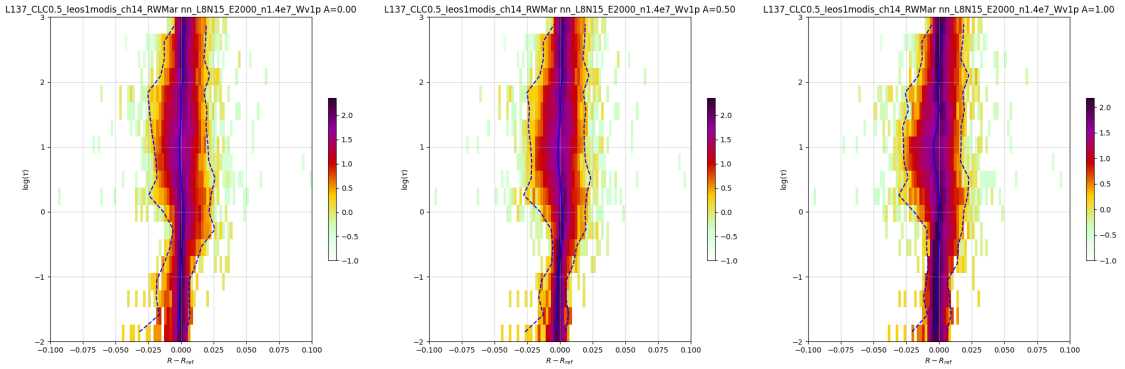

(a) (b) (c)

Figure 40: MFASIS $\Delta r_{\mathrm{MFASIS}-ref}$ as function of the cloud optical depth τ at albedo(s) of 0.00, 0.50, 1.00 (from left to right) for the instrument: EOS 1 MODIS CH14

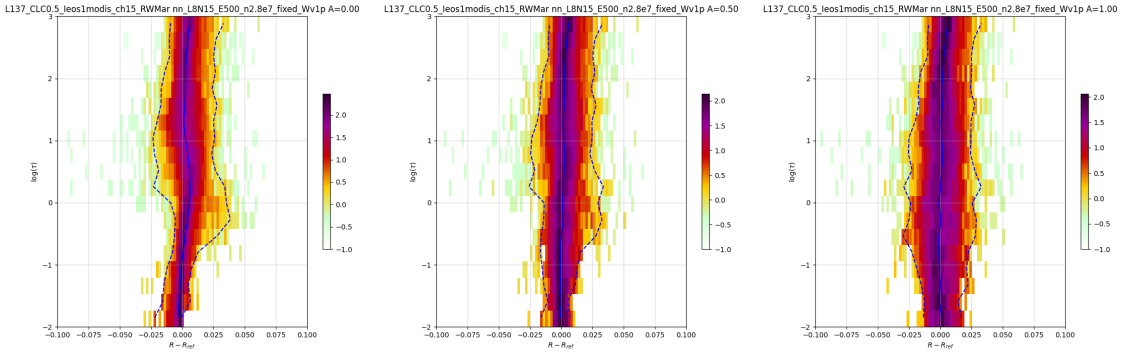

(a) (b) (c)

Figure 41: MFASIS $\Delta r_{\mathrm{MFASIS}-ref}$ as function of the cloud optical depth τ at albedo(s) of 0.00, 0.50, 1.00 (from left to right) for the instrument: EOS 1 MODIS CH15

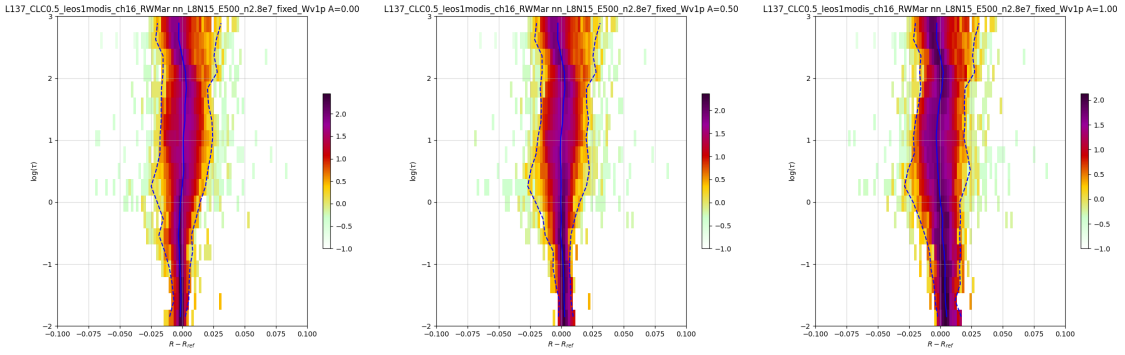

(a) (b) (c)

Figure 42: MFASIS $\Delta r_{\mathrm{MFASIS}-ref}$ as function of the cloud optical depth τ at albedo(s) of 0.00, 0.50, 1.00 (from left to right) for the instrument: EOS 1 MODIS CH16

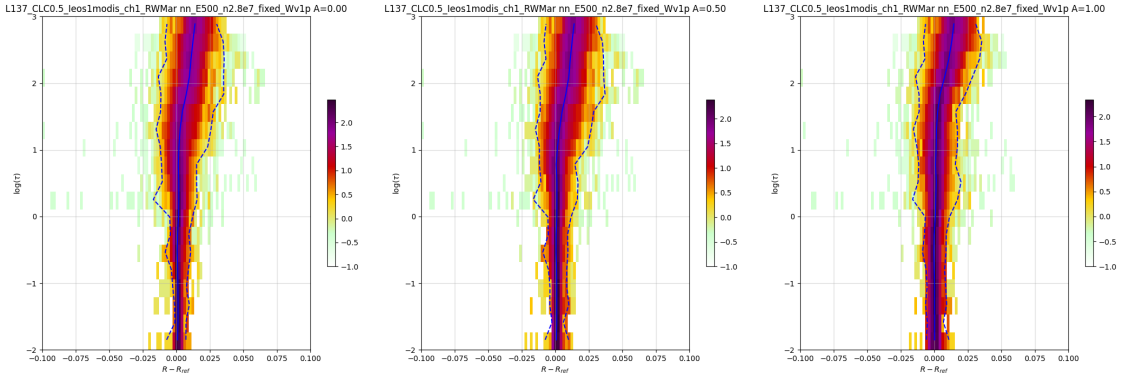

(a) (b) (c)

Figure 43: MFASIS $\Delta r_{\mathrm{MFASIS}-ref}$ as function of the cloud optical depth τ at albedo(s) of 0.00, 0.50, 1.00 (from left to right) for the instrument: EOS 1 MODIS CH1

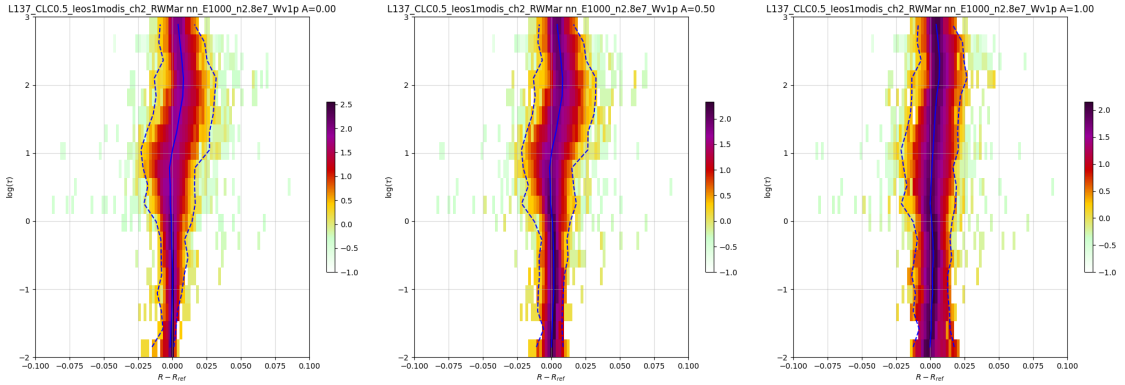

(a) (b) (c)

Figure 44: MFASIS $\Delta r_{\mathrm{MFASIS}-ref}$ as function of the cloud optical depth τ at albedo(s) of 0.00, 0.50, 1.00 (from left to right) for the instrument: EOS 1 MODIS CH2

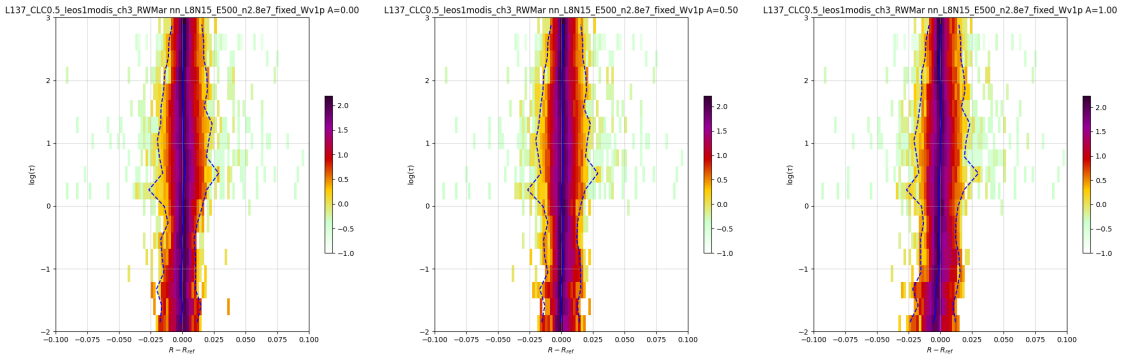

(a) (b) (c)

Figure 45: MFASIS $\Delta r_{\mathrm{MFASIS}-ref}$ as function of the cloud optical depth τ at albedo(s) of 0.00, 0.50, 1.00 (from left to right) for the instrument: EOS 1 MODIS CH3

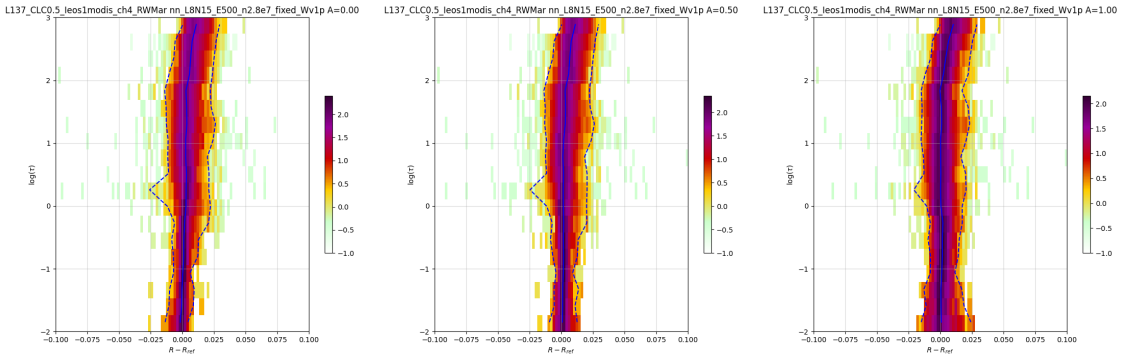

(a) (b) (c)

Figure 46: MFASIS $\Delta r_{\mathrm{MFASIS}-ref}$ as function of the cloud optical depth τ at albedo(s) of 0.00, 0.50, 1.00 (from left to right) for the instrument: EOS 1 MODIS CH4

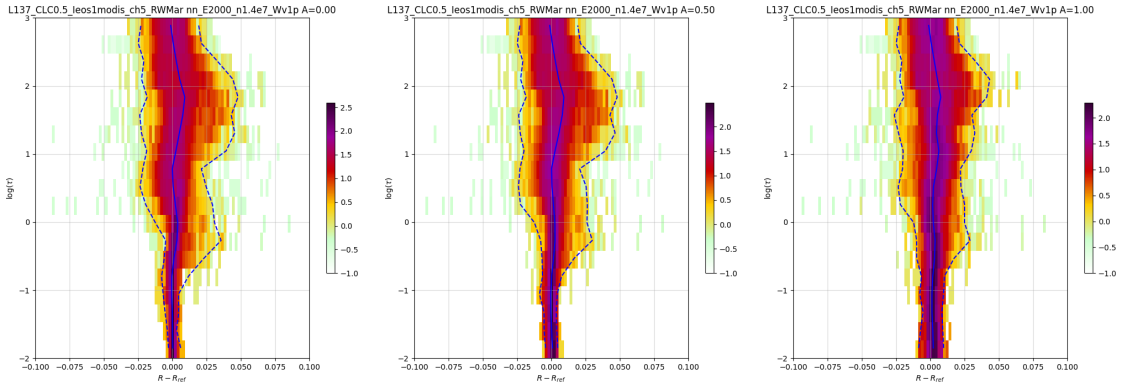

(a) (b) (c)

Figure 47: MFASIS $\Delta r_{\mathrm{MFASIS}-ref}$ as function of the cloud optical depth τ at albedo(s) of 0.00, 0.50, 1.00 (from left to right) for the instrument: EOS 1 MODIS CH5

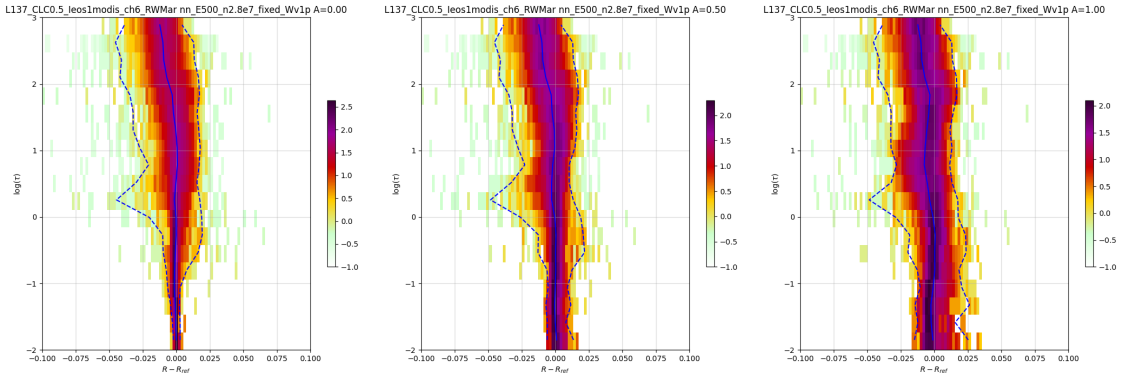

(a) (b) (c)

Figure 48: MFASIS $\Delta r_{\mathrm{MFASIS}-ref}$ as function of the cloud optical depth τ at albedo(s) of 0.00, 0.50, 1.00 (from left to right) for the instrument: EOS 1 MODIS CH6

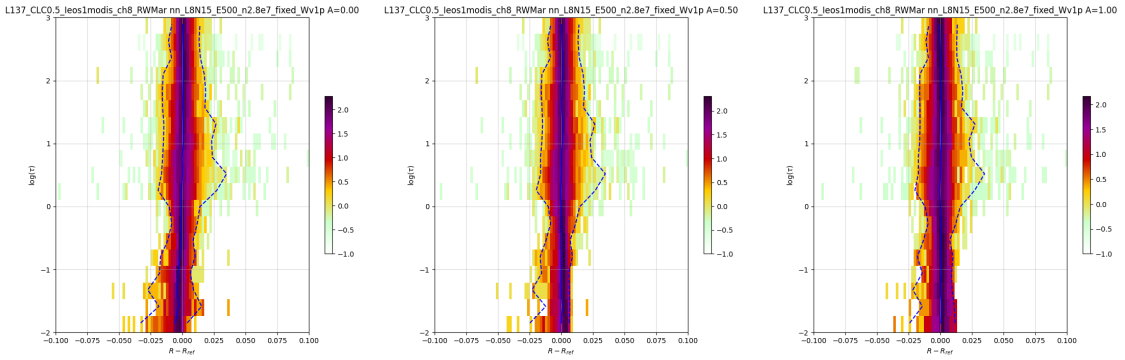

(a) (b) (c)

Figure 49: MFASIS $\Delta r_{\mathrm{MFASIS}-ref}$ as function of the cloud optical depth τ at albedo(s) of 0.00, 0.50, 1.00 (from left to right) for the instrument: EOS 1 MODIS CH8

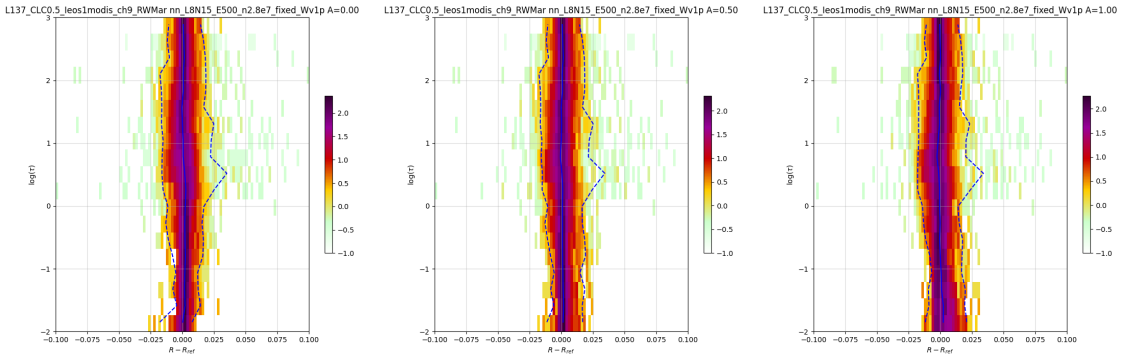

(a) (b) (c)

Figure 50: MFASIS $\Delta r_{\mathrm{MFASIS}-ref}$ as function of the cloud optical depth τ at albedo(s) of 0.00, 0.50, 1.00 (from left to right) for the instrument: EOS 1 MODIS CH9

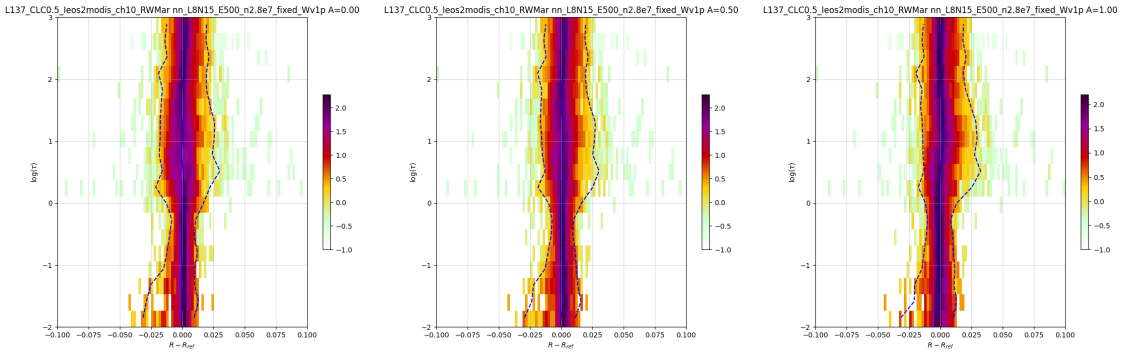

(a) (b) (c)

Figure 51: MFASIS $\Delta r_{\mathrm{MFASIS}-ref}$ as function of the cloud optical depth τ at albedo(s) of 0.00, 0.50, 1.00 (from left to right) for the instrument: EOS 2 MODIS CH10

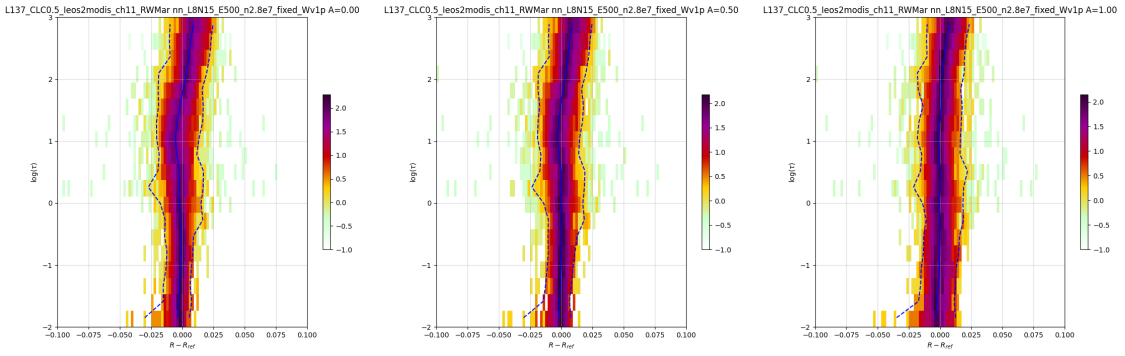

(a) (b) (c)

Figure 52: MFASIS $\Delta r_{\mathrm{MFASIS}-ref}$ as function of the cloud optical depth τ at albedo(s) of 0.00, 0.50, 1.00 (from left to right) for the instrument: EOS 2 MODIS CH11

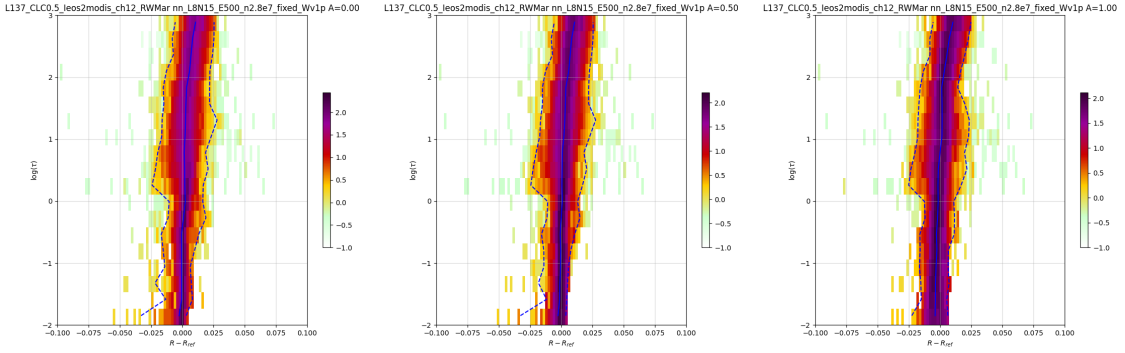

(a) (b) (c)

Figure 53: MFASIS $\Delta r_{\mathrm{MFASIS}-ref}$ as function of the cloud optical depth τ at albedo(s) of 0.00, 0.50, 1.00 (from left to right) for the instrument: EOS 2 MODIS CH12

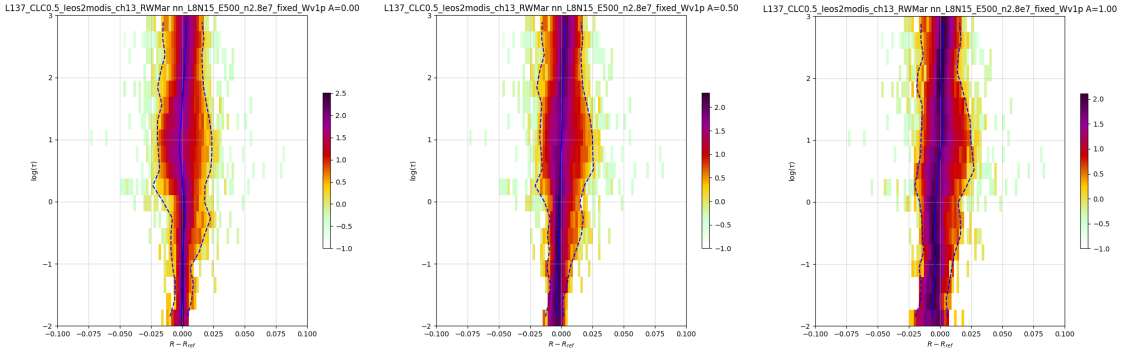

(a) (b) (c)

Figure 54: MFASIS $\Delta r_{\mathrm{MFASIS}-ref}$ as function of the cloud optical depth τ at albedo(s) of 0.00, 0.50, 1.00 (from left to right) for the instrument: EOS 2 MODIS CH13

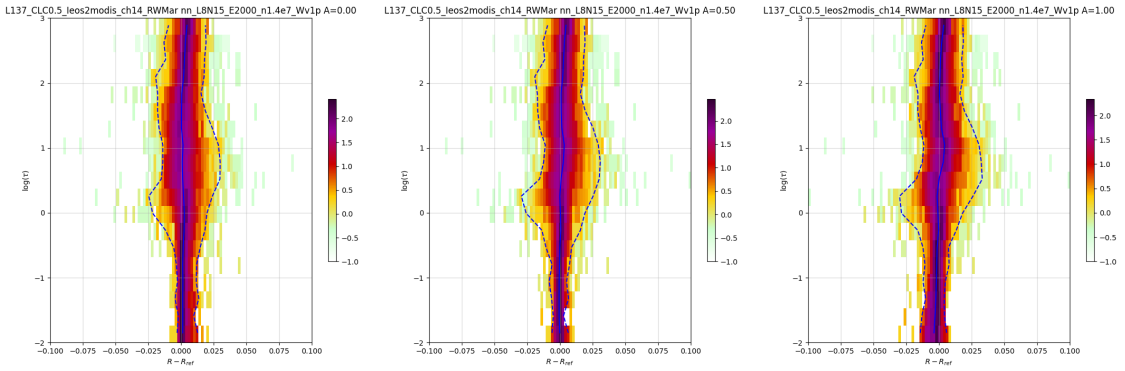

(a) (b) (c)

Figure 55: MFASIS $\Delta r_{\mathrm{MFASIS}-ref}$ as function of the cloud optical depth τ at albedo(s) of 0.00, 0.50, 1.00 (from left to right) for the instrument: EOS 2 MODIS CH14

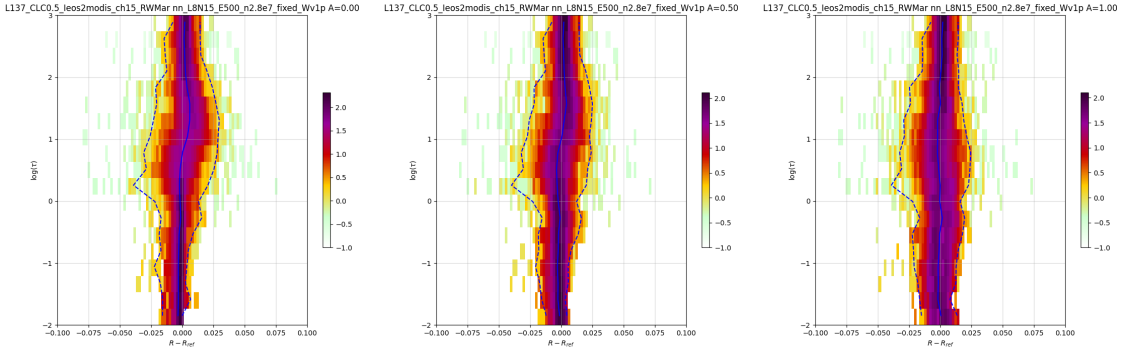

(a) (b) (c)

Figure 56: MFASIS $\Delta r_{\mathrm{MFASIS}-ref}$ as function of the cloud optical depth τ at albedo(s) of 0.00, 0.50, 1.00 (from left to right) for the instrument: EOS 2 MODIS CH15

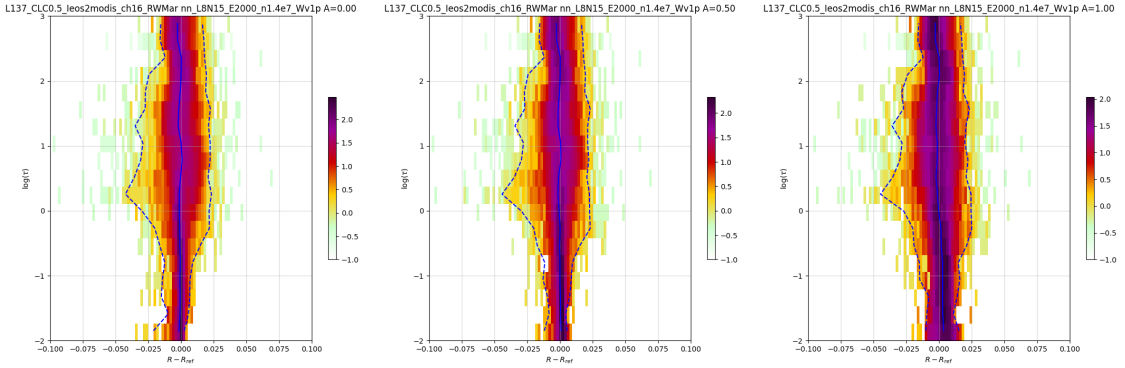

(a) (b) (c)

Figure 57: MFASIS $\Delta r_{\mathrm{MFASIS}-ref}$ as function of the cloud optical depth τ at albedo(s) of 0.00, 0.50, 1.00 (from left to right) for the instrument: EOS 2 MODIS CH16

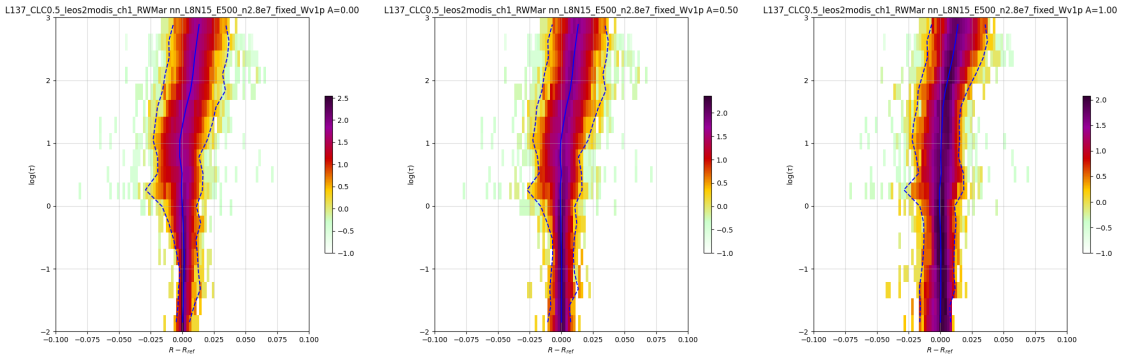

(a) (b) (c)

Figure 58: MFASIS $\Delta r_{\mathrm{MFASIS}-ref}$ as function of the cloud optical depth τ at albedo(s) of 0.00, 0.50, 1.00 (from left to right) for the instrument: EOS 2 MODIS CH1

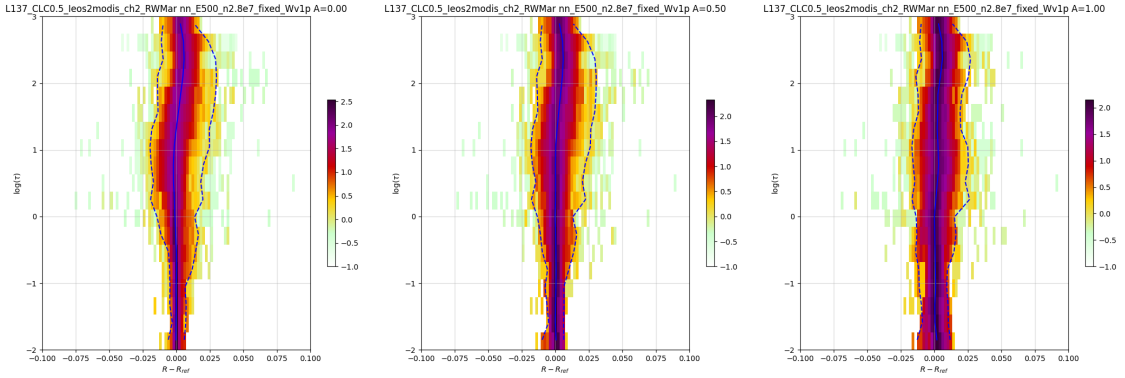

(a) (b) (c)

Figure 59: MFASIS $\Delta r_{\mathrm{MFASIS}-ref}$ as function of the cloud optical depth τ at albedo(s) of 0.00, 0.50, 1.00 (from left to right) for the instrument: EOS 2 MODIS CH2

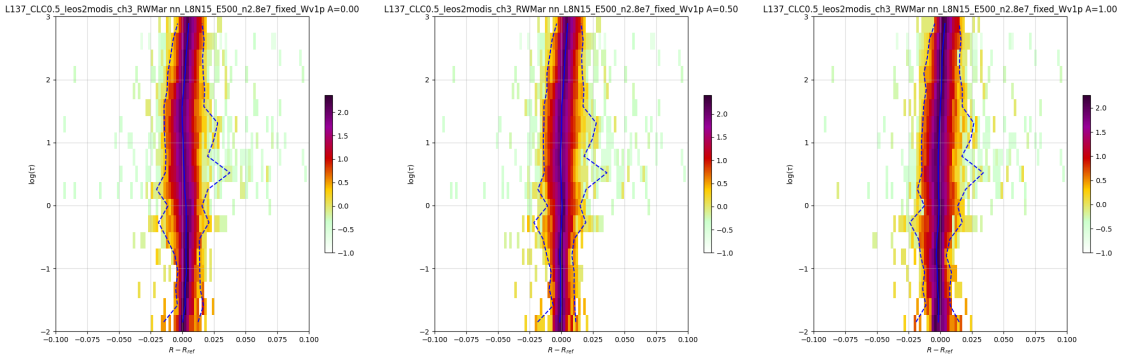

(a) (b) (c)

Figure 60: MFASIS $\Delta r_{\mathrm{MFASIS}-ref}$ as function of the cloud optical depth τ at albedo(s) of 0.00, 0.50, 1.00 (from left to right) for the instrument: EOS 2 MODIS CH3

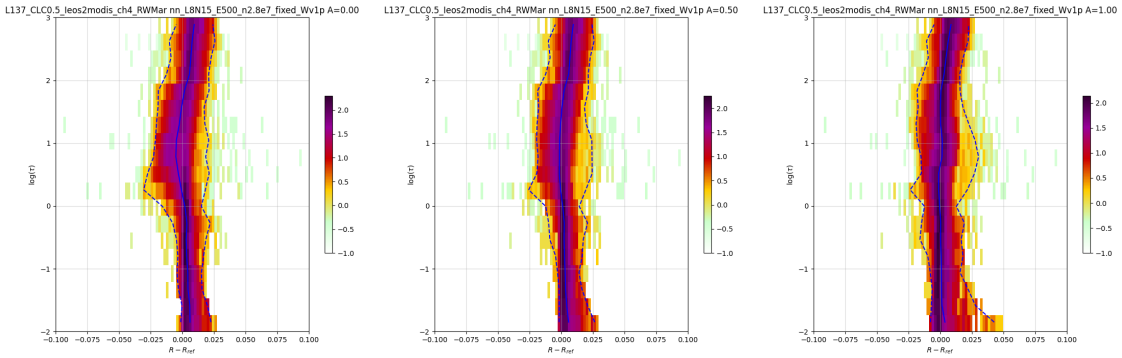

(a) (b) (c)

Figure 61: MFASIS $\Delta r_{\mathrm{MFASIS}-ref}$ as function of the cloud optical depth τ at albedo(s) of 0.00, 0.50, 1.00 (from left to right) for the instrument: EOS 2 MODIS CH4

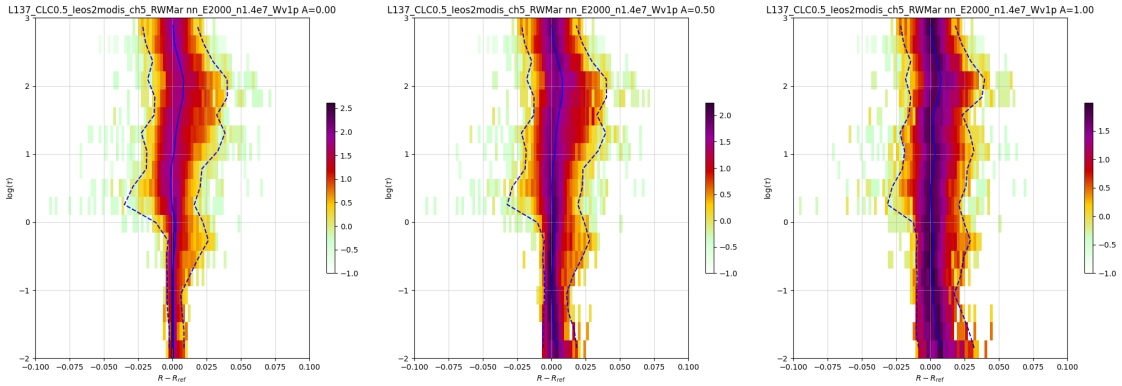

(a) (b) (c)

Figure 62: MFASIS $\Delta r_{\mathrm{MFASIS}-ref}$ as function of the cloud optical depth τ at albedo(s) of 0.00, 0.50, 1.00 (from left to right) for the instrument: EOS 2 MODIS CH5

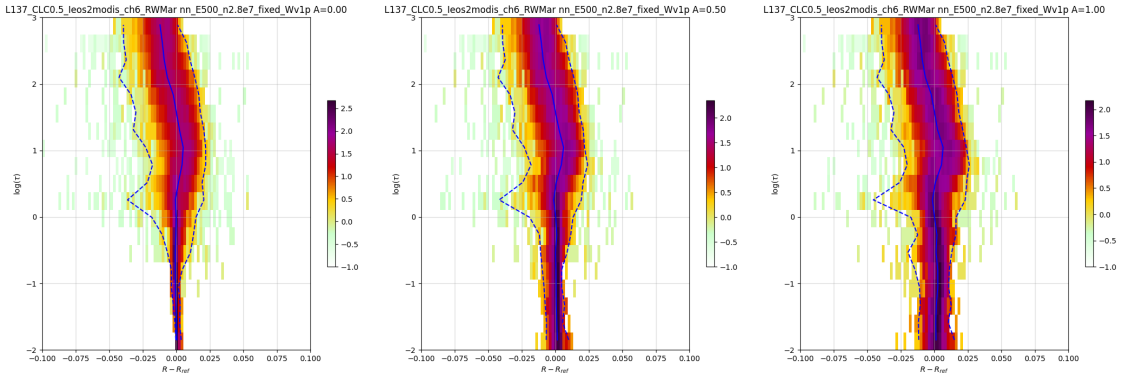

(a) (b) (c)

Figure 63: MFASIS $\Delta r_{\mathrm{MFASIS}-ref}$ as function of the cloud optical depth τ at albedo(s) of 0.00, 0.50, 1.00 (from left to right) for the instrument: EOS 2 MODIS CH6

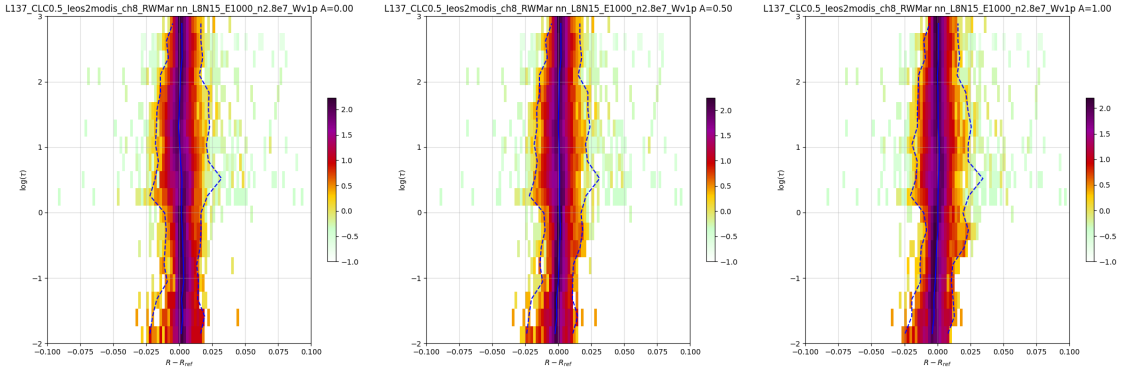

(a) (b) (c)

Figure 64: MFASIS $\Delta r_{\mathrm{MFASIS}-ref}$ as function of the cloud optical depth τ at albedo(s) of 0.00, 0.50, 1.00 (from left to right) for the instrument: EOS 2 MODIS CH8

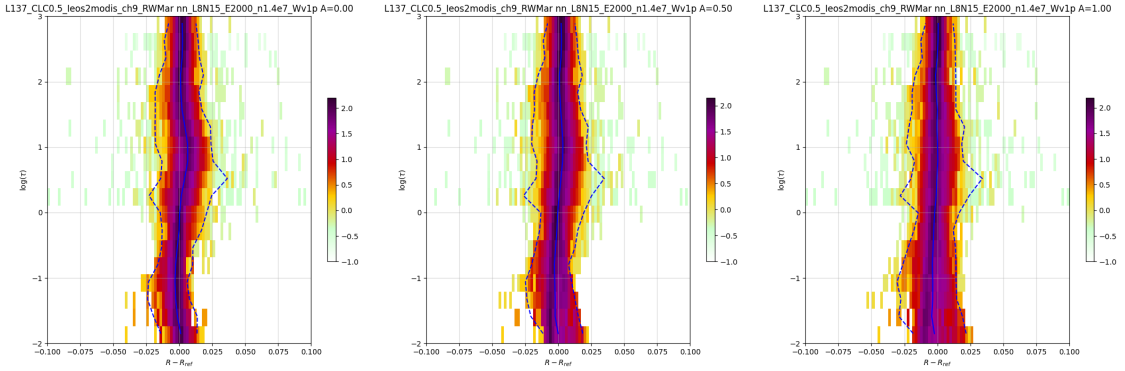

(a) (b) (c)

Figure 65: MFASIS $\Delta r_{\mathrm{MFASIS}-ref}$ as function of the cloud optical depth τ at albedo(s) of 0.00, 0.50, 1.00 (from left to right) for the instrument: EOS 2 MODIS CH9

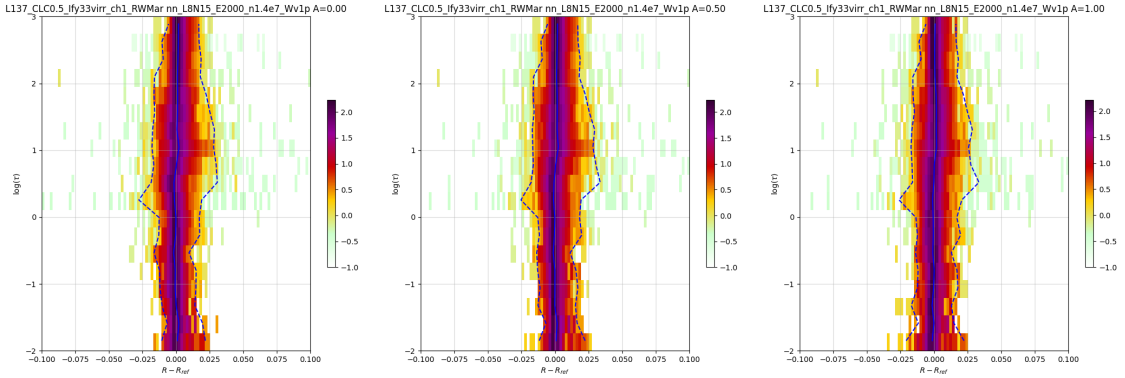

(a) (b) (c)

Figure 66: MFASIS $\Delta r_{\mathrm{MFASIS}-ref}$ as function of the cloud optical depth τ at albedo(s) of 0.00, 0.50, 1.00 (from left to right) for the instrument: FY3 3 VIRR CH1

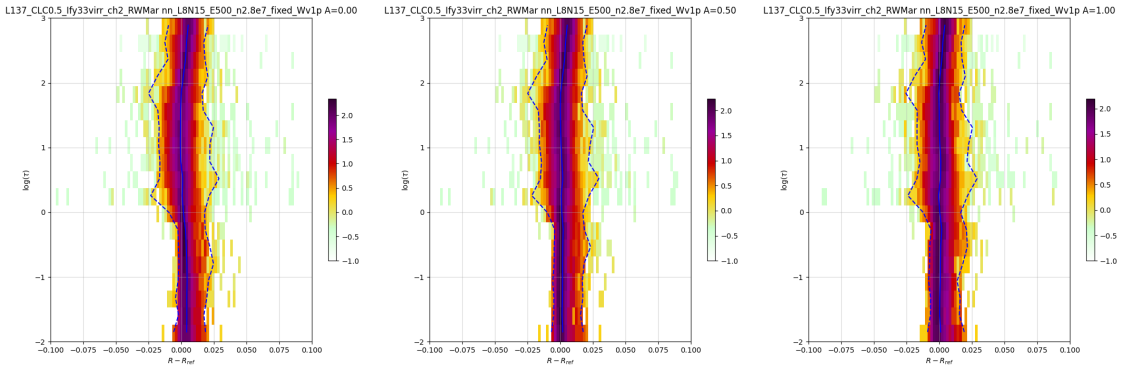

(a) (b) (c)

Figure 67: MFASIS $\Delta r_{\mathrm{MFASIS}-ref}$ as function of the cloud optical depth τ at albedo(s) of 0.00, 0.50, 1.00 (from left to right) for the instrument: FY3 3 VIRR CH2

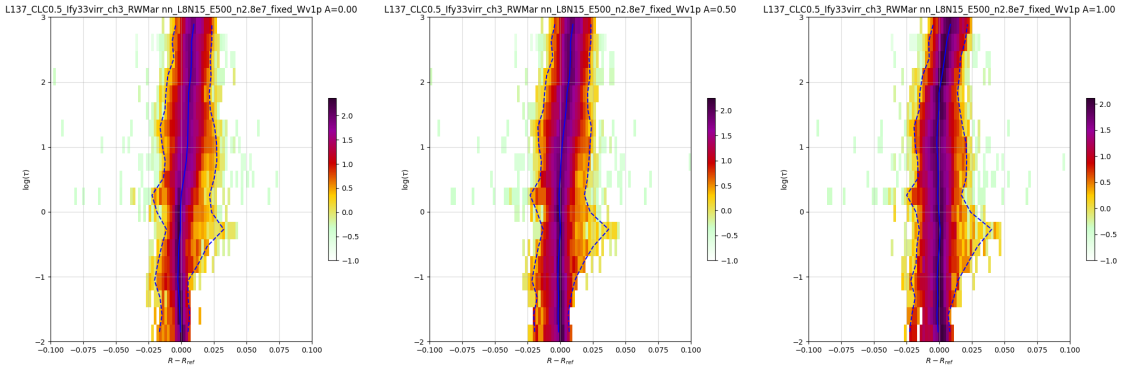

(a) (b) (c)

Figure 68: MFASIS $\Delta r_{\mathrm{MFASIS}-ref}$ as function of the cloud optical depth τ at albedo(s) of 0.00, 0.50, 1.00 (from left to right) for the instrument: FY3 3 VIRR CH3

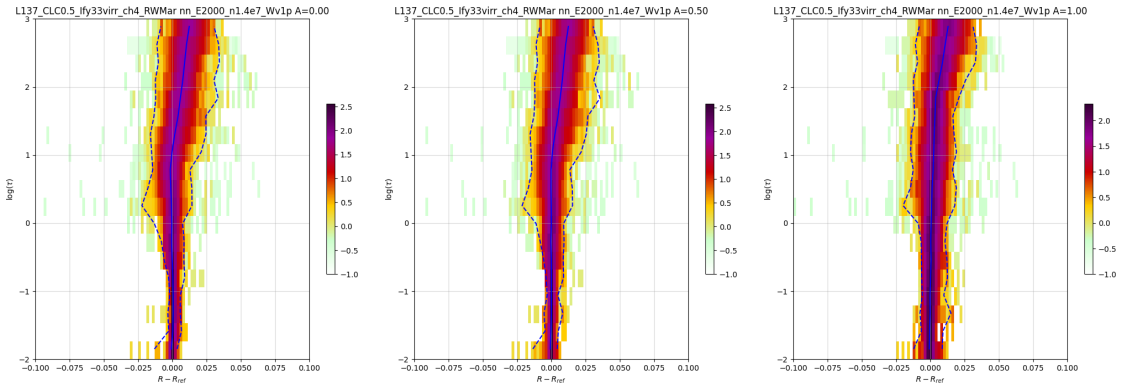

(a) (b) (c)

Figure 69: MFASIS $\Delta r_{\mathrm{MFASIS}-ref}$ as function of the cloud optical depth τ at albedo(s) of 0.00, 0.50, 1.00 (from left to right) for the instrument: FY3 3 VIRR CH4

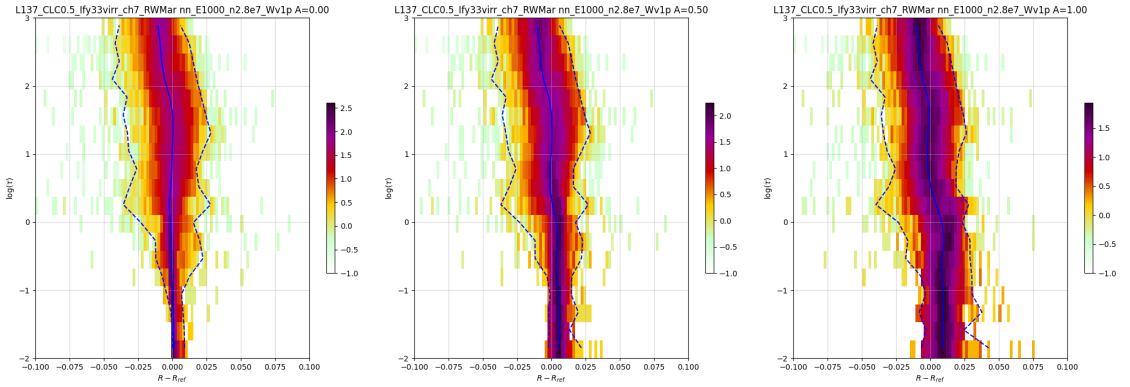

(a) (b) (c)

Figure 70: MFASIS $\Delta r_{\mathrm{MFASIS}-ref}$ as function of the cloud optical depth τ at albedo(s) of 0.00, 0.50, 1.00 (from left to right) for the instrument: FY3 3 VIRR CH7

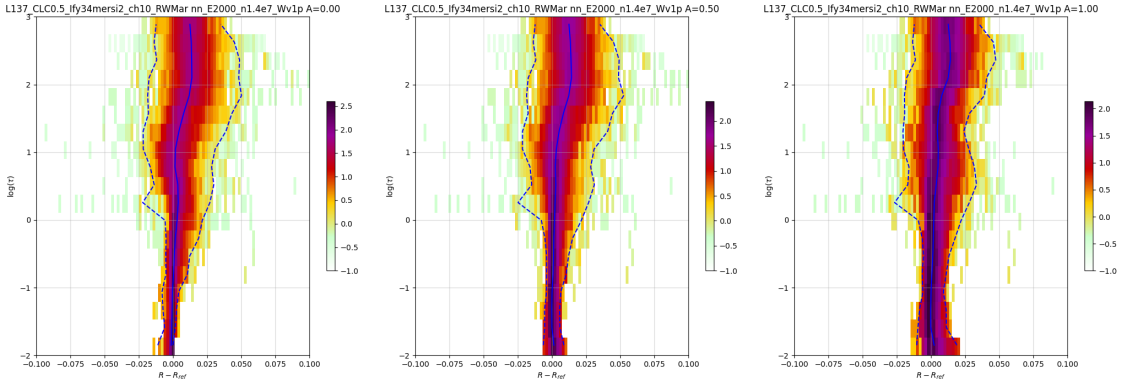

(a) (b) (c)

Figure 71: MFASIS $\Delta r_{\mathrm{MFASIS}-ref}$ as function of the cloud optical depth τ at albedo(s) of 0.00, 0.50, 1.00 (from left to right) for the instrument: FY3 4 MERSI2 CH10

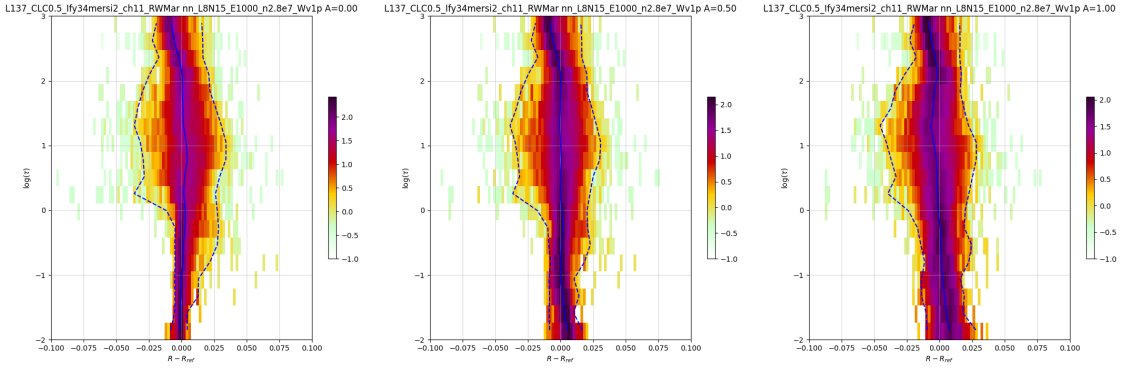

(a) (b) (c)

Figure 72: MFASIS $\Delta r_{\mathrm{MFASIS}-ref}$ as function of the cloud optical depth τ at albedo(s) of 0.00, 0.50, 1.00 (from left to right) for the instrument: FY3 4 MERSI2 CH11

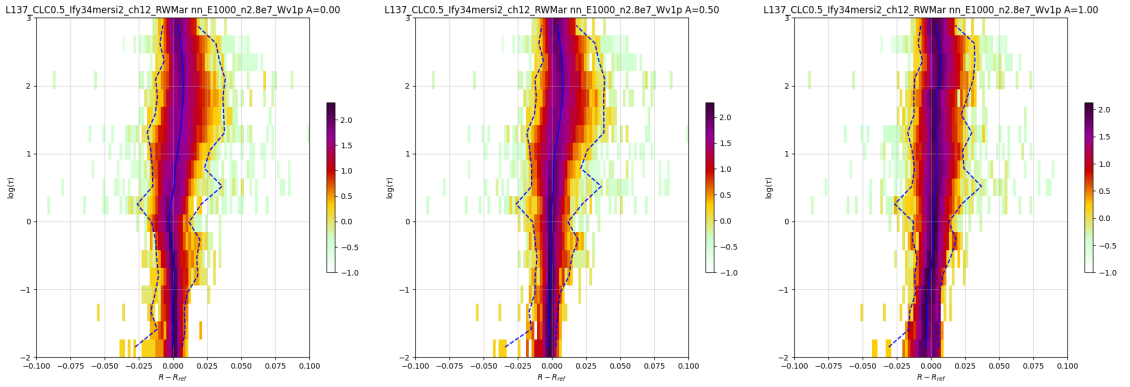

(a) (b) (c)

Figure 73: MFASIS $\Delta r_{\mathrm{MFASIS}-ref}$ as function of the cloud optical depth τ at albedo(s) of 0.00, 0.50, 1.00 (from left to right) for the instrument: FY3 4 MERSI2 CH12

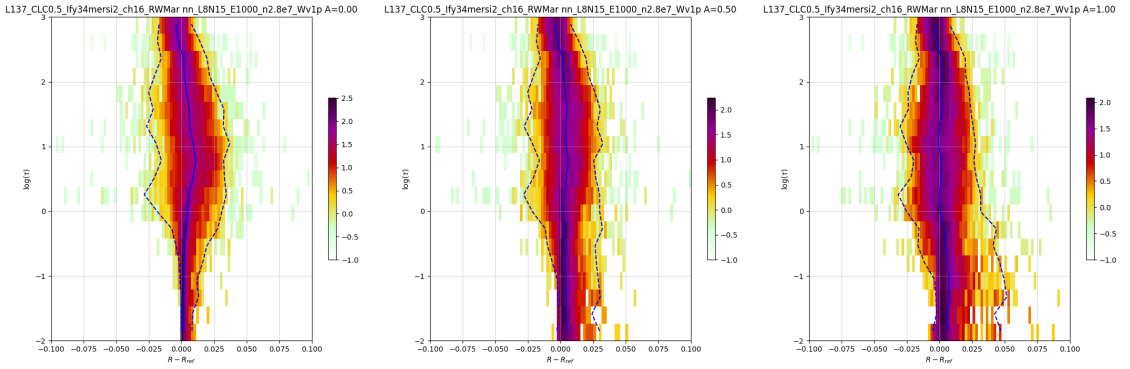

(a) (b) (c)

Figure 74: MFASIS $\Delta r_{\mathrm{MFASIS}-ref}$ as function of the cloud optical depth τ at albedo(s) of 0.00, 0.50, 1.00 (from left to right) for the instrument: FY3 4 MERSI2 CH16

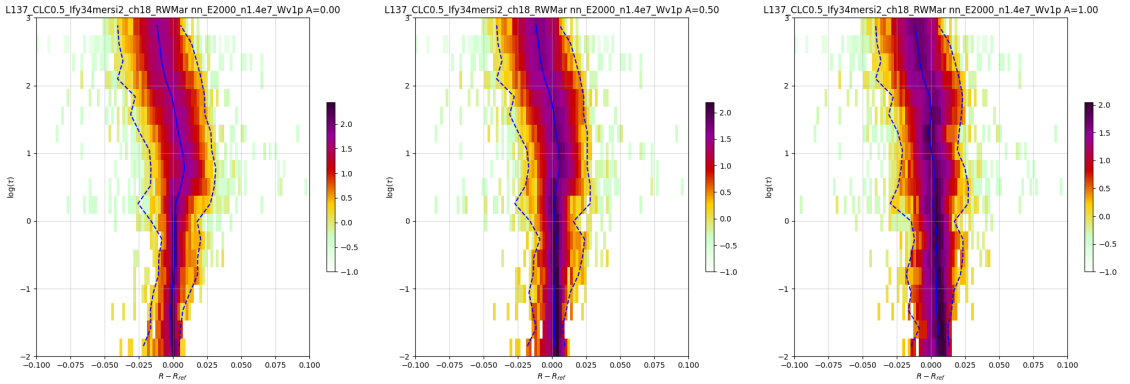

(a) (b) (c)

Figure 75: MFASIS $\Delta r_{\mathrm{MFASIS}-ref}$ as function of the cloud optical depth τ at albedo(s) of 0.00, 0.50, 1.00 (from left to right) for the instrument: FY3 4 MERSI2 CH18

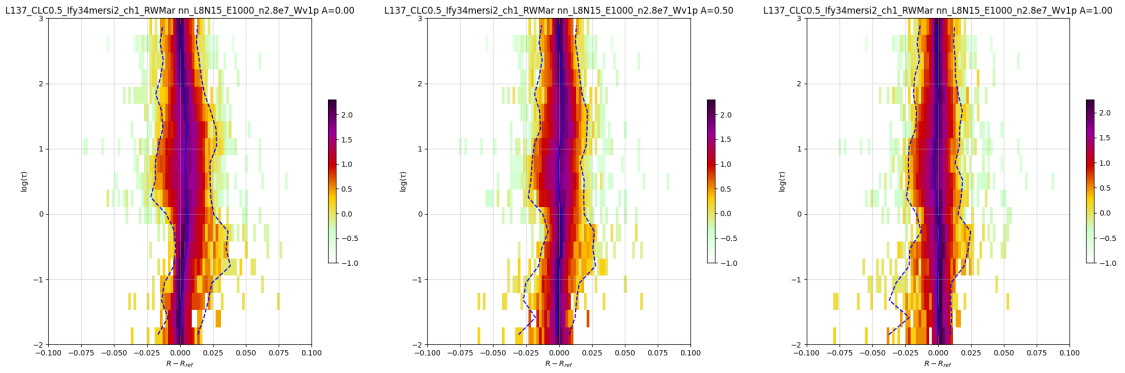

(a) (b) (c)

Figure 76: MFASIS $\Delta r_{\mathrm{MFASIS}-ref}$ as function of the cloud optical depth τ at albedo(s) of 0.00, 0.50, 1.00 (from left to right) for the instrument: FY3 4 MERSI2 CH1

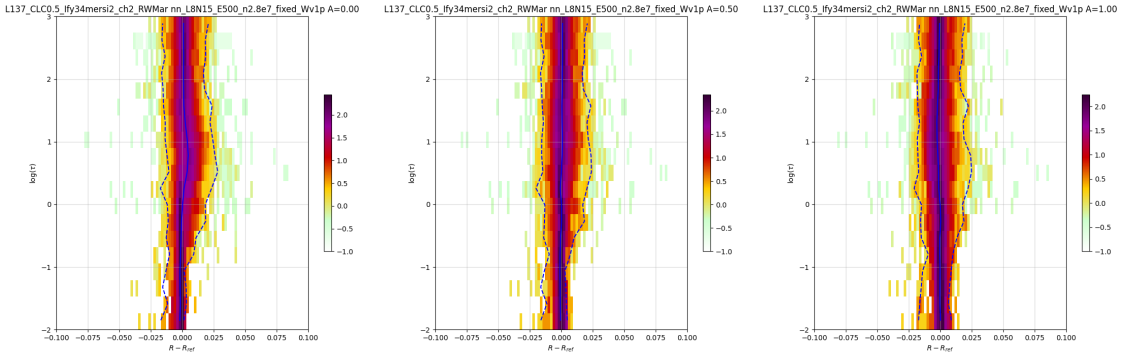

(a) (b) (c)

Figure 77: MFASIS $\Delta r_{\mathrm{MFASIS}-ref}$ as function of the cloud optical depth τ at albedo(s) of 0.00, 0.50, 1.00 (from left to right) for the instrument: FY3 4 MERSI2 CH2

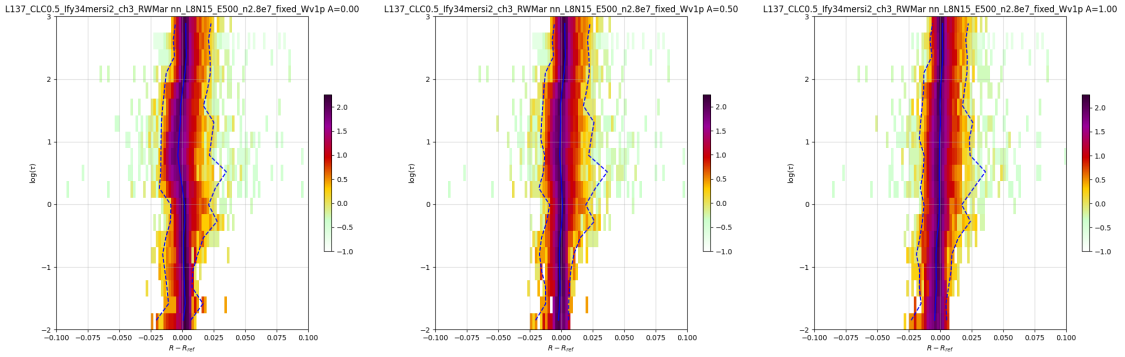

(a) (b) (c)

Figure 78: MFASIS $\Delta r_{\mathrm{MFASIS}-ref}$ as function of the cloud optical depth τ at albedo(s) of 0.00, 0.50, 1.00 (from left to right) for the instrument: FY3 4 MERSI2 CH3

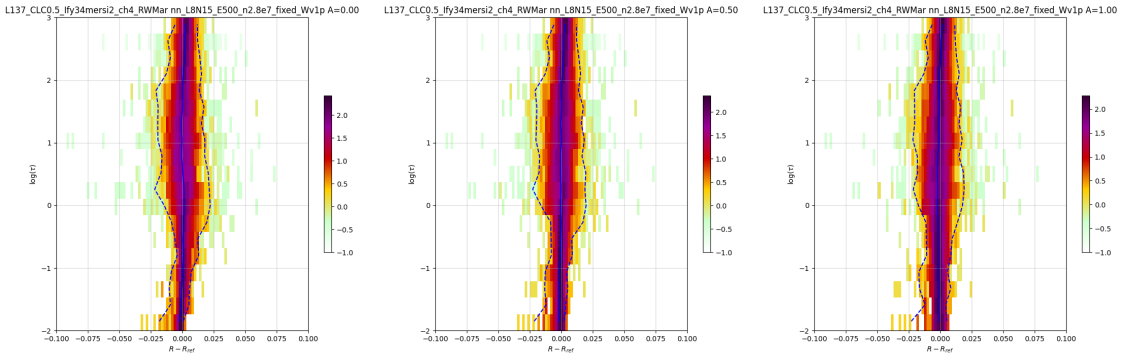

(a) (b) (c)

Figure 79: MFASIS $\Delta r_{\mathrm{MFASIS}-ref}$ as function of the cloud optical depth τ at albedo(s) of 0.00, 0.50, 1.00 (from left to right) for the instrument: FY3 4 MERSI2 CH4

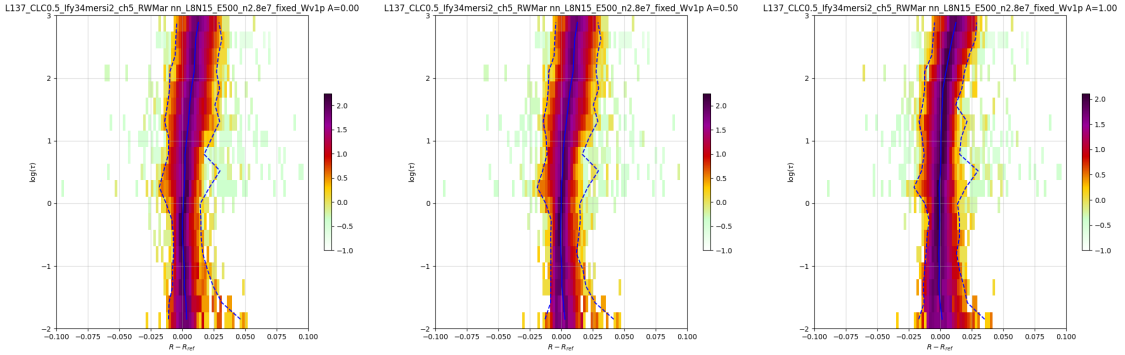

(a) (b) (c)

Figure 80: MFASIS $\Delta r_{\mathrm{MFASIS}-ref}$ as function of the cloud optical depth τ at albedo(s) of 0.00, 0.50, 1.00 (from left to right) for the instrument: FY3 4 MERSI2 CH5

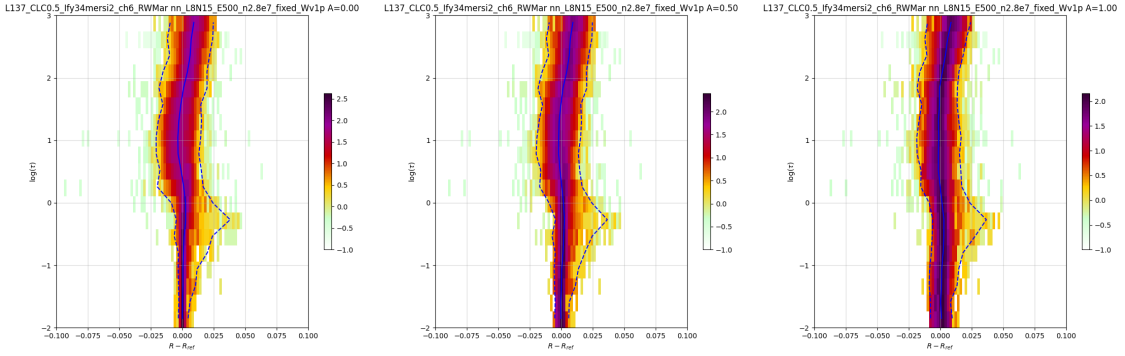

(a) (b) (c)

Figure 81: MFASIS $\Delta r_{\mathrm{MFASIS}-ref}$ as function of the cloud optical depth τ at albedo(s) of 0.00, 0.50, 1.00 (from left to right) for the instrument: FY3 4 MERSI2 CH6

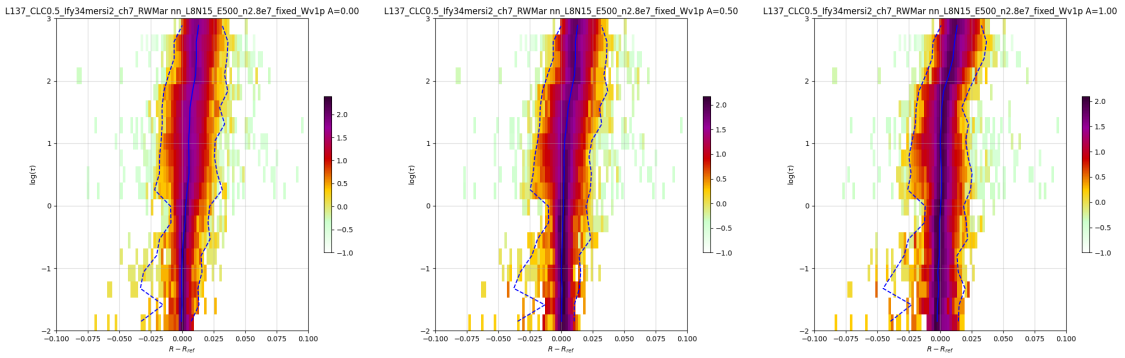

(a) (b) (c)

Figure 82: MFASIS $\Delta r_{\mathrm{MFASIS}-ref}$ as function of the cloud optical depth τ at albedo(s) of 0.00, 0.50, 1.00 (from left to right) for the instrument: FY3 4 MERSI2 CH7

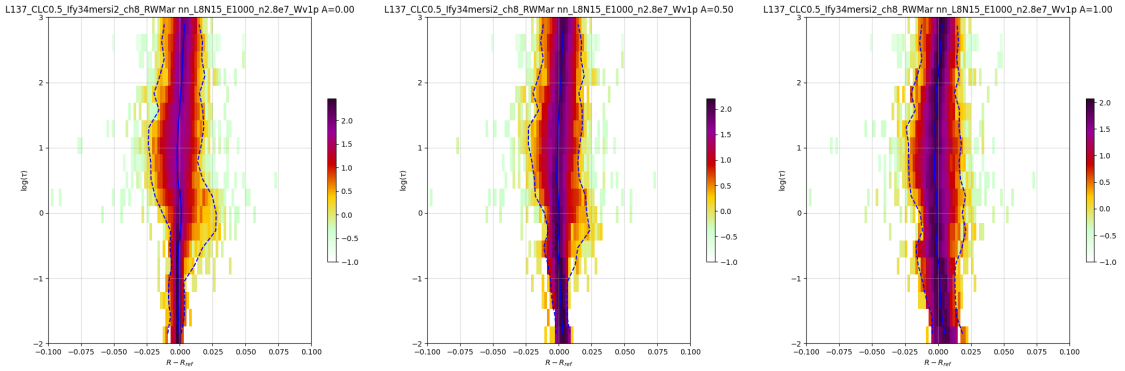

(a) (b) (c)

Figure 83: MFASIS $\Delta r_{\mathrm{MFASIS}-ref}$ as function of the cloud optical depth τ at albedo(s) of 0.00, 0.50, 1.00 (from left to right) for the instrument: FY3 4 MERSI2 CH8

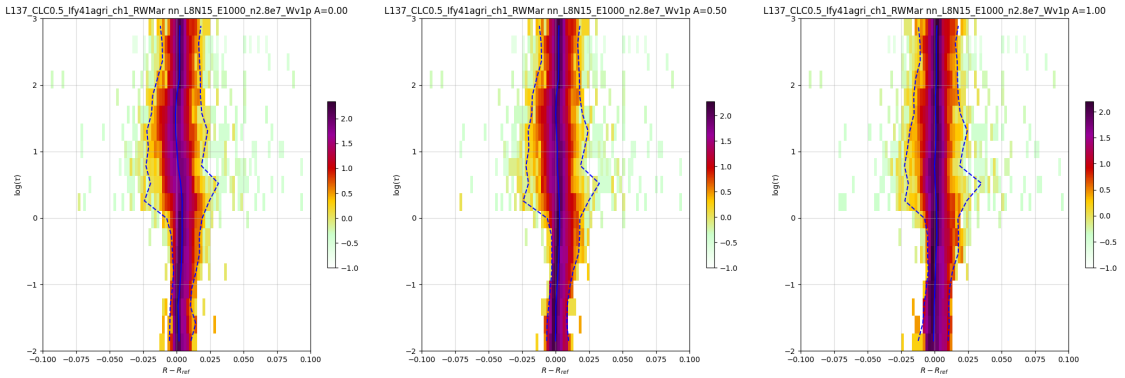

(a) (b) (c)

Figure 84: MFASIS $\Delta r_{\mathrm{MFASIS}-ref}$ as function of the cloud optical depth τ at albedo(s) of 0.00, 0.50, 1.00 (from left to right) for the instrument: FY4 1 AGRI CH1

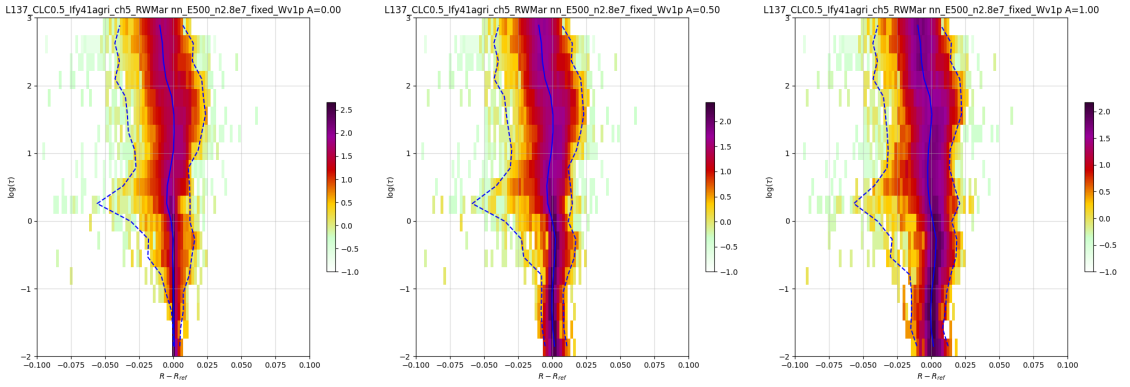

(a) (b) (c)

Figure 85: MFASIS $\Delta r_{\mathrm{MFASIS}-ref}$ as function of the cloud optical depth τ at albedo(s) of 0.00, 0.50, 1.00 (from left to right) for the instrument: FY4 1 AGRI CH5

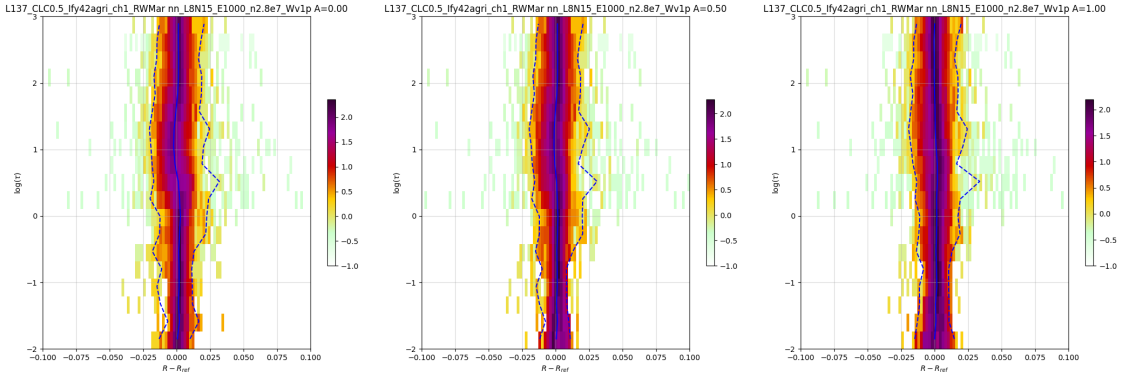

(a) (b) (c)

Figure 86: MFASIS $\Delta r_{\mathrm{MFASIS}-ref}$ as function of the cloud optical depth τ at albedo(s) of 0.00, 0.50, 1.00 (from left to right) for the instrument: FY4 2 AGRI CH1

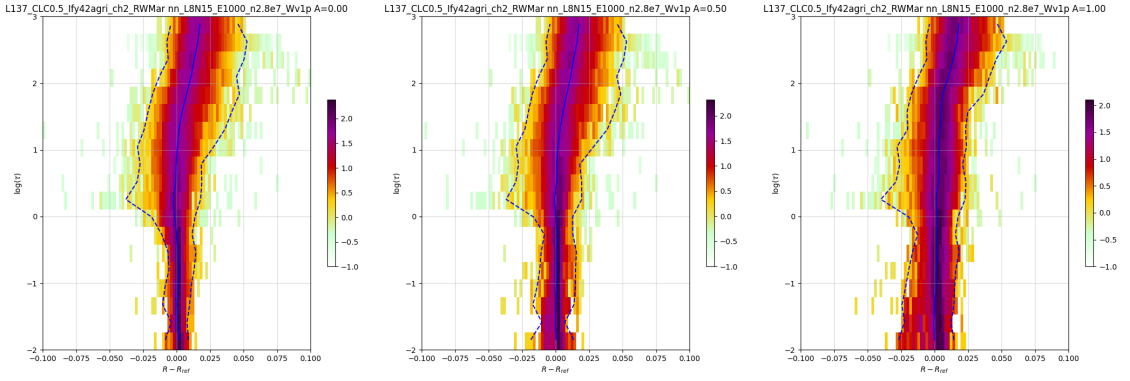

(a) (b) (c)

Figure 87: MFASIS $\Delta r_{\mathrm{MFASIS}-ref}$ as function of the cloud optical depth τ at albedo(s) of 0.00, 0.50, 1.00 (from left to right) for the instrument: FY4 2 AGRI CH2

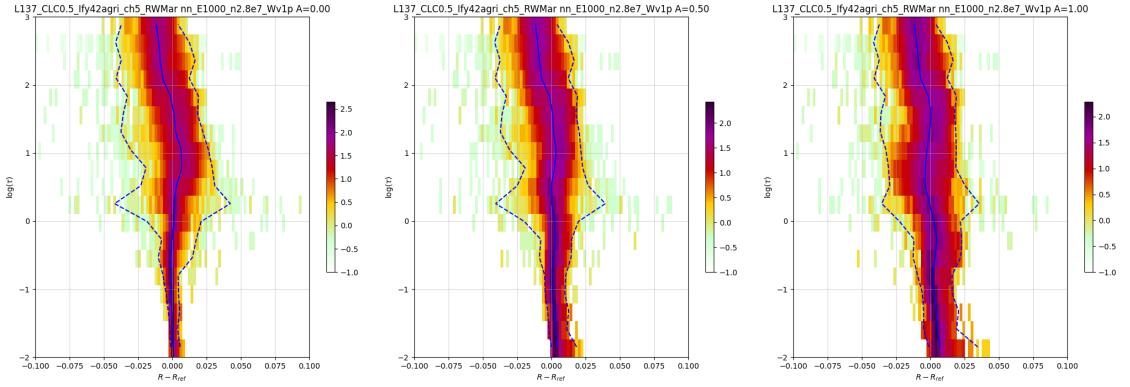

(a) (b) (c)

Figure 88: MFASIS $\Delta r_{\mathrm{MFASIS}-ref}$ as function of the cloud optical depth τ at albedo(s) of 0.00, 0.50, 1.00 (from left to right) for the instrument: FY4 2 AGRI CH5

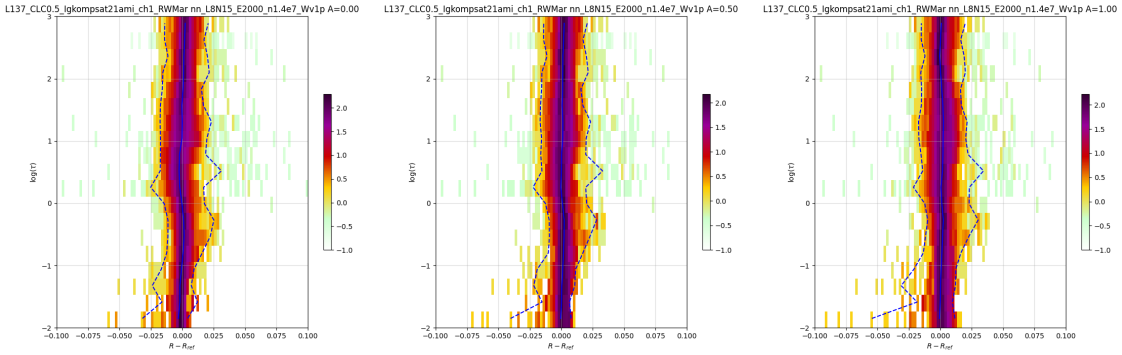

(a) (b) (c)

Figure 89: MFASIS $\Delta r_{\mathrm{MFASIS}-ref}$ as function of the cloud optical depth τ at albedo(s) of 0.00, 0.50, 1.00 (from left to right) for the instrument: GKOMPSAT2 1 AMI CH1

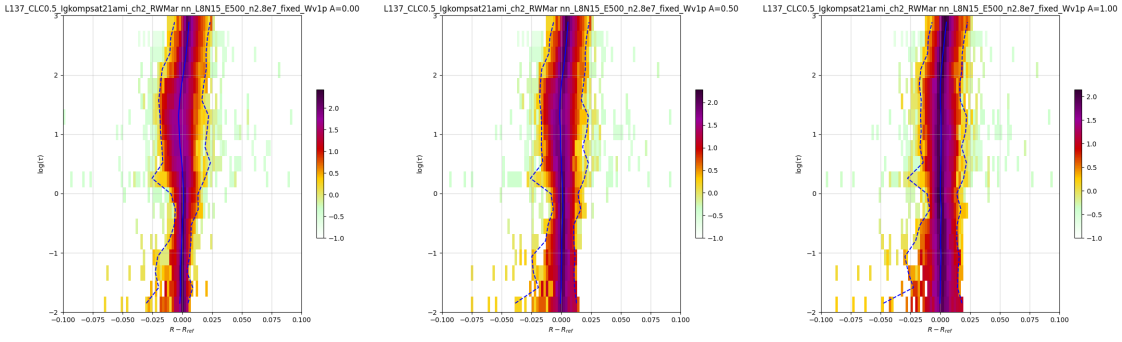

(a) (b) (c)

Figure 90: MFASIS $\Delta r_{\mathrm{MFASIS}-ref}$ as function of the cloud optical depth τ at albedo(s) of 0.00, 0.50, 1.00 (from left to right) for the instrument: GKOMPSAT2 1 AMI CH2

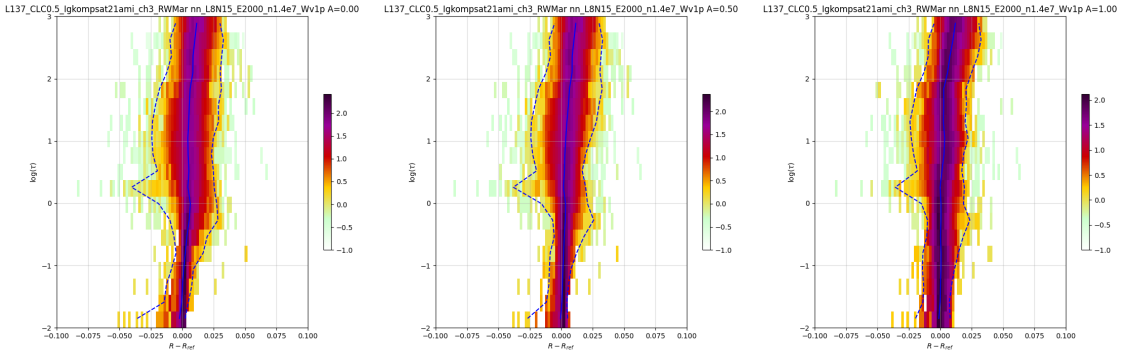

(a) (b) (c)

Figure 91: MFASIS $\Delta r_{\mathrm{MFASIS}-ref}$ as function of the cloud optical depth τ at albedo(s) of 0.00, 0.50, 1.00 (from left to right) for the instrument: GKOMPSAT2 1 AMI CH3

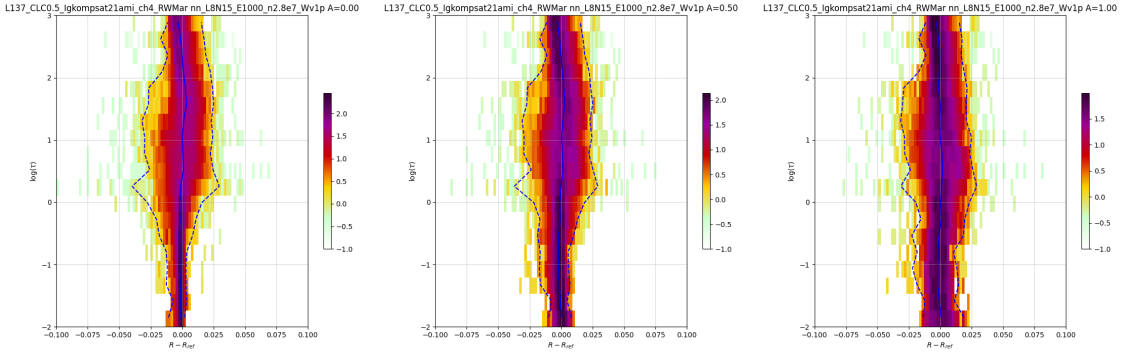

(a) (b) (c)

Figure 92: MFASIS $\Delta r_{\mathrm{MFASIS}-ref}$ as function of the cloud optical depth τ at albedo(s) of 0.00, 0.50, 1.00 (from left to right) for the instrument: GKOMPSAT2 1 AMI CH4

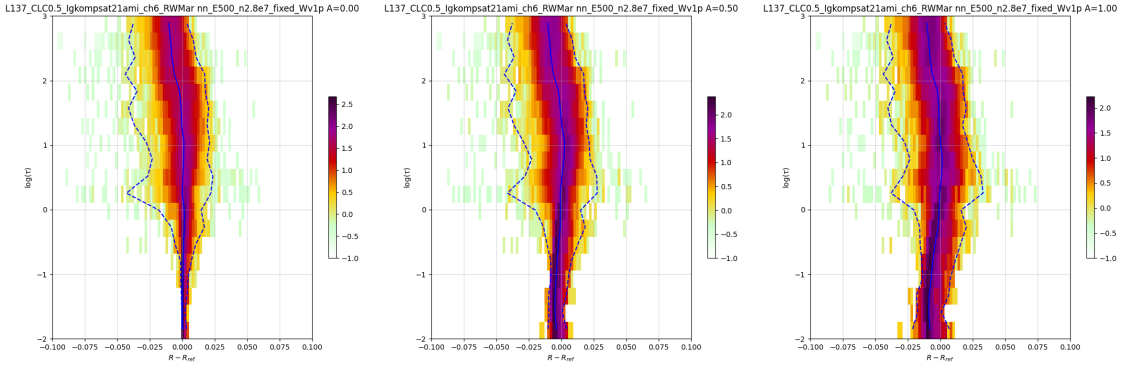

(a) (b) (c)

Figure 93: MFASIS $\Delta r_{\mathrm{MFASIS}-ref}$ as function of the cloud optical depth τ at albedo(s) of 0.00, 0.50, 1.00 (from left to right) for the instrument: GKOMPSAT2 1 AMI CH6

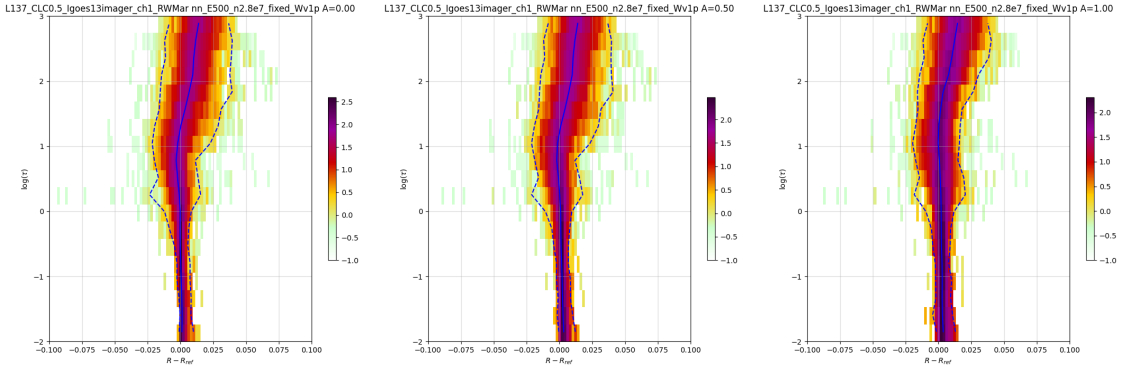

(a) (b) (c)

Figure 94: MFASIS $\Delta r_{\mathrm{MFASIS}-ref}$ as function of the cloud optical depth τ at albedo(s) of 0.00, 0.50, 1.00 (from left to right) for the instrument: GOES 13 IMAGER CH1

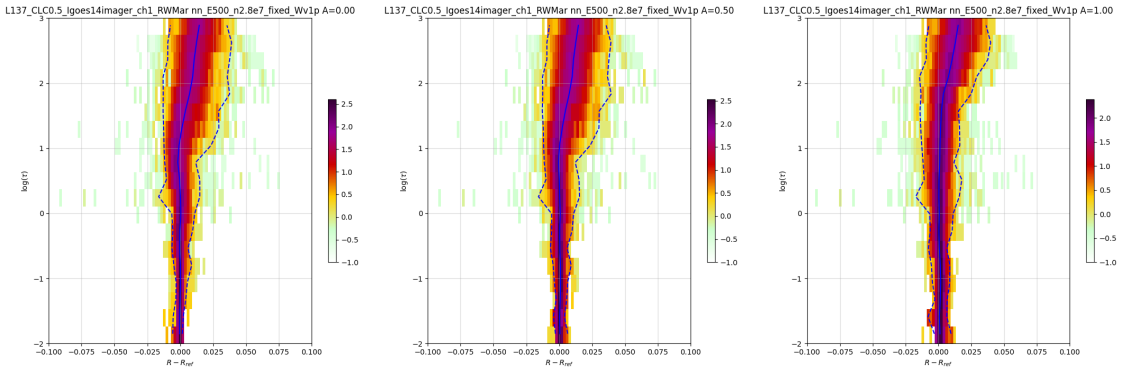

(a) (b) (c)

Figure 95: MFASIS $\Delta r_{\mathrm{MFASIS}-ref}$ as function of the cloud optical depth τ at albedo(s) of 0.00, 0.50, 1.00 (from left to right) for the instrument: GOES 14 IMAGER CH1

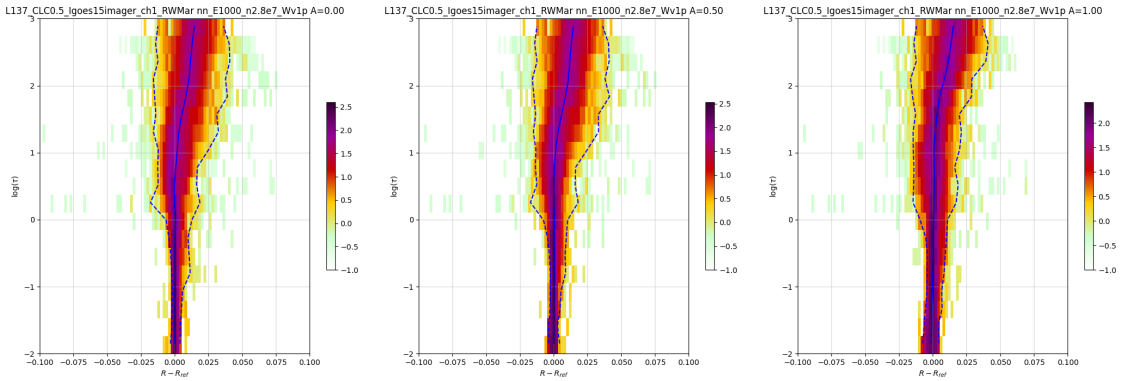

(a) (b) (c)

Figure 96: MFASIS $\Delta r_{\mathrm{MFASIS}-ref}$ as function of the cloud optical depth τ at albedo(s) of 0.00, 0.50, 1.00 (from left to right) for the instrument: GOES 15 IMAGER CH1

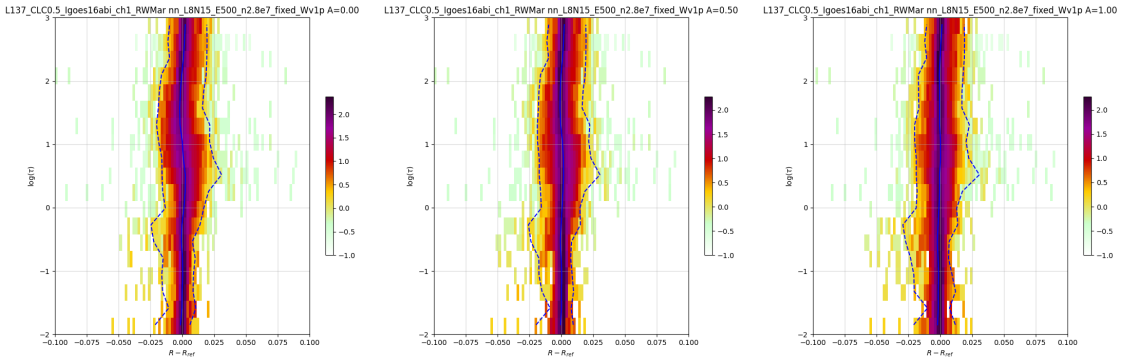

(a) (b) (c)

Figure 97: MFASIS $\Delta r_{\mathrm{MFASIS}-ref}$ as function of the cloud optical depth τ at albedo(s) of 0.00, 0.50, 1.00 (from left to right) for the instrument: GOES 16 ABI CH1

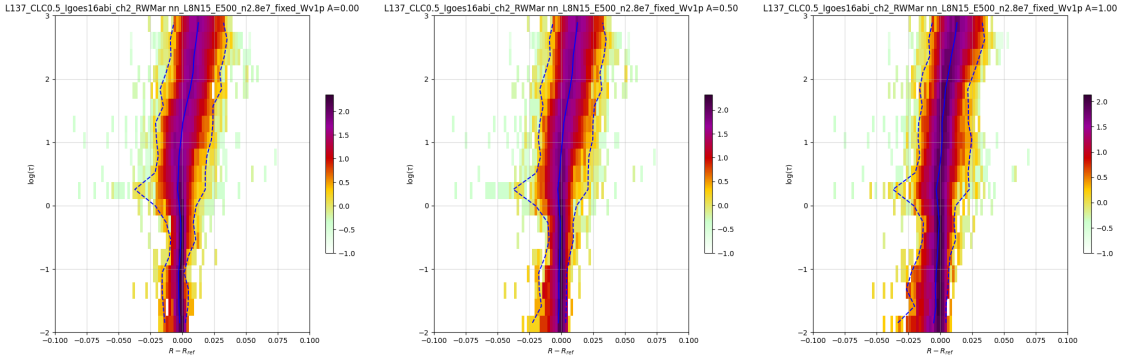

(a) (b) (c)

Figure 98: MFASIS $\Delta r_{\mathrm{MFASIS}-ref}$ as function of the cloud optical depth τ at albedo(s) of 0.00, 0.50, 1.00 (from left to right) for the instrument: GOES 16 ABI CH2

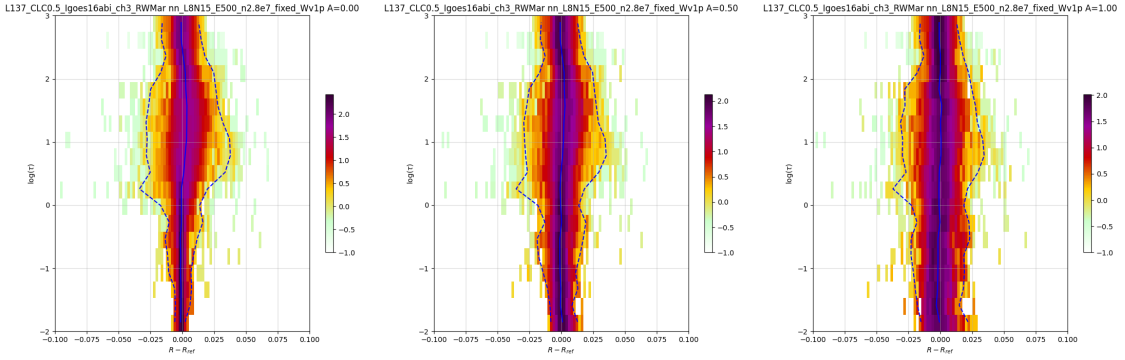

(a) (b) (c)

Figure 99: MFASIS $\Delta r_{\mathrm{MFASIS}-ref}$ as function of the cloud optical depth τ at albedo(s) of 0.00, 0.50, 1.00 (from left to right) for the instrument: GOES 16 ABI CH3

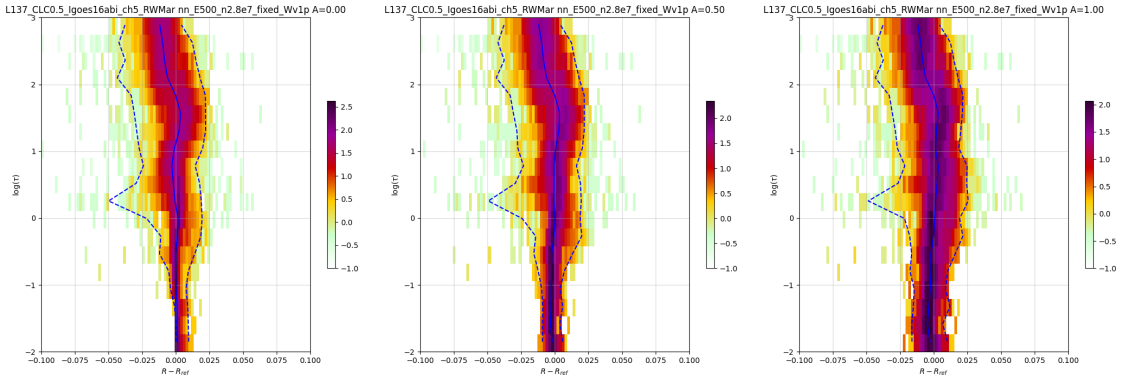

(a) (b) (c)

Figure 100: MFASIS $\Delta r_{\mathrm{MFASIS}-ref}$ as function of the cloud optical depth τ at albedo(s) of 0.00, 0.50, 1.00 (from left to right) for the instrument: GOES 16 ABI CH5

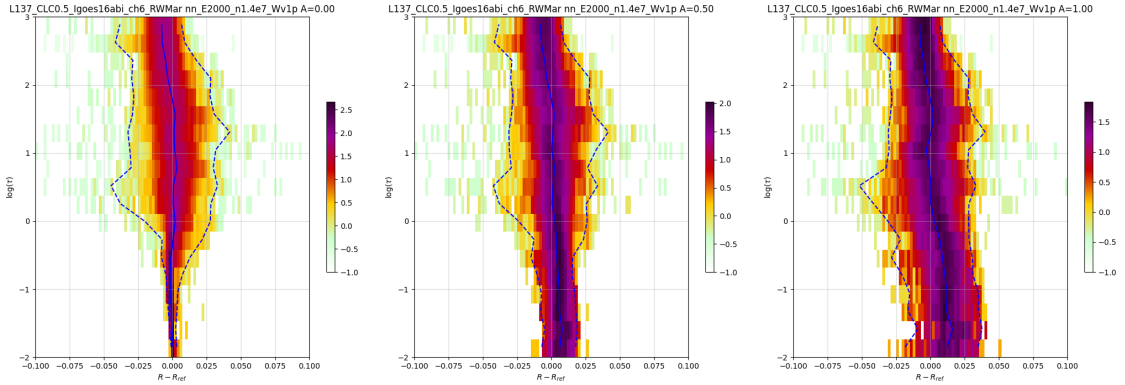

(a) (b) (c)

Figure 101: MFASIS $\Delta r_{\mathrm{MFASIS}-ref}$ as function of the cloud optical depth τ at albedo(s) of 0.00, 0.50, 1.00 (from left to right) for the instrument: GOES 16 ABI CH6

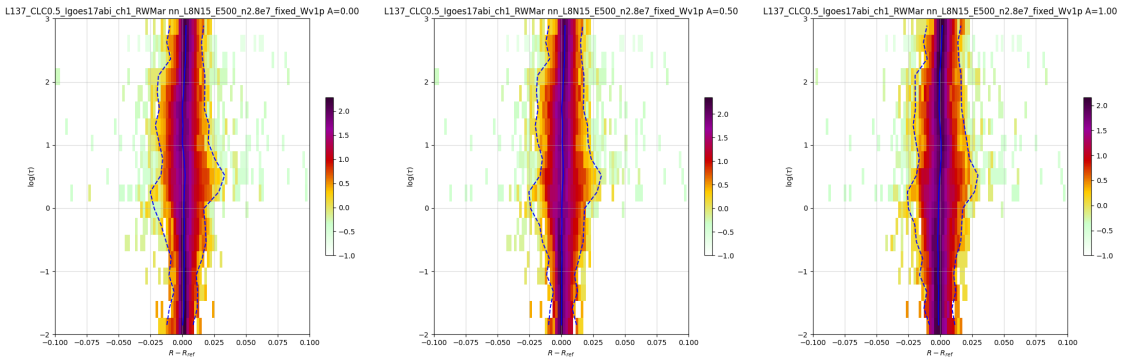

(a) (b) (c)

Figure 102: MFASIS $\Delta r_{\mathrm{MFASIS}-ref}$ as function of the cloud optical depth τ at albedo(s) of 0.00, 0.50, 1.00 (from left to right) for the instrument: GOES 17 ABI CH1

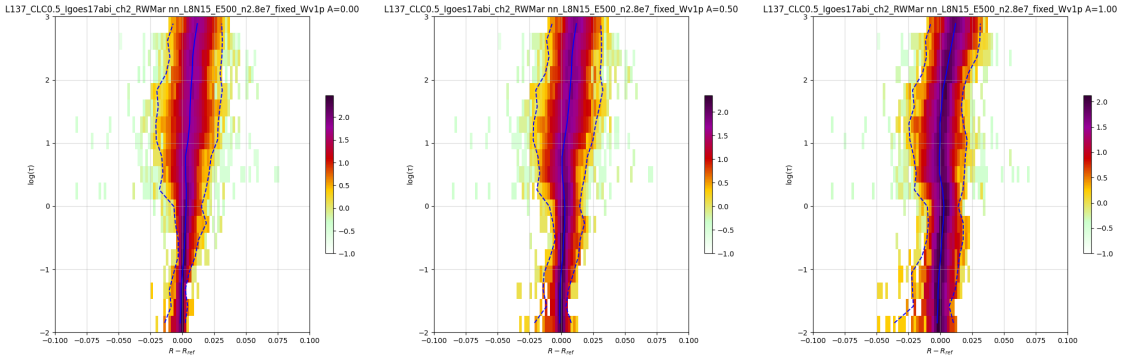

(a) (b) (c)

Figure 103: MFASIS $\Delta r_{\mathrm{MFASIS}-ref}$ as function of the cloud optical depth τ at albedo(s) of 0.00, 0.50, 1.00 (from left to right) for the instrument: GOES 17 ABI CH2

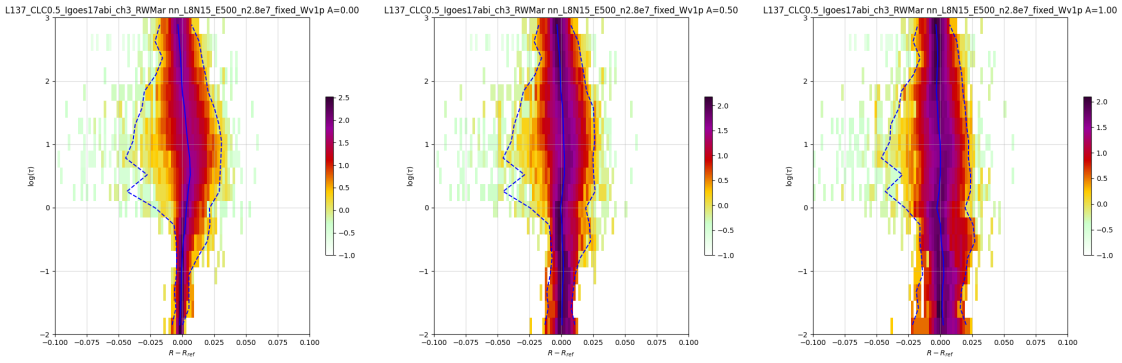

(a) (b) (c)

Figure 104: MFASIS $\Delta r_{\mathrm{MFASIS}-ref}$ as function of the cloud optical depth τ at albedo(s) of 0.00, 0.50, 1.00 (from left to right) for the instrument: GOES 17 ABI CH3

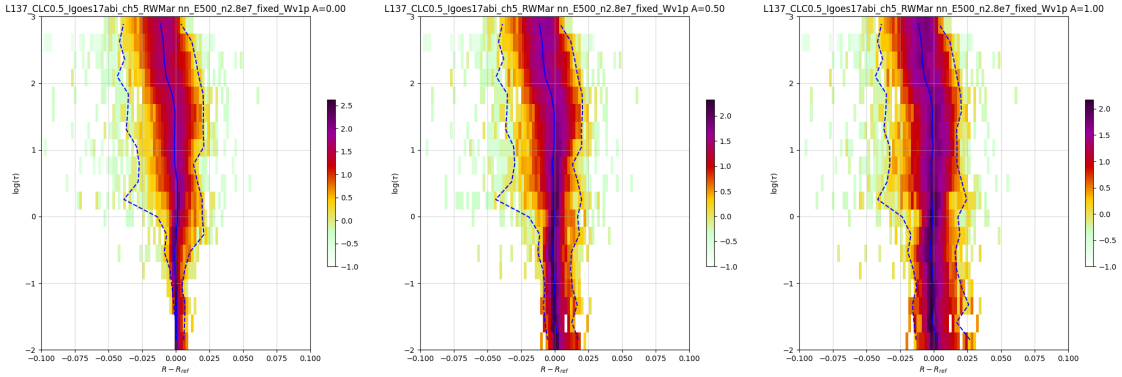

(a) (b) (c)

Figure 105: MFASIS $\Delta r_{\mathrm{MFASIS}-ref}$ as function of the cloud optical depth τ at albedo(s) of 0.00, 0.50, 1.00 (from left to right) for the instrument: GOES 17 ABI CH5

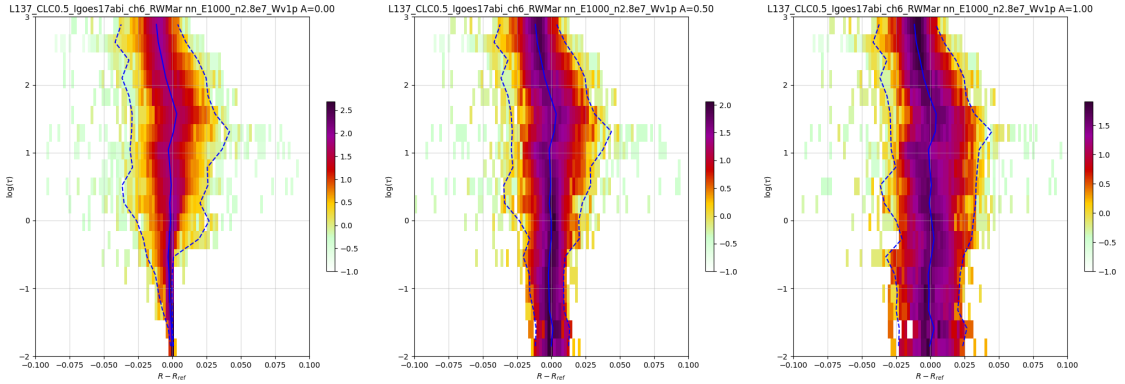

(a) (b) (c)

Figure 106: MFASIS $\Delta r_{\mathrm{MFASIS}-ref}$ as function of the cloud optical depth τ at albedo(s) of 0.00, 0.50, 1.00 (from left to right) for the instrument: GOES 17 ABI CH6

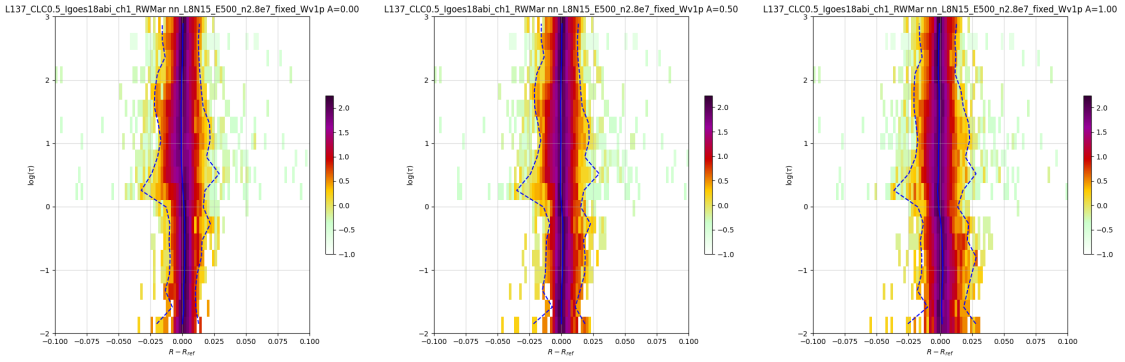

(a) (b) (c)

Figure 107: MFASIS $\Delta r_{\mathrm{MFASIS}-ref}$ as function of the cloud optical depth τ at albedo(s) of 0.00, 0.50, 1.00 (from left to right) for the instrument: GOES 18 ABI CH1

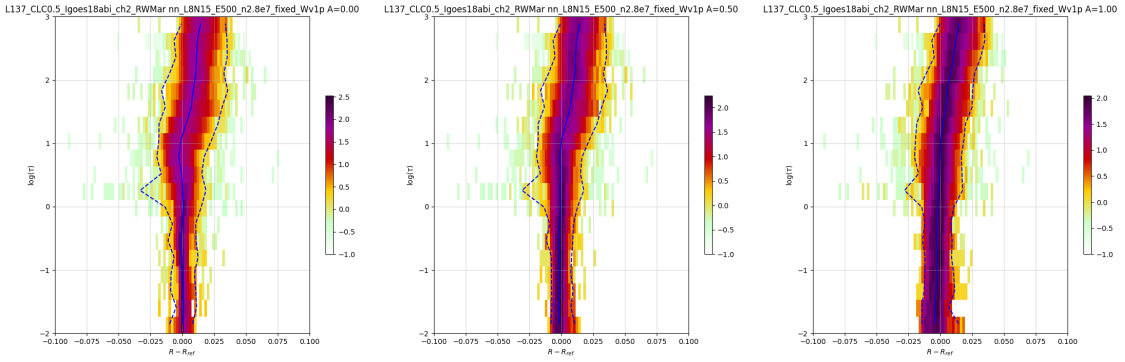

(a) (b) (c)

Figure 108: MFASIS $\Delta r_{\mathrm{MFASIS}-ref}$ as function of the cloud optical depth τ at albedo(s) of 0.00, 0.50, 1.00 (from left to right) for the instrument: GOES 18 ABI CH2

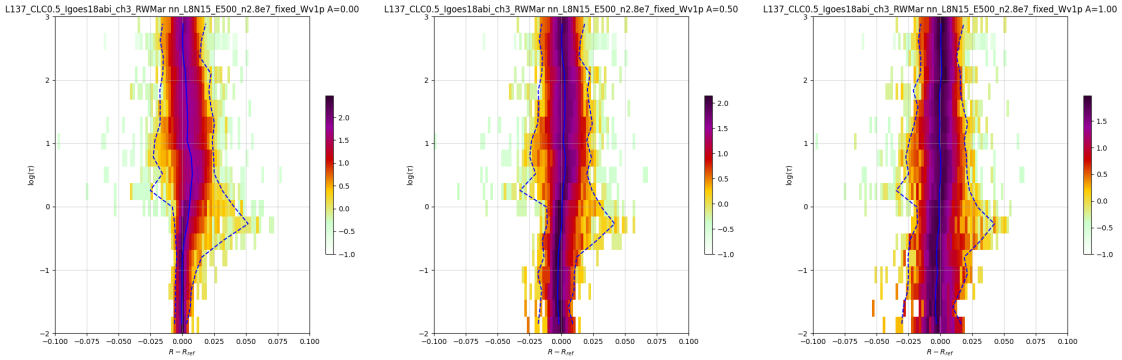

(a) (b) (c)

Figure 109: MFASIS $\Delta r_{\mathrm{MFASIS}-ref}$ as function of the cloud optical depth τ at albedo(s) of 0.00, 0.50, 1.00 (from left to right) for the instrument: GOES 18 ABI CH3

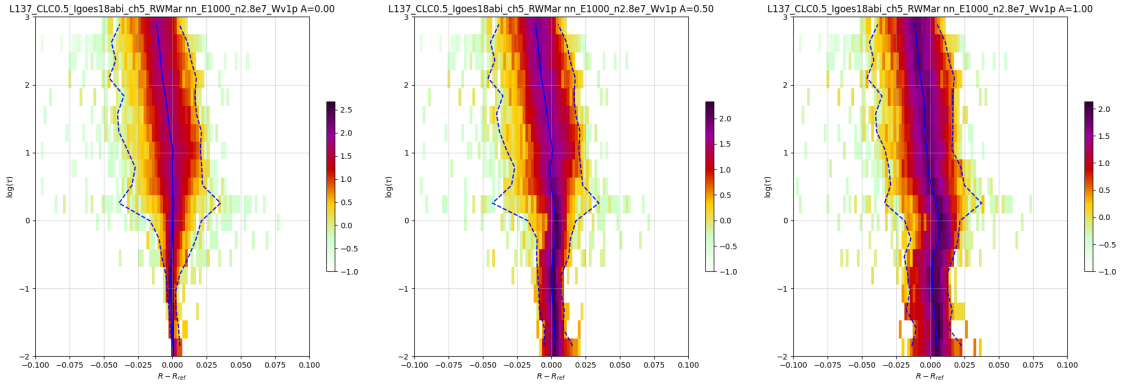

(a) (b) (c)

Figure 110: MFASIS $\Delta r_{\mathrm{MFASIS}-ref}$ as function of the cloud optical depth τ at albedo(s) of 0.00, 0.50, 1.00 (from left to right) for the instrument: GOES 18 ABI CH5

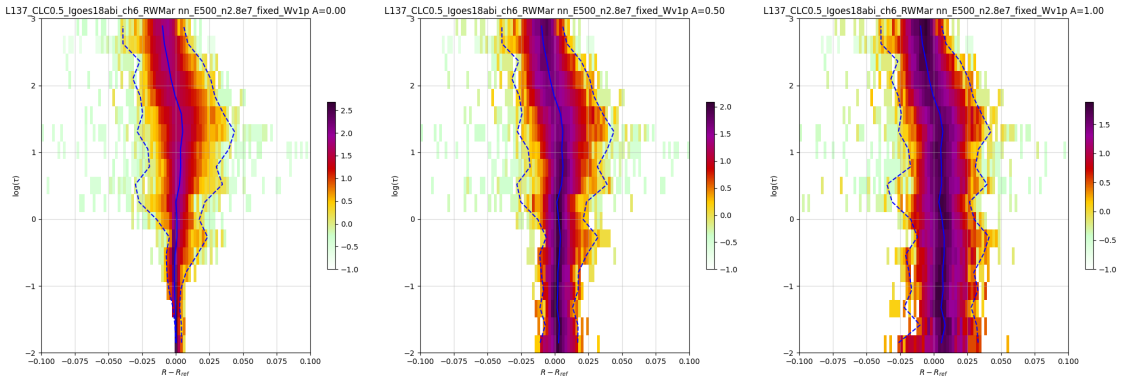

(a) (b) (c)

Figure 111: MFASIS $\Delta r_{\mathrm{MFASIS}-ref}$ as function of the cloud optical depth τ at albedo(s) of 0.00, 0.50, 1.00 (from left to right) for the instrument: GOES 18 ABI CH6

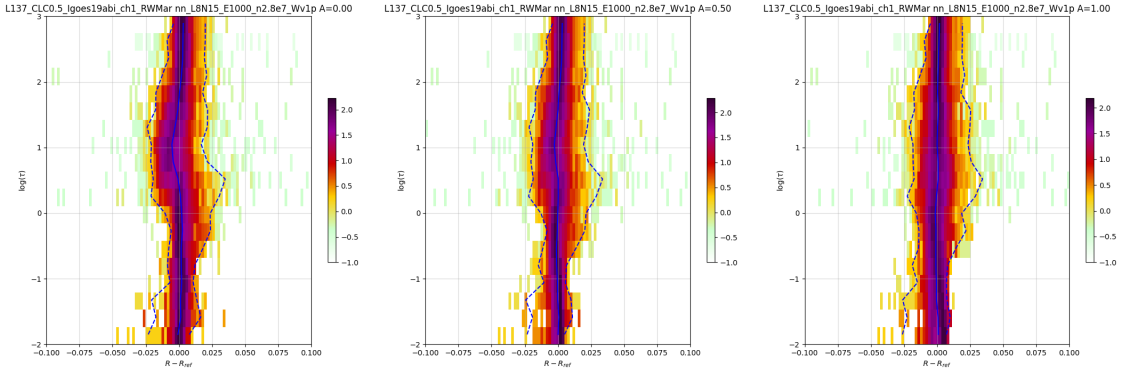

(a) (b) (c)

Figure 112: MFASIS $\Delta r_{\mathrm{MFASIS}-ref}$ as function of the cloud optical depth τ at albedo(s) of 0.00, 0.50, 1.00 (from left to right) for the instrument: GOES 19 ABI CH1

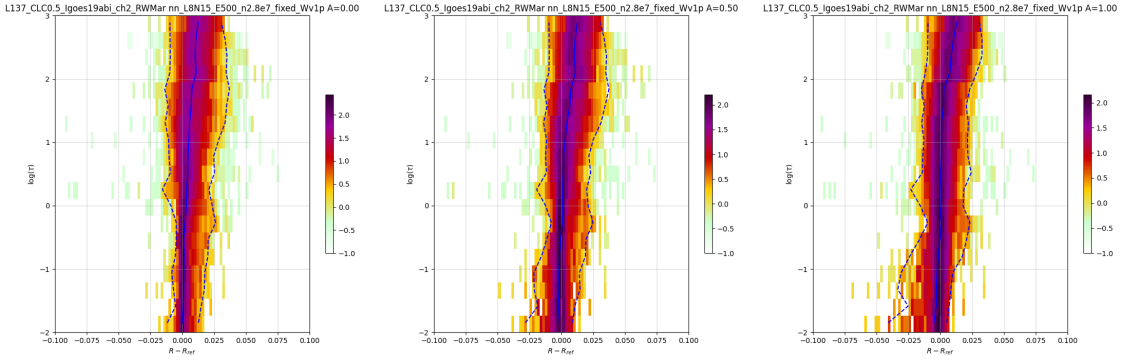

(a) (b) (c)

Figure 113: MFASIS $\Delta r_{\mathrm{MFASIS}-ref}$ as function of the cloud optical depth τ at albedo(s) of 0.00, 0.50, 1.00 (from left to right) for the instrument: GOES 19 ABI CH2

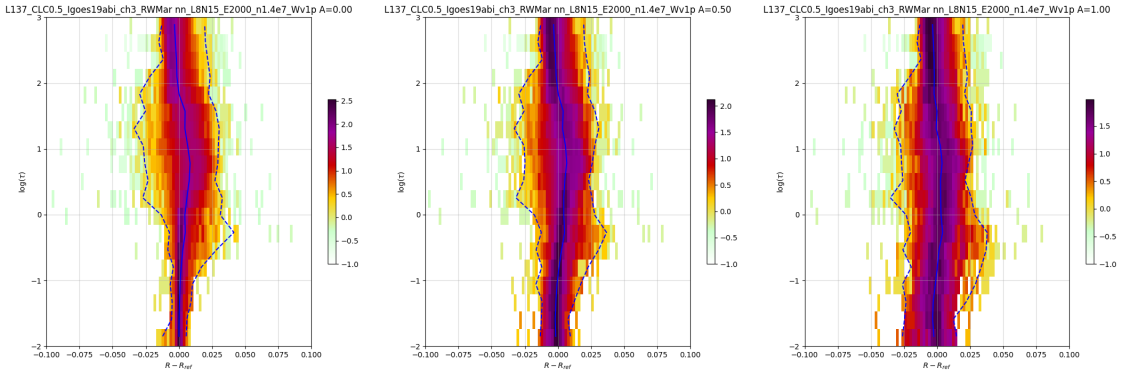

(a) (b) (c)

Figure 114: MFASIS $\Delta r_{\mathrm{MFASIS}-ref}$ as function of the cloud optical depth τ at albedo(s) of 0.00, 0.50, 1.00 (from left to right) for the instrument: GOES 19 ABI CH3

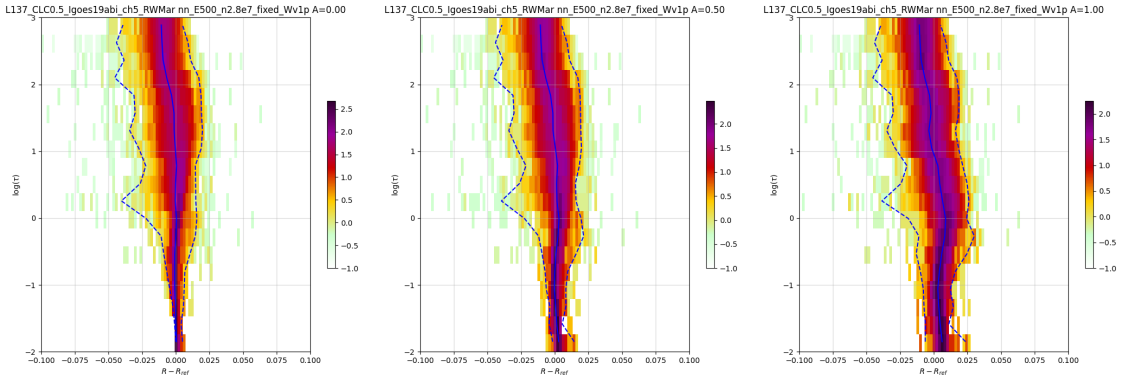

(a) (b) (c)

Figure 115: MFASIS $\Delta r_{\mathrm{MFASIS}-ref}$ as function of the cloud optical depth τ at albedo(s) of 0.00, 0.50, 1.00 (from left to right) for the instrument: GOES 19 ABI CH5

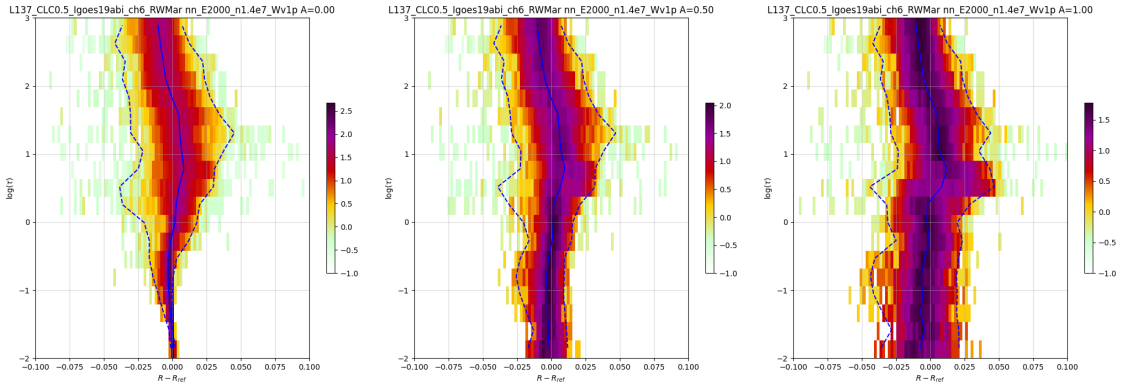

(a) (b) (c)

Figure 116: MFASIS $\Delta r_{\mathrm{MFASIS}-ref}$ as function of the cloud optical depth τ at albedo(s) of 0.00, 0.50, 1.00 (from left to right) for the instrument: GOES 19 ABI CH6

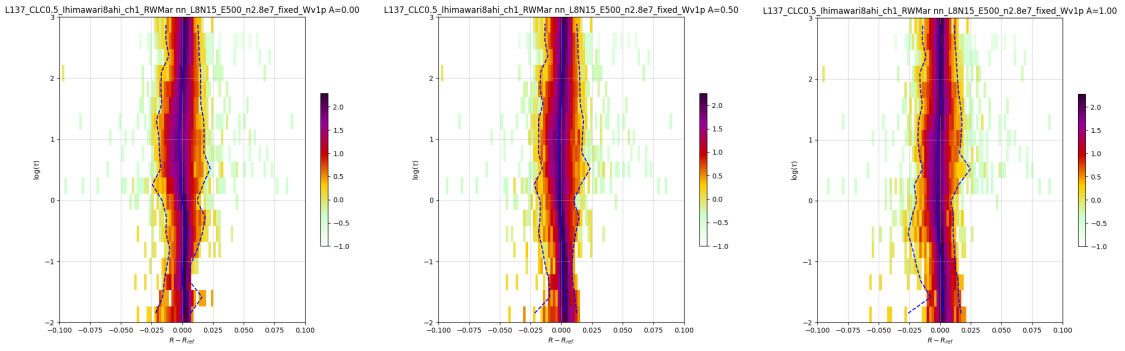

(a) (b) (c)

Figure 117: MFASIS $\Delta r_{\mathrm{MFASIS}-ref}$ as function of the cloud optical depth τ at albedo(s) of 0.00, 0.50, 1.00 (from left to right) for the instrument: HIMAWARI 8 AHI CH1

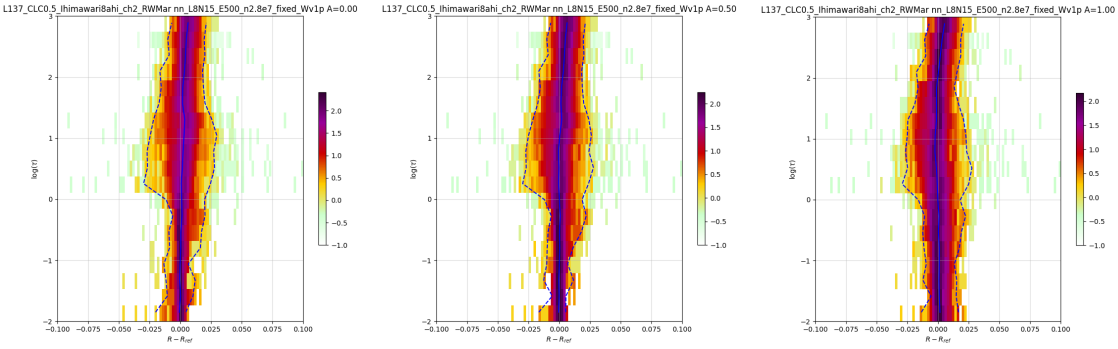

(a) (b) (c)

Figure 118: MFASIS $\Delta r_{\mathrm{MFASIS}-ref}$ as function of the cloud optical depth τ at albedo(s) of 0.00, 0.50, 1.00 (from left to right) for the instrument: HIMAWARI 8 AHI CH2

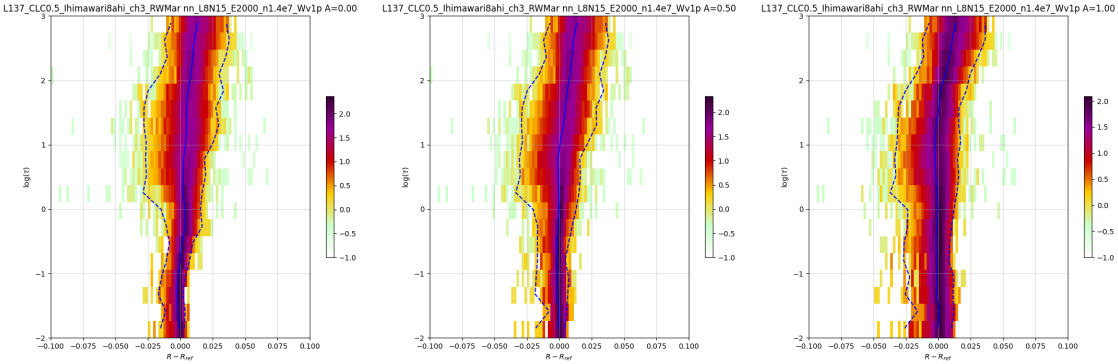

(a) (b) (c)

Figure 119: MFASIS $\Delta r_{\mathrm{MFASIS}-ref}$ as function of the cloud optical depth τ at albedo(s) of 0.00, 0.50, 1.00 (from left to right) for the instrument: HIMAWARI 8 AHI CH3

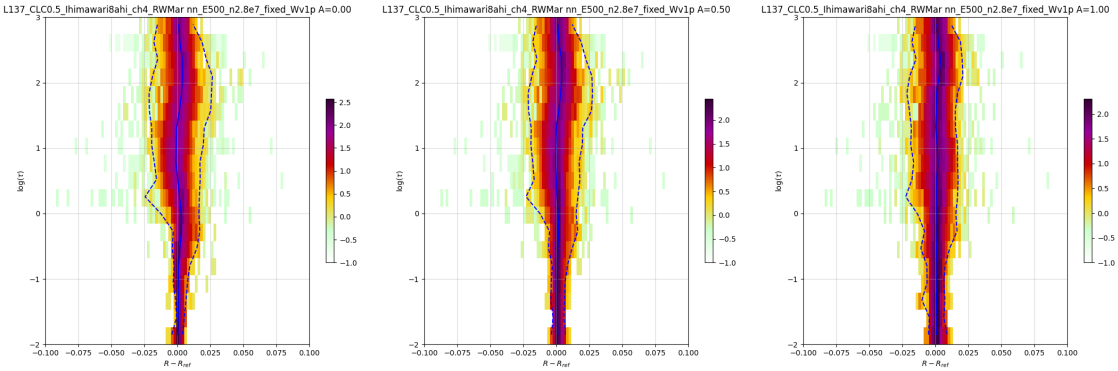

(a) (b) (c)

Figure 120: MFASIS $\Delta r_{\mathrm{MFASIS}-ref}$ as function of the cloud optical depth τ at albedo(s) of 0.00, 0.50, 1.00 (from left to right) for the instrument: HIMAWARI 8 AHI CH4

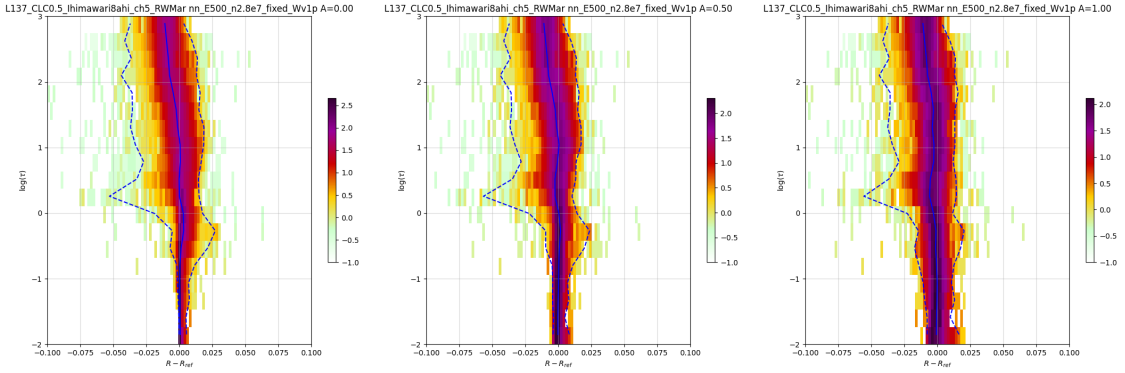

(a) (b) (c)

Figure 121: MFASIS $\Delta r_{\mathrm{MFASIS}-ref}$ as function of the cloud optical depth τ at albedo(s) of 0.00, 0.50, 1.00 (from left to right) for the instrument: HIMAWARI 8 AHI CH5

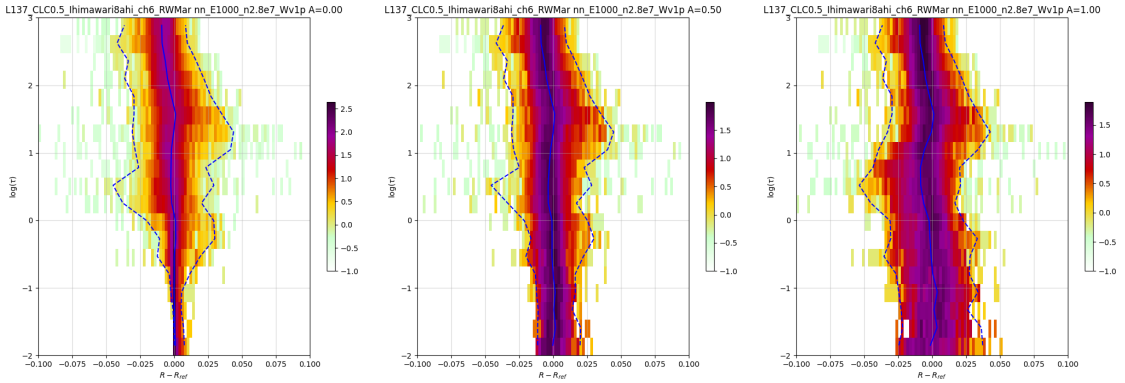

(a) (b) (c)

Figure 122: MFASIS $\Delta r_{\mathrm{MFASIS}-ref}$ as function of the cloud optical depth τ at albedo(s) of 0.00, 0.50, 1.00 (from left to right) for the instrument: HIMAWARI 8 AHI CH6

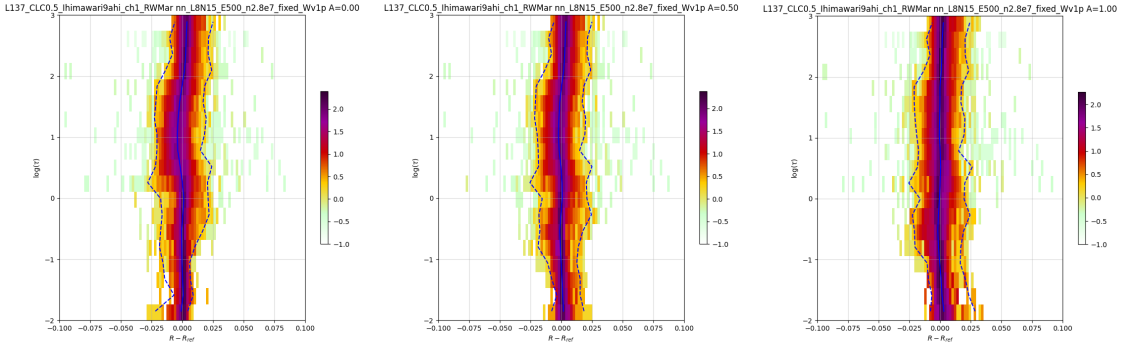

(a) (b) (c)

Figure 123: MFASIS $\Delta r_{\mathrm{MFASIS}-ref}$ as function of the cloud optical depth τ at albedo(s) of 0.00, 0.50, 1.00 (from left to right) for the instrument: HIMAWARI 9 AHI CH1

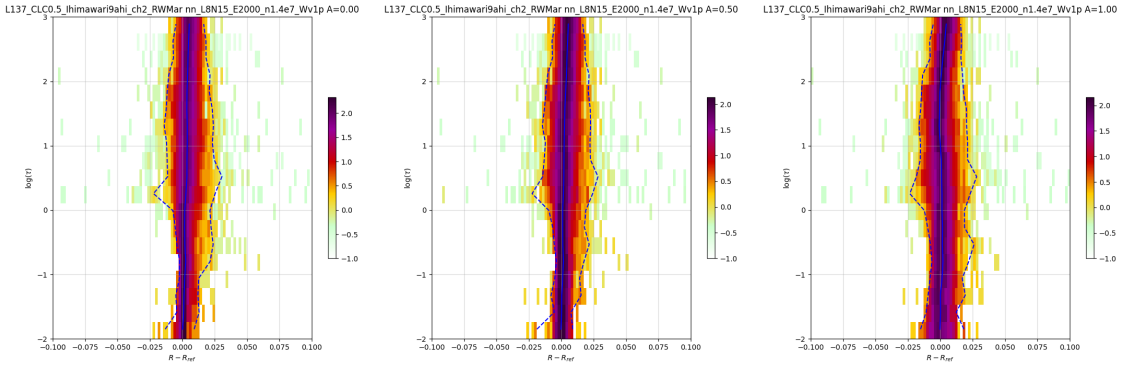

(a) (b) (c)

Figure 124: MFASIS $\Delta r_{\mathrm{MFASIS}-ref}$ as function of the cloud optical depth τ at albedo(s) of 0.00, 0.50, 1.00 (from left to right) for the instrument: HIMAWARI 9 AHI CH2

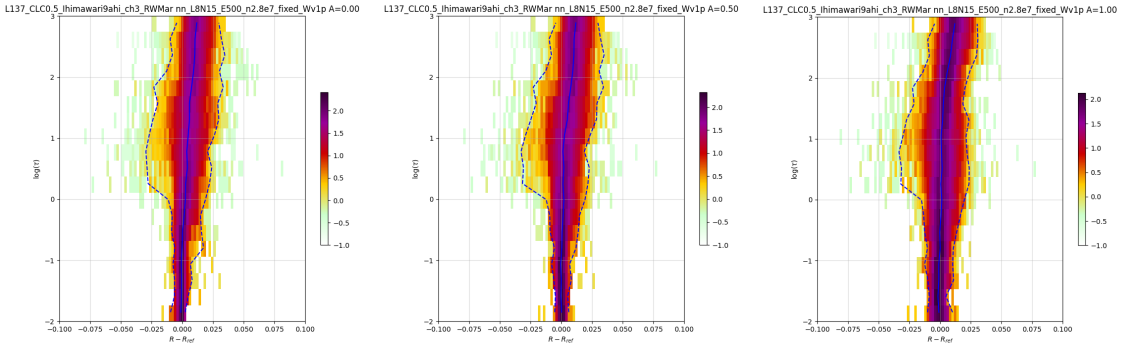

(a) (b) (c)

Figure 125: MFASIS $\Delta r_{\mathrm{MFASIS}-ref}$ as function of the cloud optical depth τ at albedo(s) of 0.00, 0.50, 1.00 (from left to right) for the instrument: HIMAWARI 9 AHI CH3

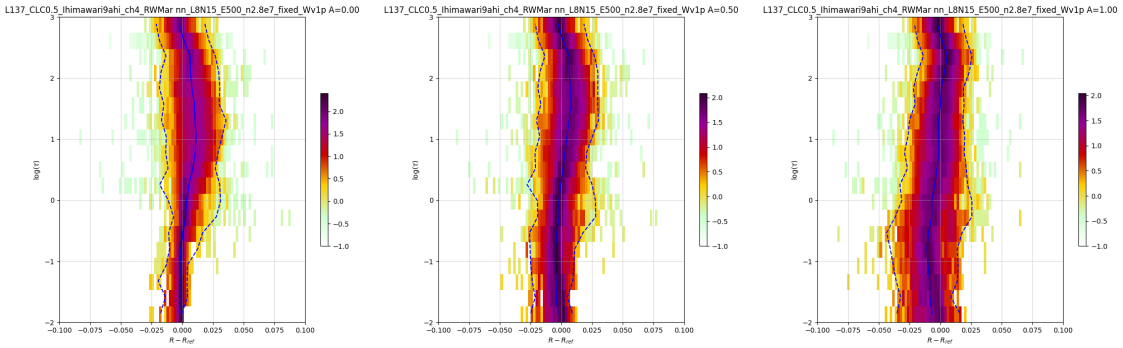

(a) (b) (c)

Figure 126: MFASIS $\Delta r_{\mathrm{MFASIS}-ref}$ as function of the cloud optical depth τ at albedo(s) of 0.00, 0.50, 1.00 (from left to right) for the instrument: HIMAWARI 9 AHI CH4

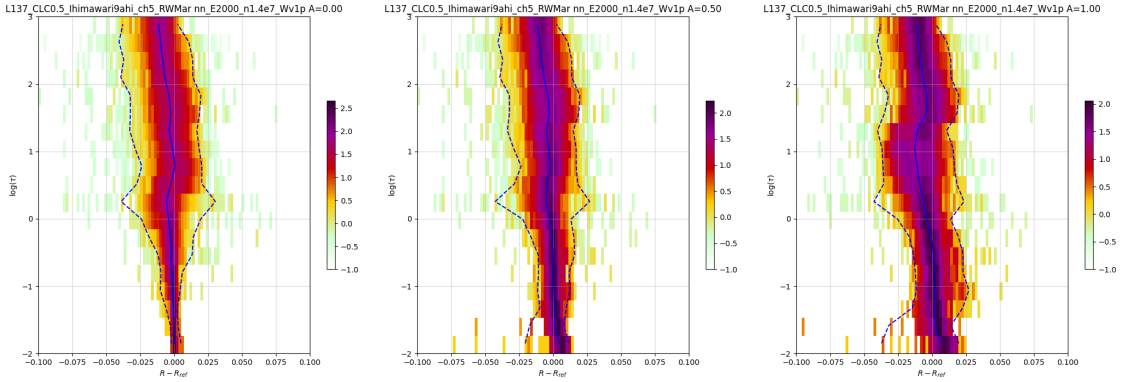

(a) (b) (c)

Figure 127: MFASIS $\Delta r_{\mathrm{MFASIS}-ref}$ as function of the cloud optical depth τ at albedo(s) of 0.00, 0.50, 1.00 (from left to right) for the instrument: HIMAWARI 9 AHI CH5

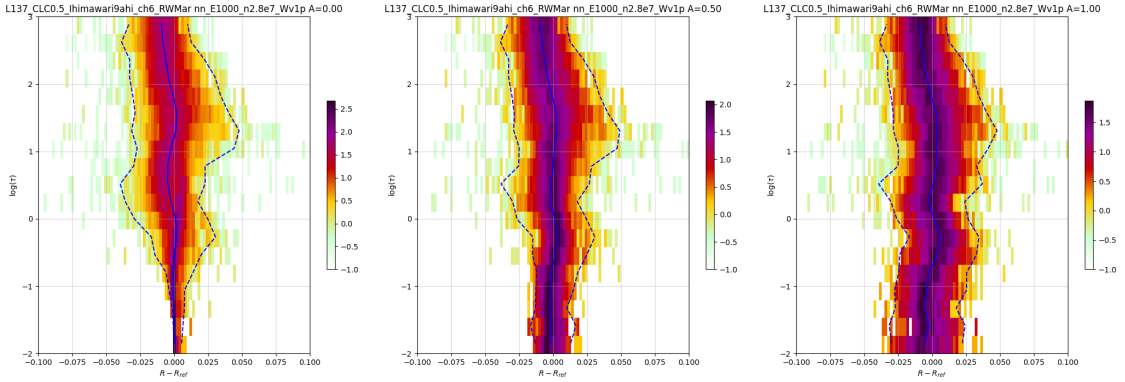

(a) (b) (c)

Figure 128: MFASIS $\Delta r_{\mathrm{MFASIS}-ref}$ as function of the cloud optical depth τ at albedo(s) of 0.00, 0.50, 1.00 (from left to right) for the instrument: HIMAWARI 9 AHI CH6

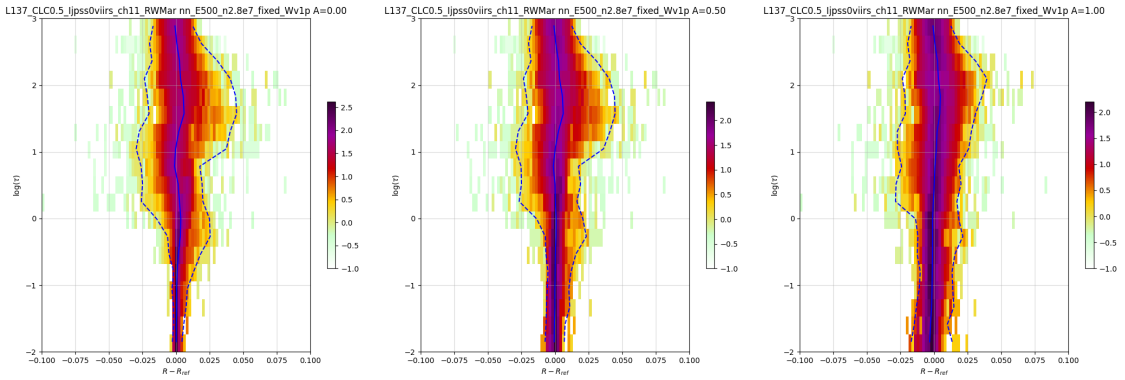

(a) (b) (c)

Figure 129: MFASIS $\Delta r_{\mathrm{MFASIS}-ref}$ as function of the cloud optical depth τ at albedo(s) of 0.00, 0.50, 1.00 (from left to right) for the instrument: JPSS 0 VIIRS CH11

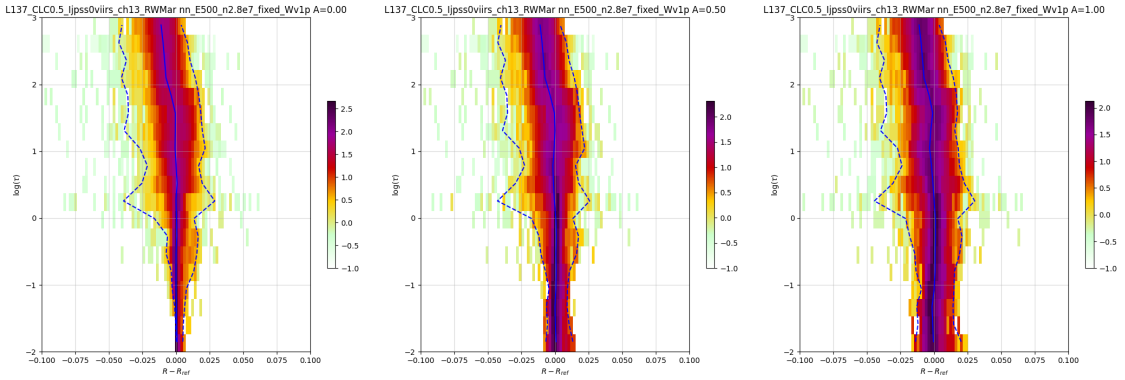

(a) (b) (c)

Figure 130: MFASIS $\Delta r_{\mathrm{MFASIS}-ref}$ as function of the cloud optical depth τ at albedo(s) of 0.00, 0.50, 1.00 (from left to right) for the instrument: JPSS 0 VIIRS CH13

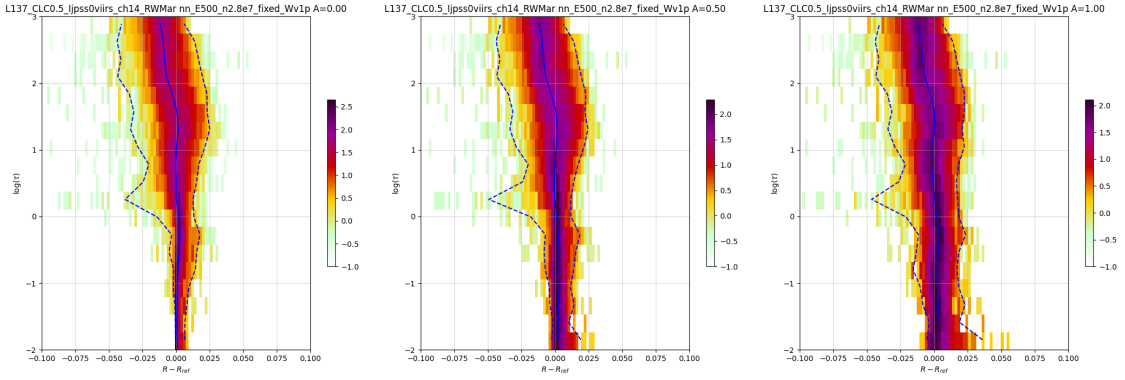

(a) (b) (c)

Figure 131: MFASIS $\Delta r_{\mathrm{MFASIS}-ref}$ as function of the cloud optical depth τ at albedo(s) of 0.00, 0.50, 1.00 (from left to right) for the instrument: JPSS 0 VIIRS CH14

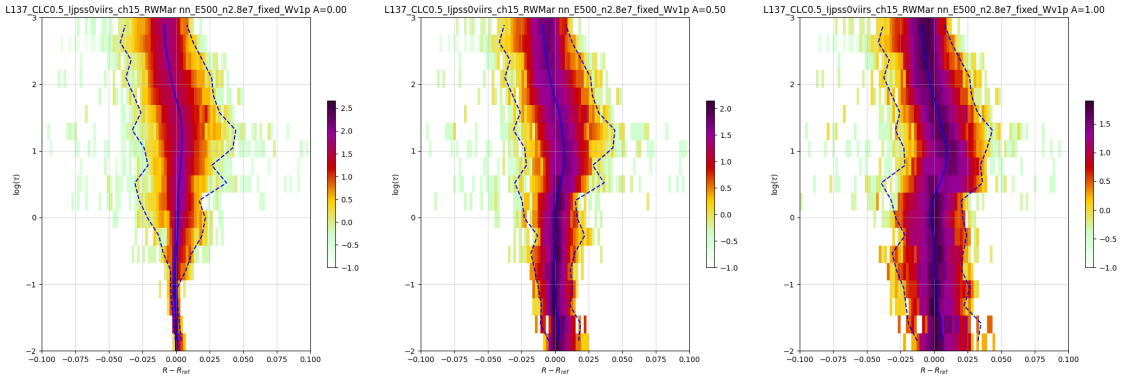

(a) (b) (c)

Figure 132: MFASIS $\Delta r_{\mathrm{MFASIS}-ref}$ as function of the cloud optical depth τ at albedo(s) of 0.00, 0.50, 1.00 (from left to right) for the instrument: JPSS 0 VIIRS CH15

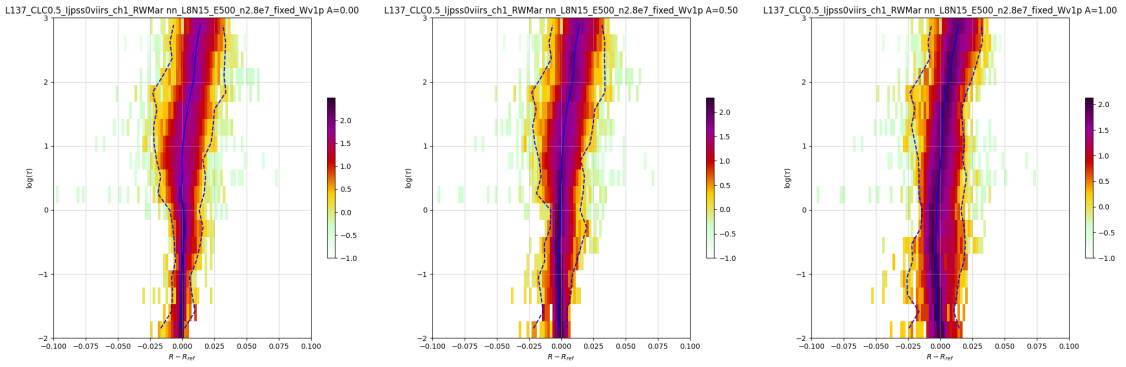

(a) (b) (c)

Figure 133: MFASIS $\Delta r_{\mathrm{MFASIS}-ref}$ as function of the cloud optical depth τ at albedo(s) of 0.00, 0.50, 1.00 (from left to right) for the instrument: JPSS 0 VIIRS CH1

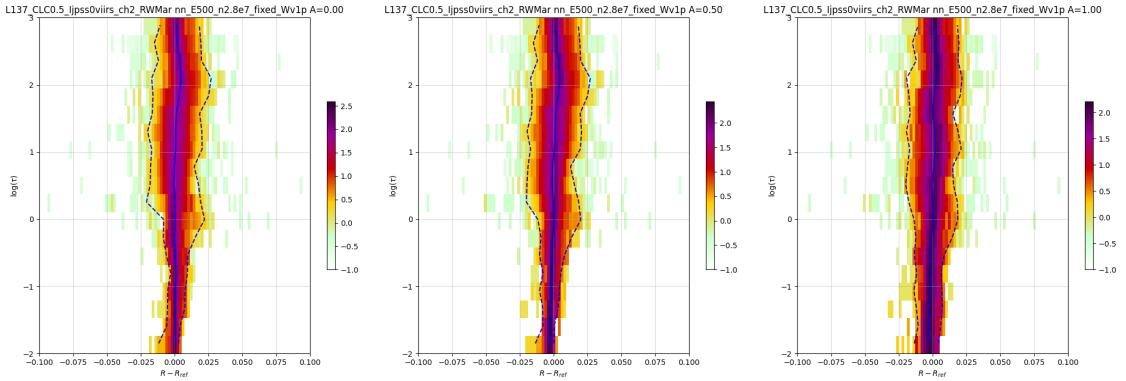

(a) (b) (c)

Figure 134: MFASIS $\Delta r_{\mathrm{MFASIS}-ref}$ as function of the cloud optical depth τ at albedo(s) of 0.00, 0.50, 1.00 (from left to right) for the instrument: JPSS 0 VIIRS CH2

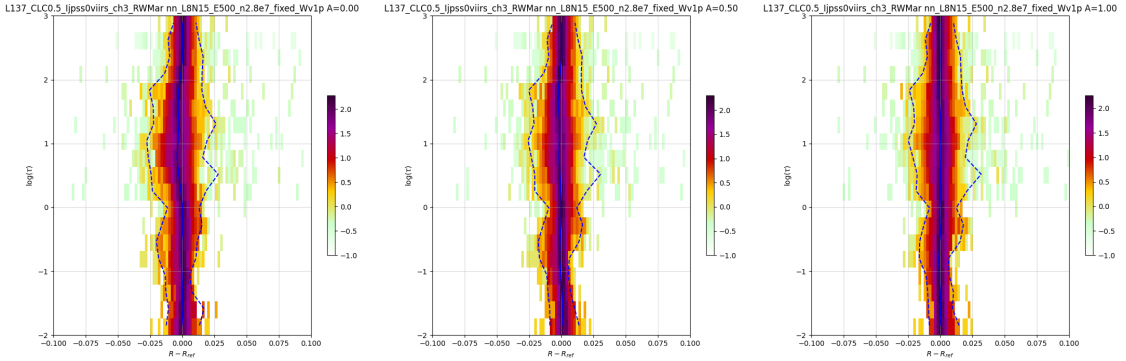

(a) (b) (c)

Figure 135: MFASIS $\Delta r_{\mathrm{MFASIS}-ref}$ as function of the cloud optical depth τ at albedo(s) of 0.00, 0.50, 1.00 (from left to right) for the instrument: JPSS 0 VIIRS CH3

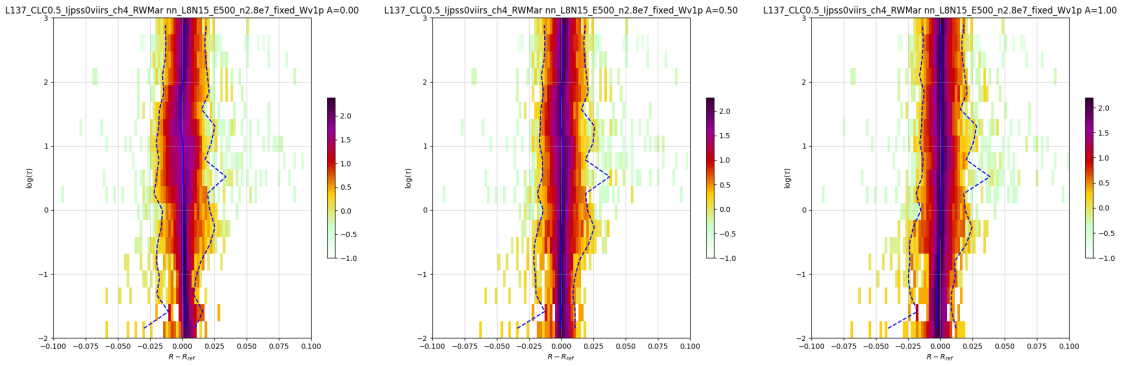

(a) (b) (c)

Figure 136: MFASIS $\Delta r_{\mathrm{MFASIS}-ref}$ as function of the cloud optical depth τ at albedo(s) of 0.00, 0.50, 1.00 (from left to right) for the instrument: JPSS 0 VIIRS CH4

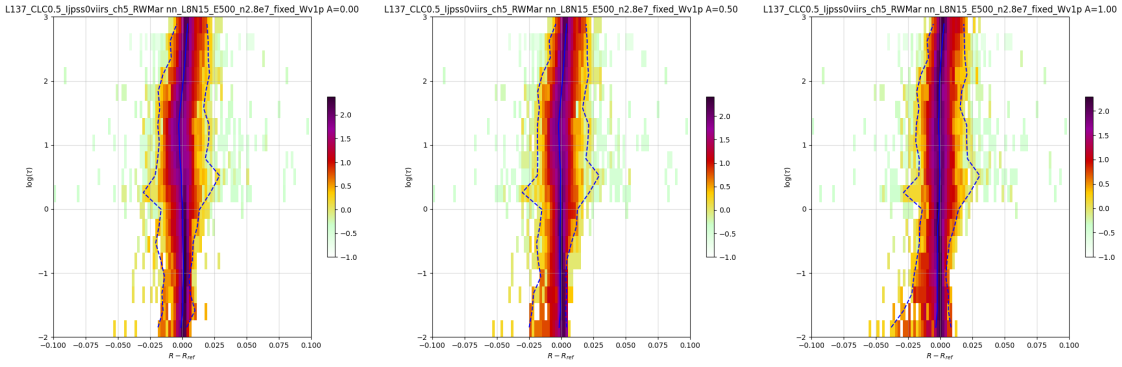

(a) (b) (c)

Figure 137: MFASIS $\Delta r_{\mathrm{MFASIS}-ref}$ as function of the cloud optical depth τ at albedo(s) of 0.00, 0.50, 1.00 (from left to right) for the instrument: JPSS 0 VIIRS CH5

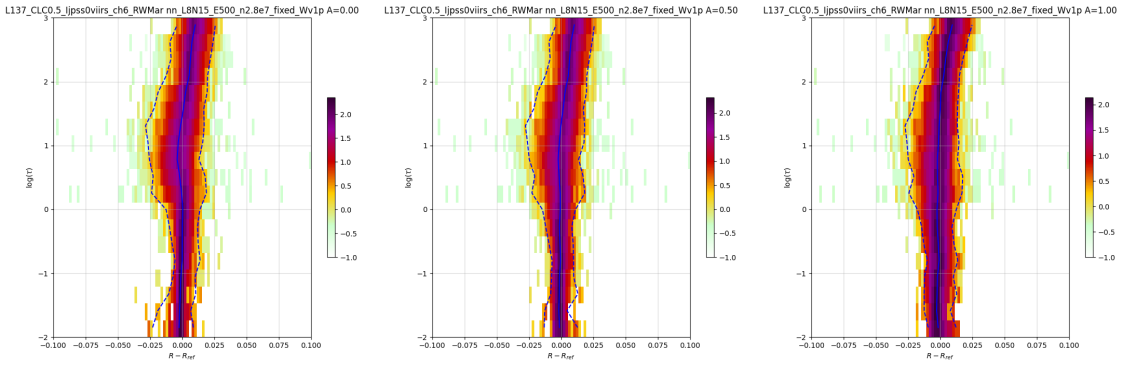

(a) (b) (c)

Figure 138: MFASIS $\Delta r_{\mathrm{MFASIS}-ref}$ as function of the cloud optical depth τ at albedo(s) of 0.00, 0.50, 1.00 (from left to right) for the instrument: JPSS 0 VIIRS CH6

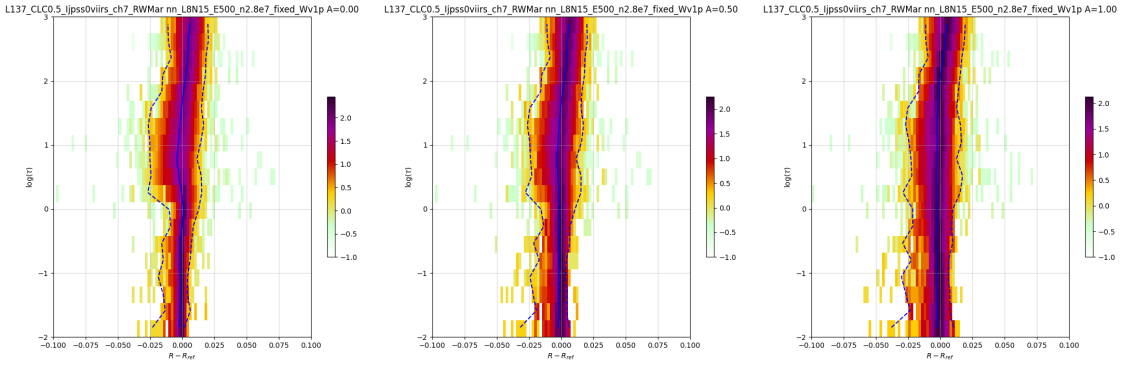

(a) (b) (c)

Figure 139: MFASIS $\Delta r_{\mathrm{MFASIS}-ref}$ as function of the cloud optical depth τ at albedo(s) of 0.00, 0.50, 1.00 (from left to right) for the instrument: JPSS 0 VIIRS CH7

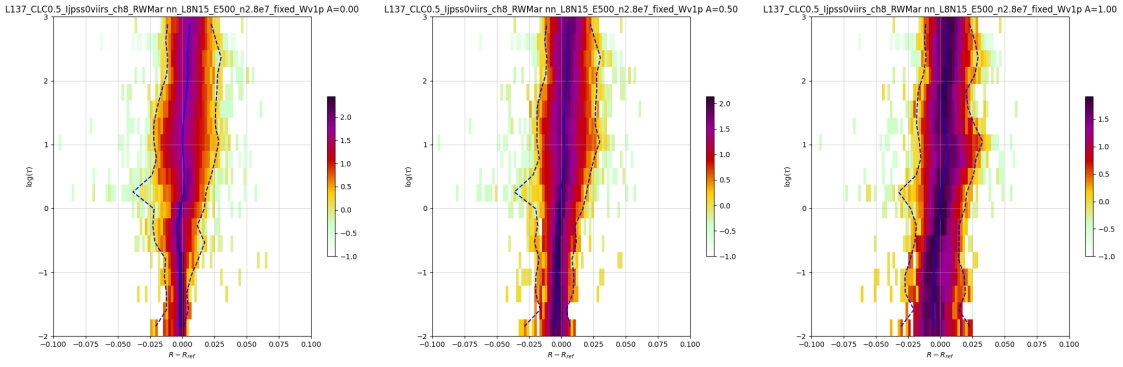

(a) (b) (c)

Figure 140: MFASIS $\Delta r_{\mathrm{MFASIS}-ref}$ as function of the cloud optical depth τ at albedo(s) of 0.00, 0.50, 1.00 (from left to right) for the instrument: JPSS 0 VIIRS CH8

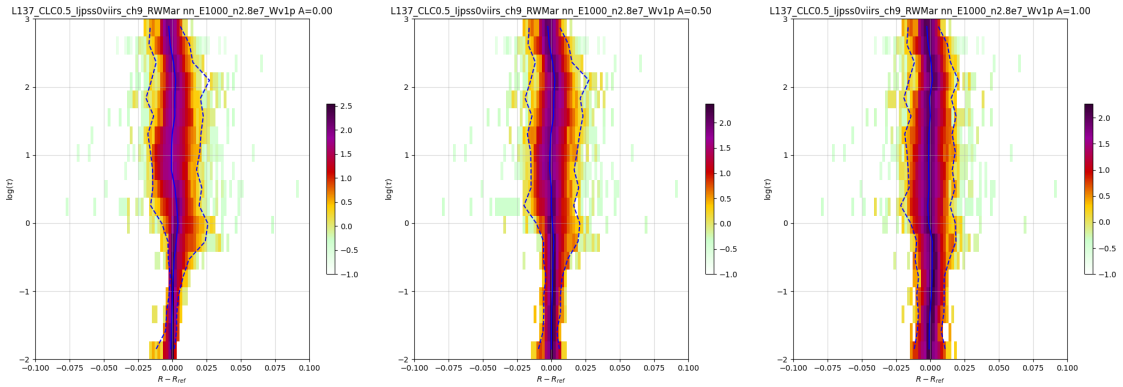

(a) (b) (c)

Figure 141: MFASIS $\Delta r_{\mathrm{MFASIS}-ref}$ as function of the cloud optical depth τ at albedo(s) of 0.00, 0.50, 1.00 (from left to right) for the instrument: JPSS 0 VIIRS CH9

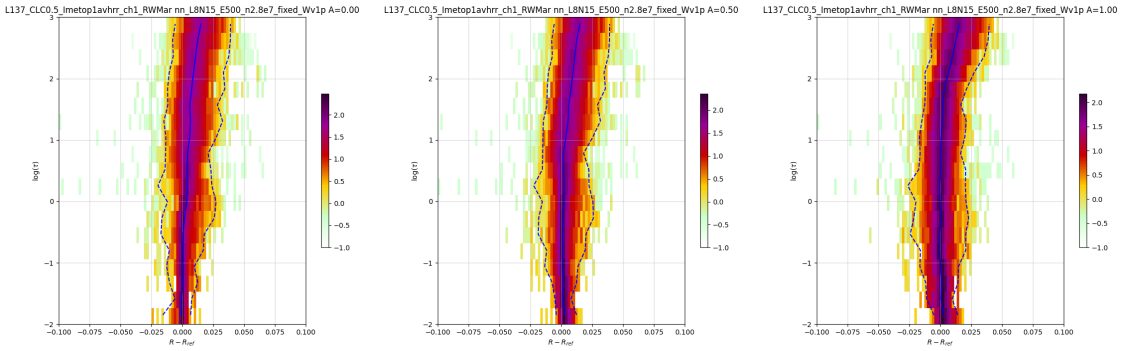

(a) (b) (c)

Figure 142: MFASIS $\Delta r_{\mathrm{MFASIS}-ref}$ as function of the cloud optical depth τ at albedo(s) of 0.00, 0.50, 1.00 (from left to right) for the instrument: METOP 1 AVHRR CH1

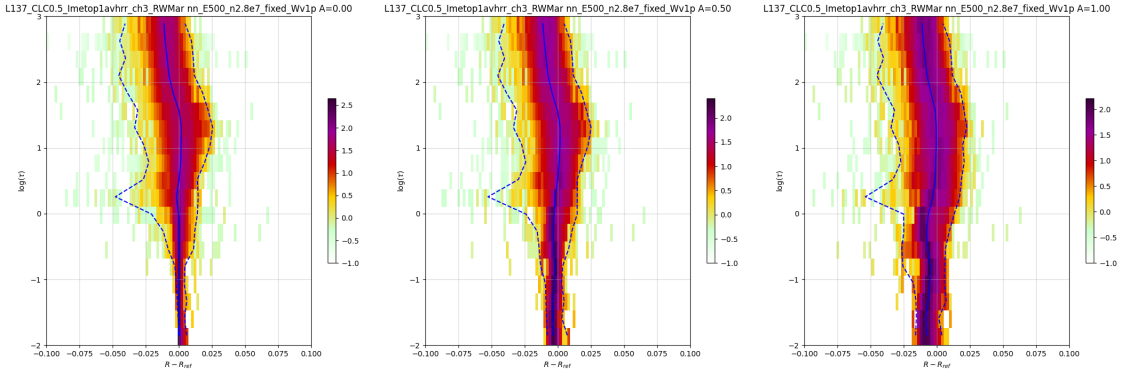

(a) (b) (c)

Figure 143: MFASIS $\Delta r_{\mathrm{MFASIS}-ref}$ as function of the cloud optical depth τ at albedo(s) of 0.00, 0.50, 1.00 (from left to right) for the instrument: METOP 1 AVHRR CH3

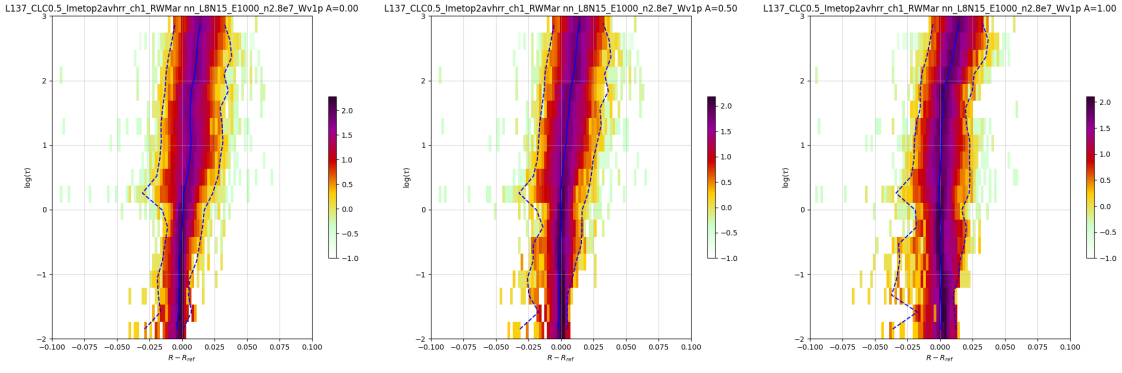

(a) (b) (c)

Figure 144: MFASIS $\Delta r_{\mathrm{MFASIS}-ref}$ as function of the cloud optical depth τ at albedo(s) of 0.00, 0.50, 1.00 (from left to right) for the instrument: METOP 2 AVHRR CH1

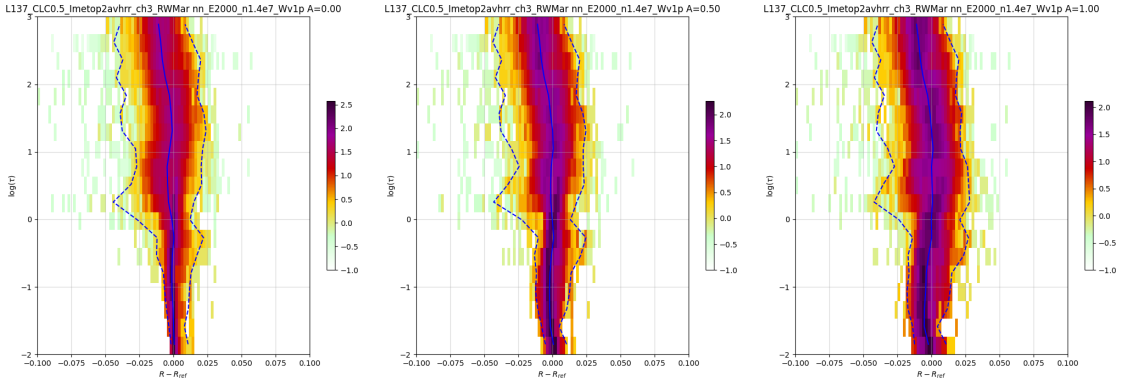

(a) (b) (c)

Figure 145: MFASIS $\Delta r_{\mathrm{MFASIS}-ref}$ as function of the cloud optical depth τ at albedo(s) of 0.00, 0.50, 1.00 (from left to right) for the instrument: METOP 2 AVHRR CH3

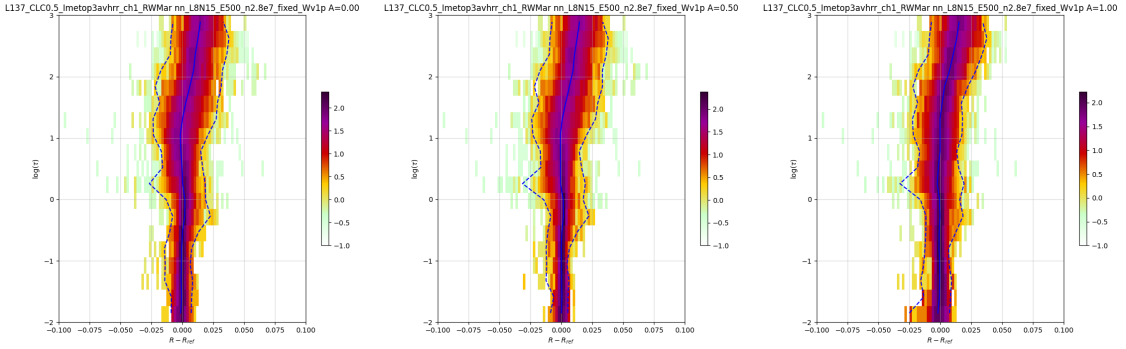

(a) (b) (c)

Figure 146: MFASIS $\Delta r_{\mathrm{MFASIS}-ref}$ as function of the cloud optical depth τ at albedo(s) of 0.00, 0.50, 1.00 (from left to right) for the instrument: METOP 3 AVHRR CH1

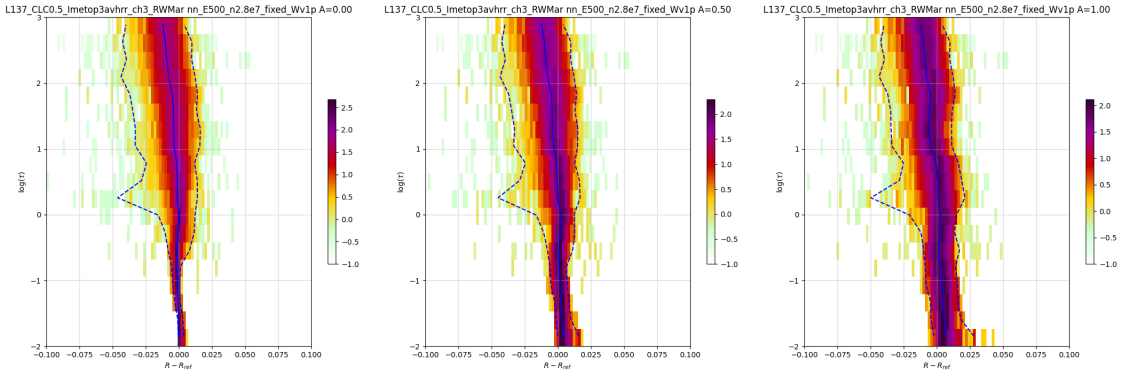

(a) (b) (c)

Figure 147: MFASIS $\Delta r_{\mathrm{MFASIS}-ref}$ as function of the cloud optical depth τ at albedo(s) of 0.00, 0.50, 1.00 (from left to right) for the instrument: METOP 3 AVHRR CH3

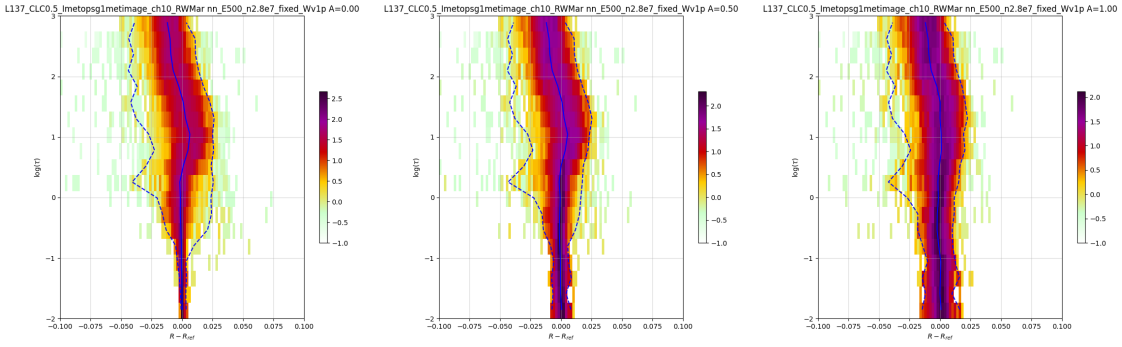

(a) (b) (c)

Figure 148: MFASIS $\Delta r_{\mathrm{MFASIS}-ref}$ as function of the cloud optical depth τ at albedo(s) of 0.00, 0.50, 1.00 (from left to right) for the instrument: METOPSG 1 METIMAGE CH10

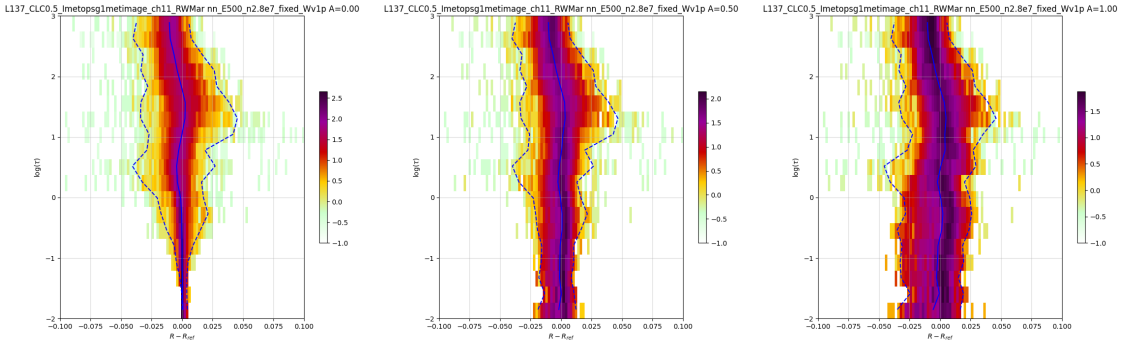

(a) (b) (c)

Figure 149: MFASIS $\Delta r_{\mathrm{MFASIS}-ref}$ as function of the cloud optical depth τ at albedo(s) of 0.00, 0.50, 1.00 (from left to right) for the instrument: METOPSG 1 METIMAGE CH11

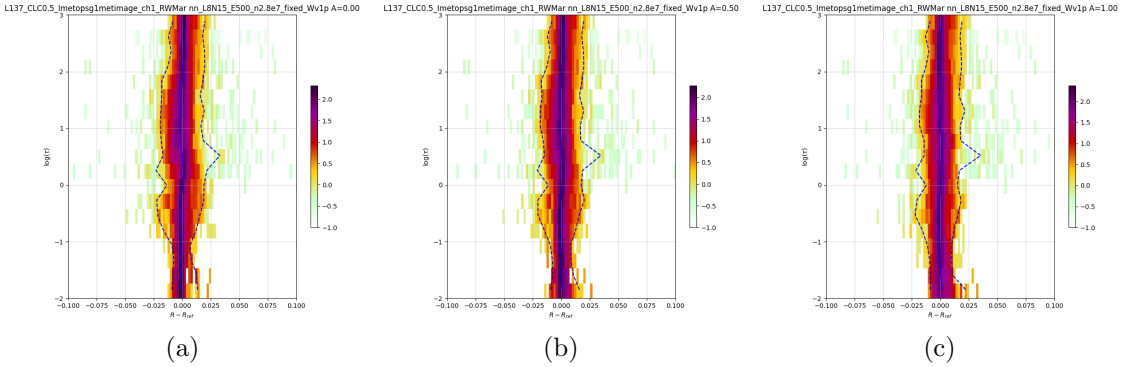

(a) (b) (c)

Figure 150: MFASIS $\Delta r_{\mathrm{MFASIS}-ref}$ as function of the cloud optical depth τ at albedo(s) of 0.00, 0.50, 1.00 (from left to right) for the instrument: METOPSG 1 METIMAGE CH1

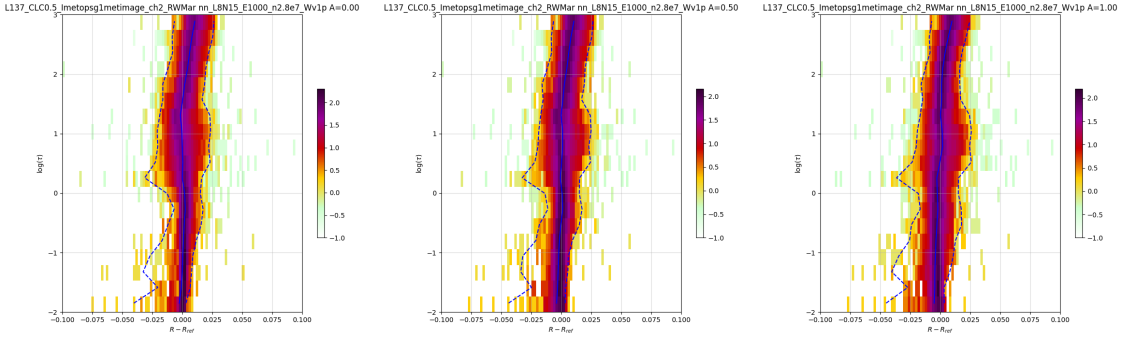

(a) (b) (c)

Figure 151: MFASIS $\Delta r_{\mathrm{MFASIS}-ref}$ as function of the cloud optical depth τ at albedo(s) of 0.00, 0.50, 1.00 (from left to right) for the instrument: METOPSG 1 METIMAGE CH2

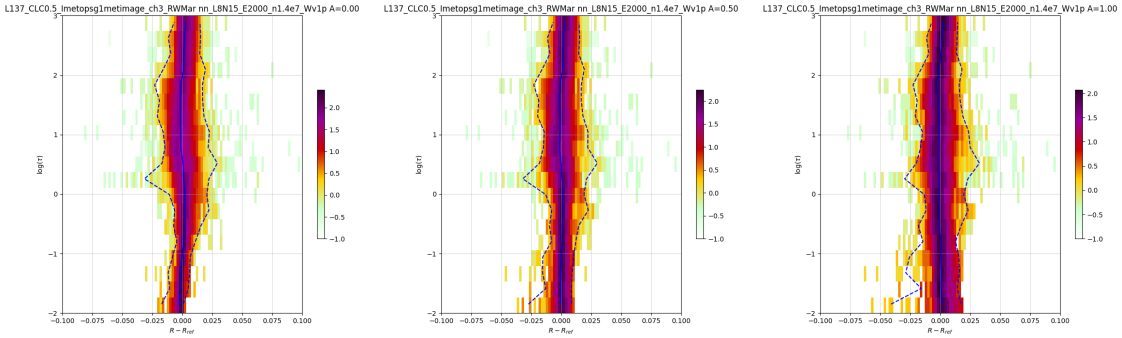

(a) (b) (c)

Figure 152: MFASIS $\Delta r_{\mathrm{MFASIS}-ref}$ as function of the cloud optical depth τ at albedo(s) of 0.00, 0.50, 1.00 (from left to right) for the instrument: METOPSG 1 METIMAGE CH3

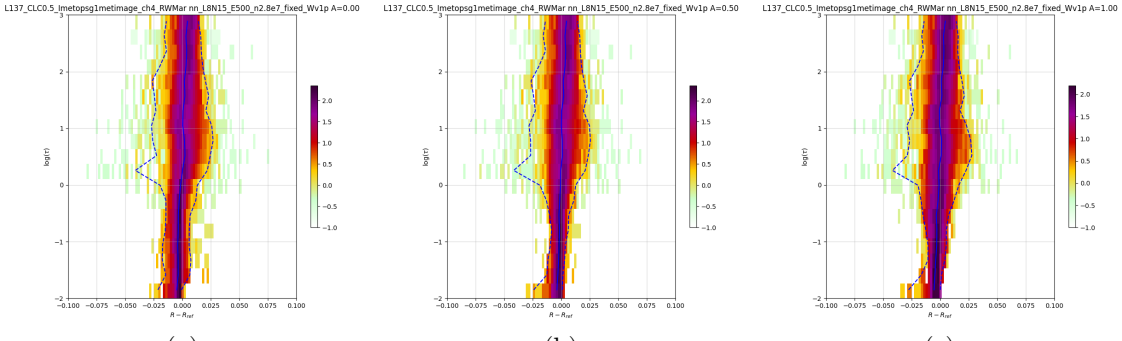

(a) (b) (c)

Figure 153: MFASIS $\Delta r_{\mathrm{MFASIS}-ref}$ as function of the cloud optical depth τ at albedo(s) of 0.00, 0.50, 1.00 (from left to right) for the instrument: METOPSG 1 METIMAGE CH4

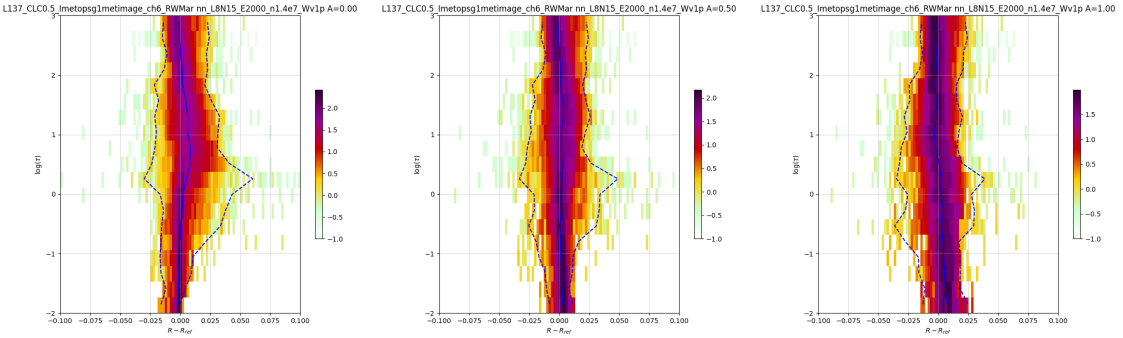

(a) (b) (c)

Figure 154: MFASIS $\Delta r_{\mathrm{MFASIS}-ref}$ as function of the cloud optical depth τ at albedo(s) of 0.00, 0.50, 1.00 (from left to right) for the instrument: METOPSG 1 METIMAGE CH6

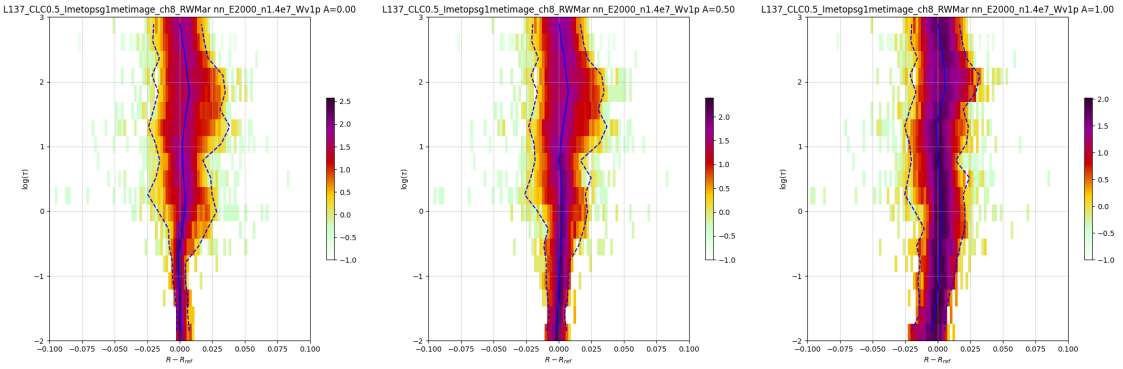

(a) (b) (c)

Figure 155: MFASIS $\Delta r_{\mathrm{MFASIS}-ref}$ as function of the cloud optical depth τ at albedo(s) of 0.00, 0.50, 1.00 (from left to right) for the instrument: METOPSG 1 METIMAGE CH8

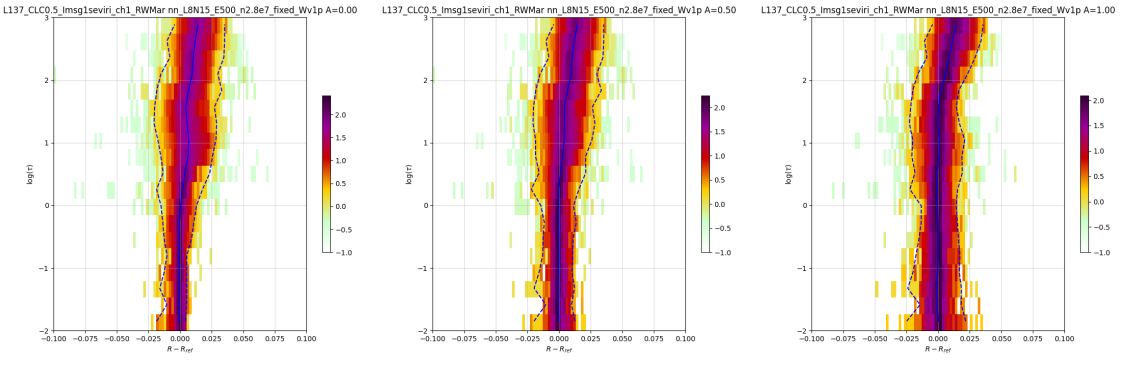

(a) (b) (c)

Figure 156: MFASIS $\Delta r_{\mathrm{MFASIS}-ref}$ as function of the cloud optical depth τ at albedo(s) of 0.00, 0.50, 1.00 (from left to right) for the instrument: MSG 1 SEVIRI CH1

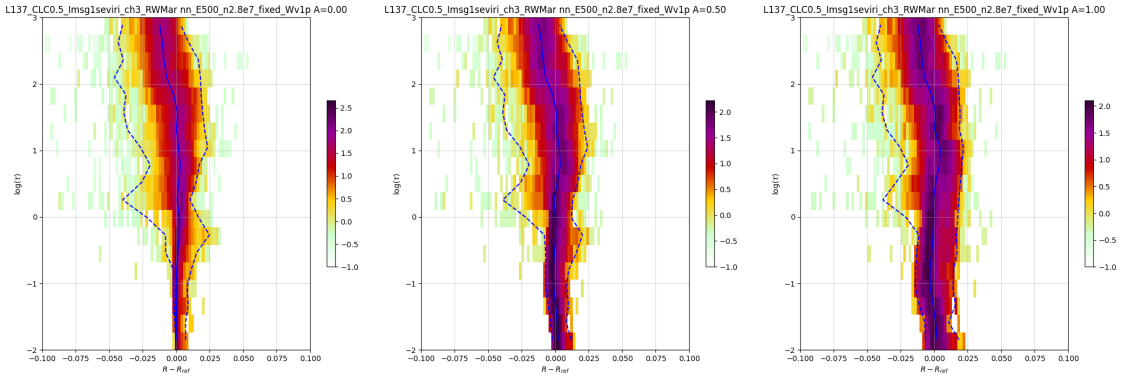

(a) (b) (c)

Figure 157: MFASIS $\Delta r_{\mathrm{MFASIS}-ref}$ as function of the cloud optical depth τ at albedo(s) of 0.00, 0.50, 1.00 (from left to right) for the instrument: MSG 1 SEVIRI CH3

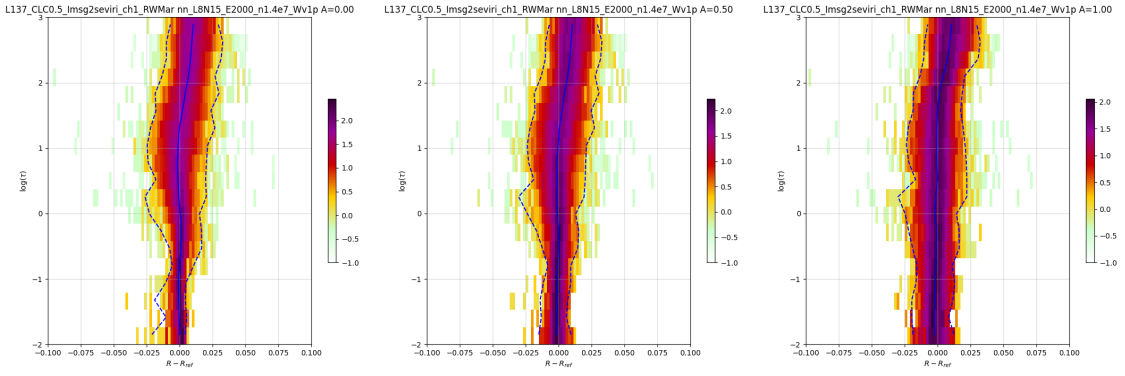

(a) (b) (c)

Figure 158: MFASIS $\Delta r_{\mathrm{MFASIS}-ref}$ as function of the cloud optical depth τ at albedo(s) of 0.00, 0.50, 1.00 (from left to right) for the instrument: MSG 2 SEVIRI CH1

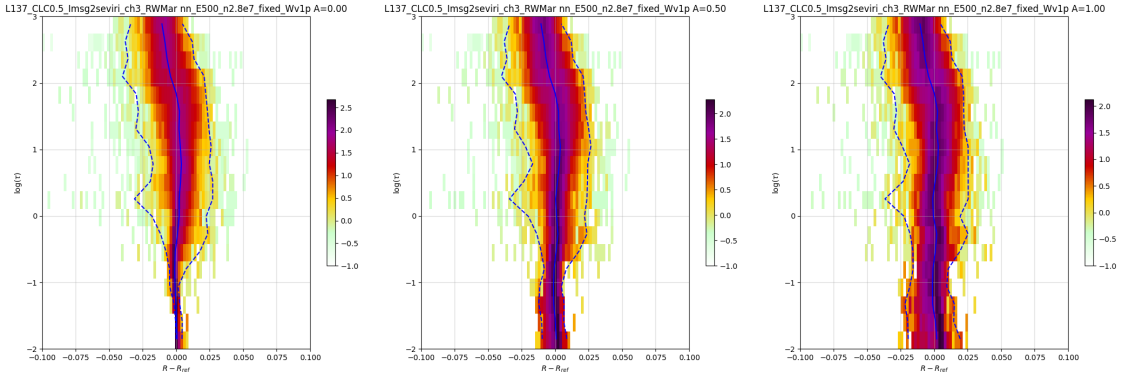

(a) (b) (c)

Figure 159: MFASIS $\Delta r_{\mathrm{MFASIS}-ref}$ as function of the cloud optical depth τ at albedo(s) of 0.00, 0.50, 1.00 (from left to right) for the instrument: MSG 2 SEVIRI CH3

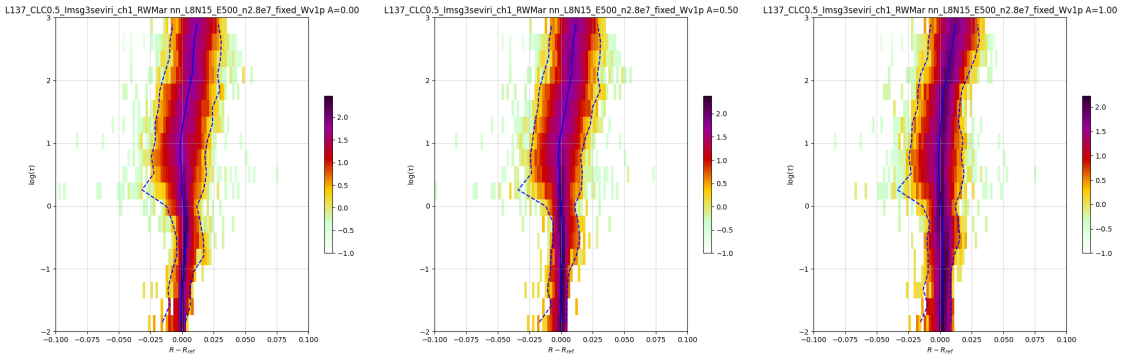

(a) (b) (c)

Figure 160: MFASIS $\Delta r_{\mathrm{MFASIS}-ref}$ as function of the cloud optical depth τ at albedo(s) of 0.00, 0.50, 1.00 (from left to right) for the instrument: MSG 3 SEVIRI CH1

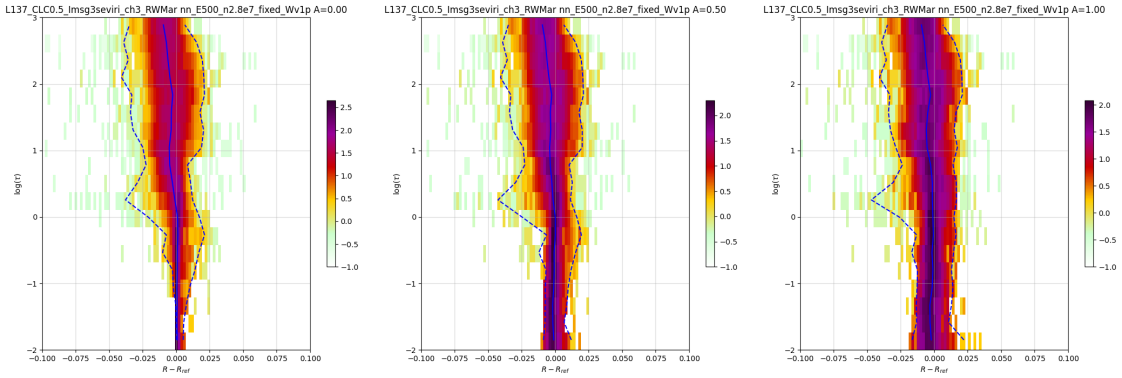

(a) (b) (c)

Figure 161: MFASIS $\Delta r_{\mathrm{MFASIS}-ref}$ as function of the cloud optical depth τ at albedo(s) of 0.00, 0.50, 1.00 (from left to right) for the instrument: MSG 3 SEVIRI CH3

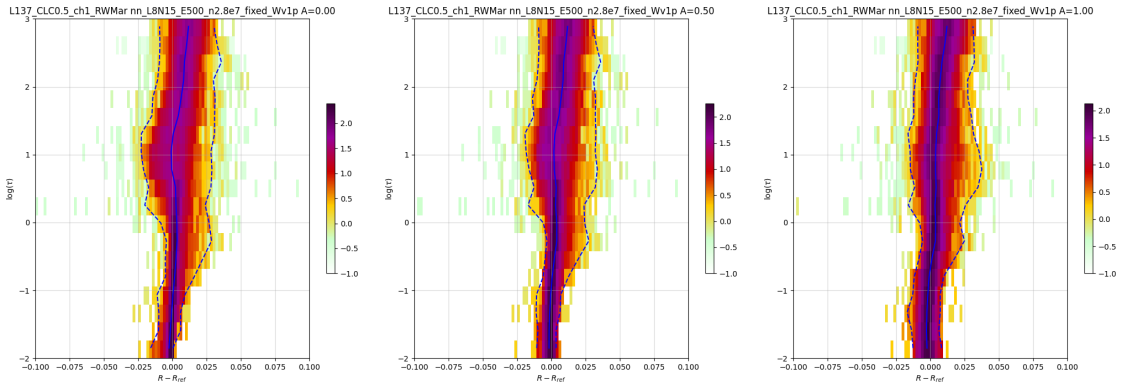

(a) (b) (c)

Figure 162: MFASIS $\Delta r_{\mathrm{MFASIS}-ref}$ as function of the cloud optical depth τ at albedo(s) of 0.00, 0.50, 1.00 (from left to right) for the instrument: MSG 4 SEVIRI CH1

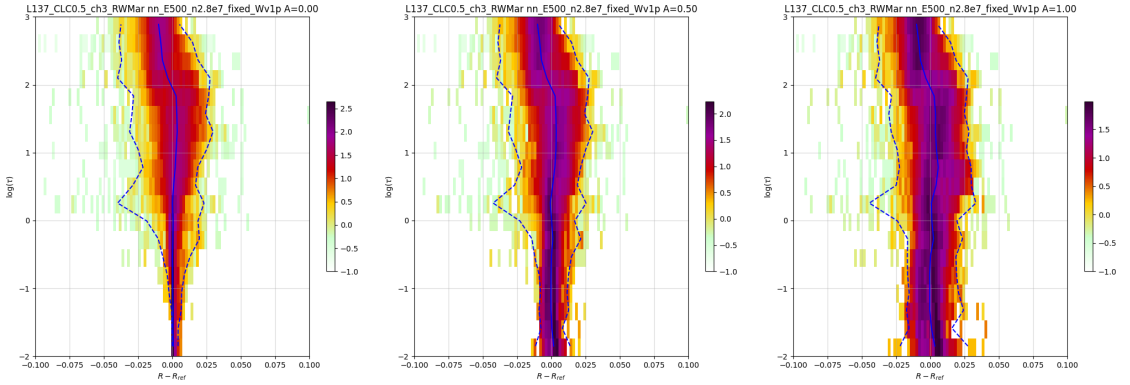

(a) (b) (c)

Figure 163: MFASIS $\Delta r_{\mathrm{MFASIS}-ref}$ as function of the cloud optical depth τ at albedo(s) of 0.00, 0.50, 1.00 (from left to right) for the instrument: MSG 4 SEVIRI CH3

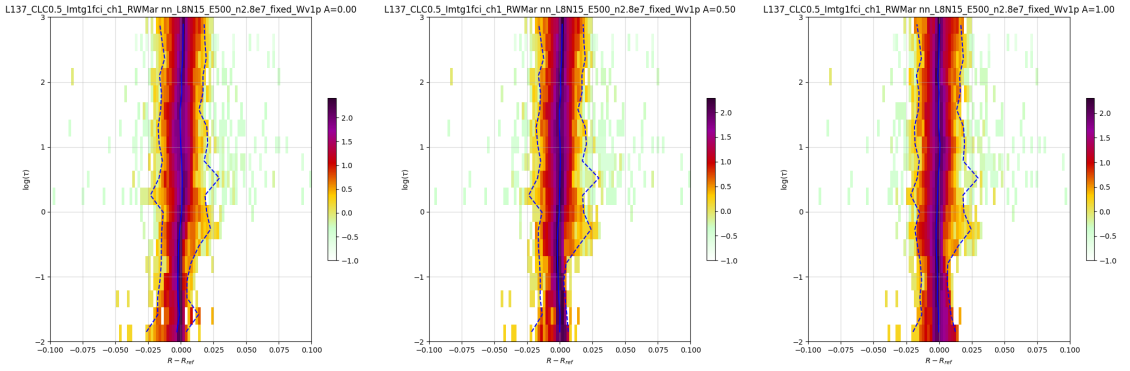

(a) (b) (c)

Figure 164: MFASIS $\Delta r_{\mathrm{MFASIS}-ref}$ as function of the cloud optical depth τ at albedo(s) of 0.00, 0.50, 1.00 (from left to right) for the instrument: MTG 1 FCI CH1

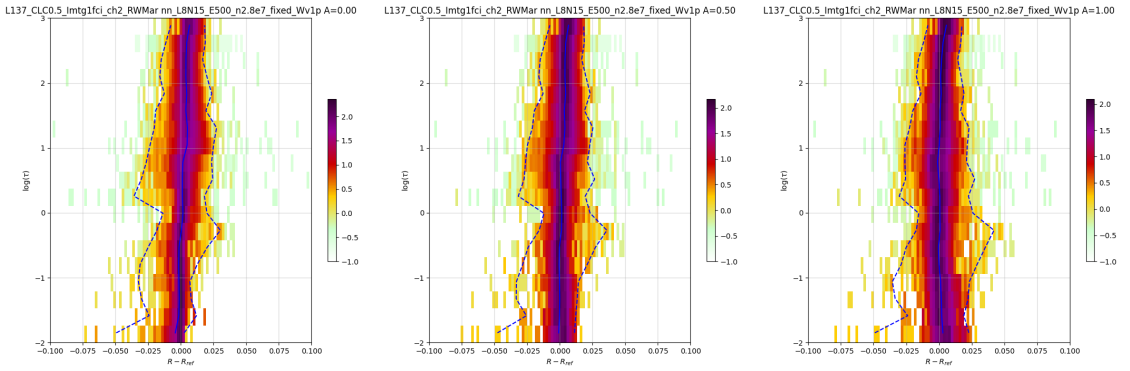

(a) (b) (c)

Figure 165: MFASIS $\Delta r_{\mathrm{MFASIS}-ref}$ as function of the cloud optical depth τ at albedo(s) of 0.00, 0.50, 1.00 (from left to right) for the instrument: MTG 1 FCI CH2

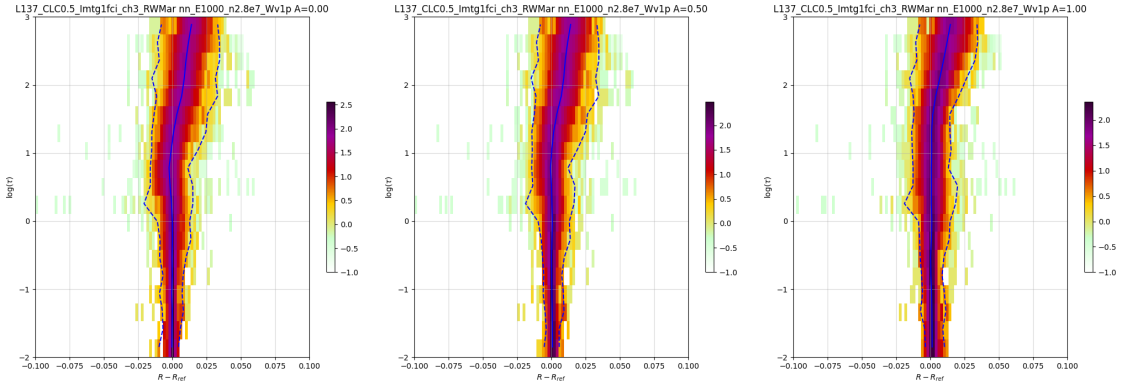

(a) (b) (c)

Figure 166: MFASIS $\Delta r_{\mathrm{MFASIS}-ref}$ as function of the cloud optical depth τ at albedo(s) of 0.00, 0.50, 1.00 (from left to right) for the instrument: MTG 1 FCI CH3

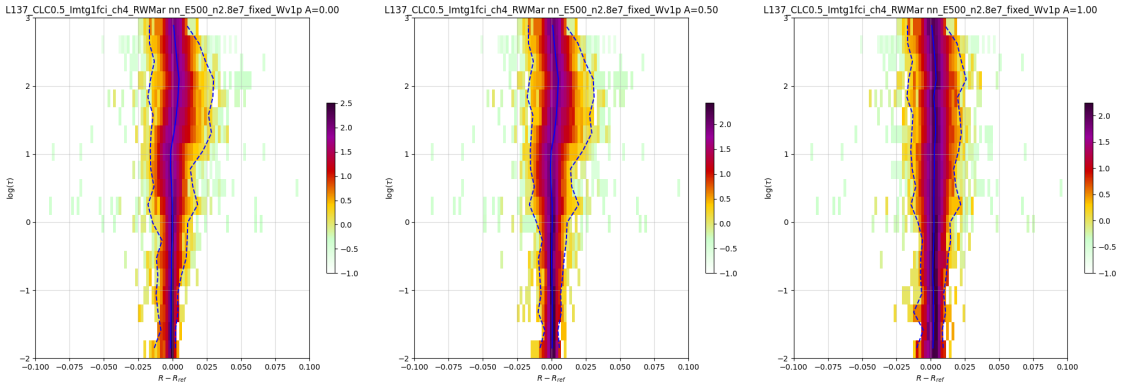

(a) (b) (c)

Figure 167: MFASIS $\Delta r_{\mathrm{MFASIS}-ref}$ as function of the cloud optical depth τ at albedo(s) of 0.00, 0.50, 1.00 (from left to right) for the instrument: MTG 1 FCI CH4

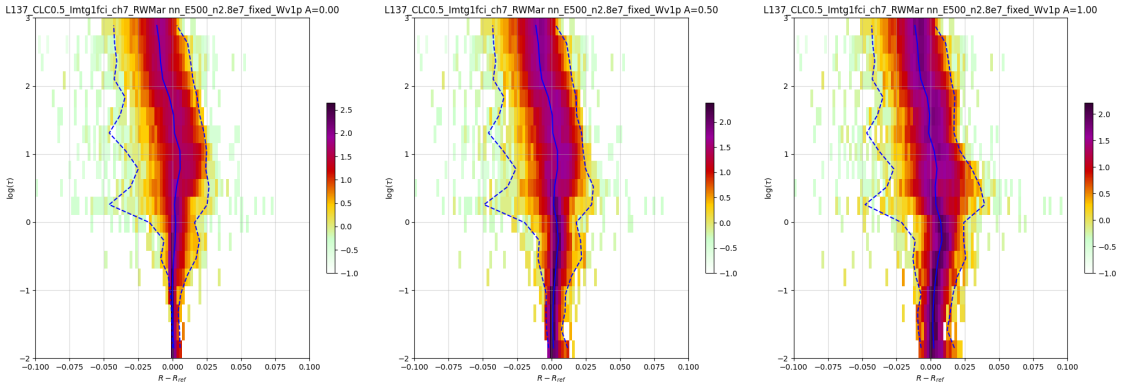

(a) (b) (c)

Figure 168: MFASIS $\Delta r_{\mathrm{MFASIS}-ref}$ as function of the cloud optical depth τ at albedo(s) of 0.00, 0.50, 1.00 (from left to right) for the instrument: MTG 1 FCI CH7

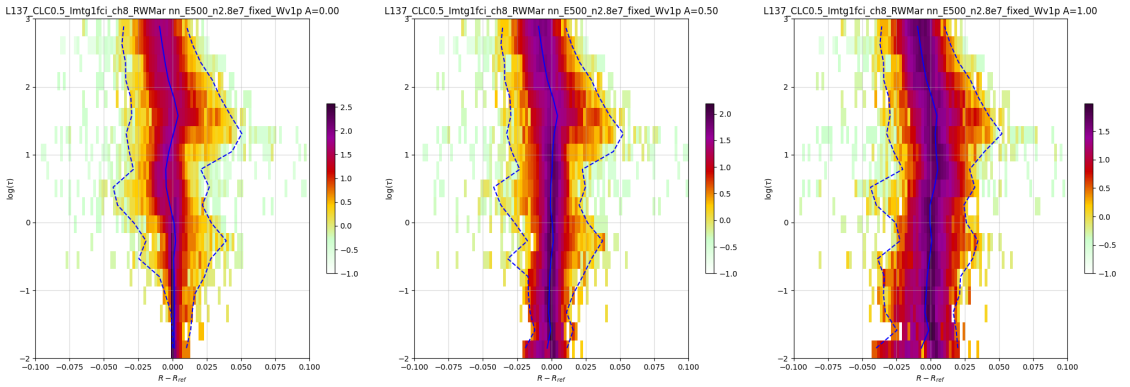

(a) (b) (c)

Figure 169: MFASIS $\Delta r_{\mathrm{MFASIS}-ref}$ as function of the cloud optical depth τ at albedo(s) of 0.00, 0.50, 1.00 (from left to right) for the instrument: MTG 1 FCI CH8

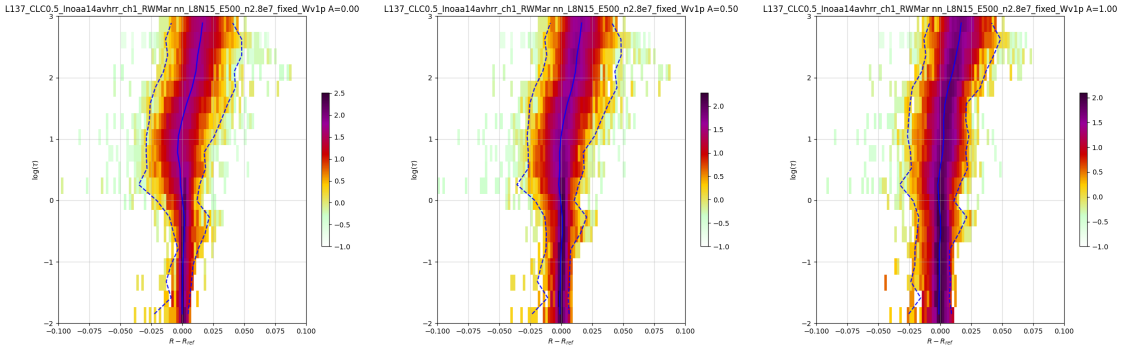

(a) (b) (c)

Figure 170: MFASIS $\Delta r_{\mathrm{MFASIS}-ref}$ as function of the cloud optical depth τ at albedo(s) of 0.00, 0.50, 1.00 (from left to right) for the instrument: NOAA 14 AVHRR CH1

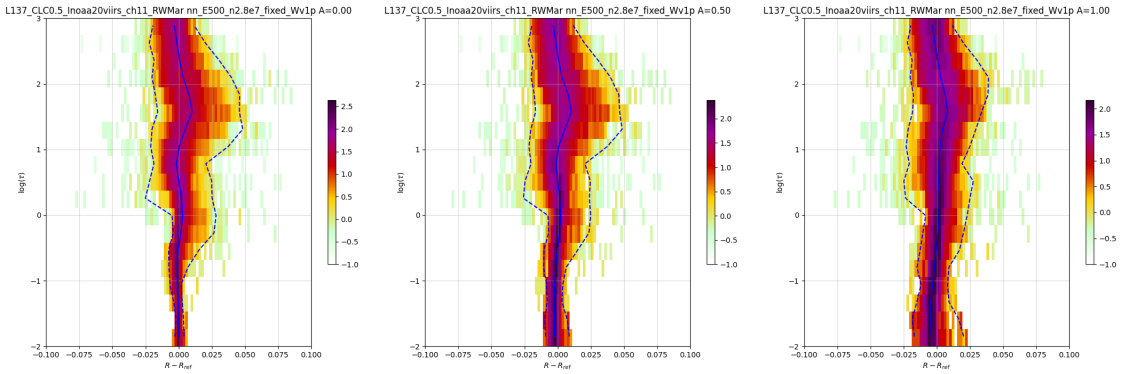

(a) (b) (c)

Figure 171: MFASIS $\Delta r_{\mathrm{MFASIS}-ref}$ as function of the cloud optical depth τ at albedo(s) of 0.00, 0.50, 1.00 (from left to right) for the instrument: NOAA 20 VIIRS CH11

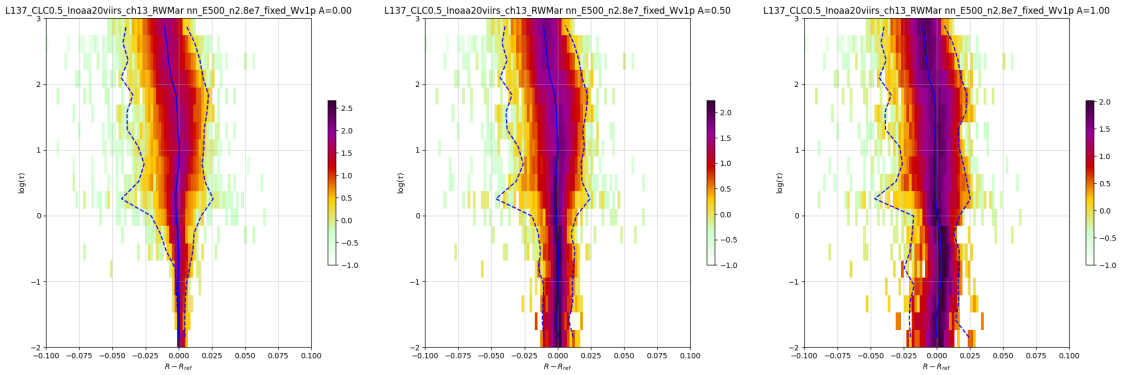

(a) (b) (c)

Figure 172: MFASIS $\Delta r_{\mathrm{MFASIS}-ref}$ as function of the cloud optical depth τ at albedo(s) of 0.00, 0.50, 1.00 (from left to right) for the instrument: NOAA 20 VIIRS CH13

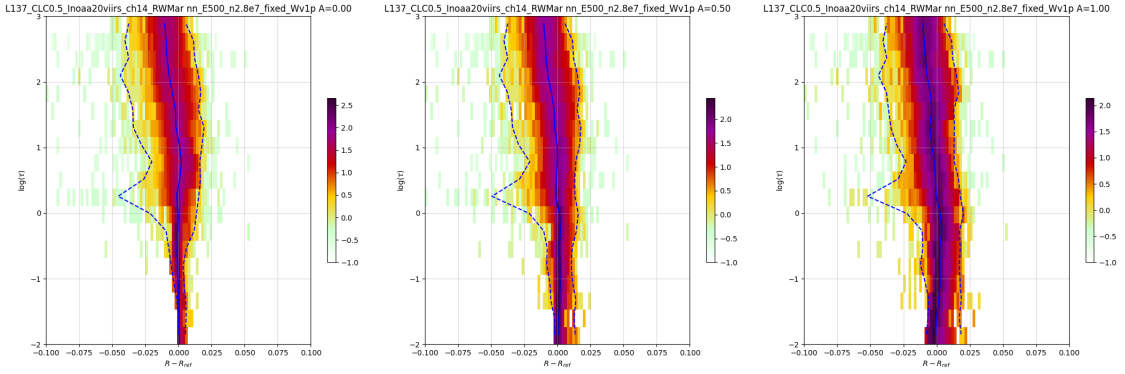

(a) (b) (c)

Figure 173: MFASIS $\Delta r_{\mathrm{MFASIS}-ref}$ as function of the cloud optical depth τ at albedo(s) of 0.00, 0.50, 1.00 (from left to right) for the instrument: NOAA 20 VIIRS CH14

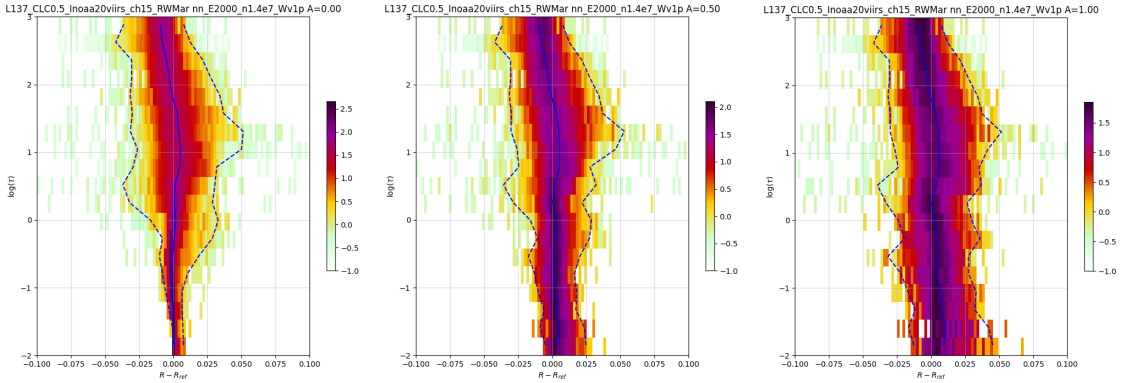

(a) (b) (c)

Figure 174: MFASIS $\Delta r_{\mathrm{MFASIS}-ref}$ as function of the cloud optical depth τ at albedo(s) of 0.00, 0.50, 1.00 (from left to right) for the instrument: NOAA 20 VIIRS CH15

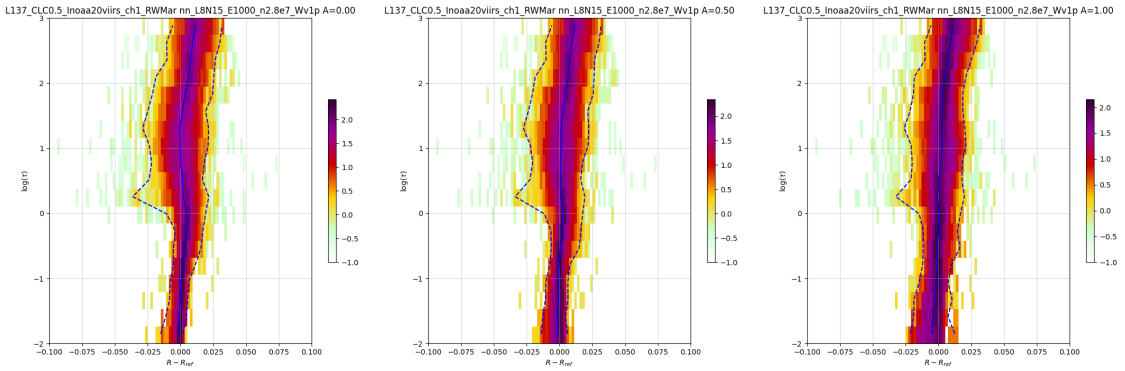

(a) (b) (c)

Figure 175: MFASIS $\Delta r_{\mathrm{MFASIS}-ref}$ as function of the cloud optical depth τ at albedo(s) of 0.00, 0.50, 1.00 (from left to right) for the instrument: NOAA 20 VIIRS CH1

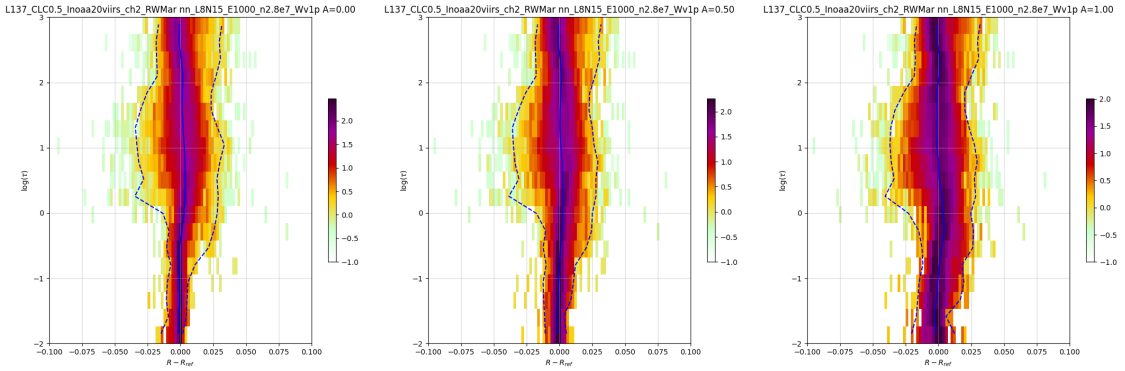

(a) (b) (c)

Figure 176: MFASIS $\Delta r_{\mathrm{MFASIS}-ref}$ as function of the cloud optical depth τ at albedo(s) of 0.00, 0.50, 1.00 (from left to right) for the instrument: NOAA 20 VIIRS CH2

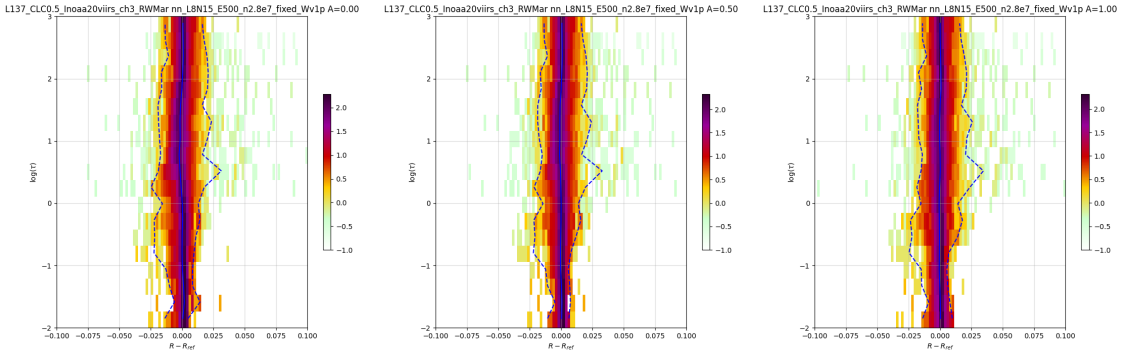

(a) (b) (c)

Figure 177: MFASIS $\Delta r_{\mathrm{MFASIS}-ref}$ as function of the cloud optical depth τ at albedo(s) of 0.00, 0.50, 1.00 (from left to right) for the instrument: NOAA 20 VIIRS CH3

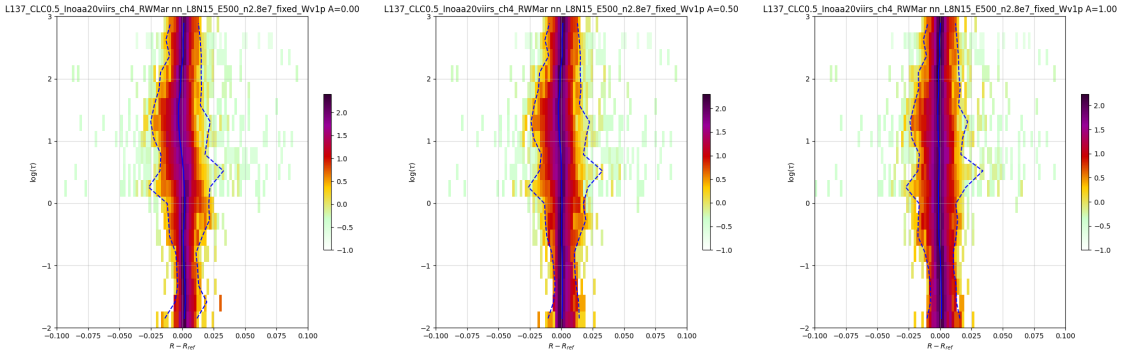

(a) (b) (c)

Figure 178: MFASIS $\Delta r_{\mathrm{MFASIS}-ref}$ as function of the cloud optical depth τ at albedo(s) of 0.00, 0.50, 1.00 (from left to right) for the instrument: NOAA 20 VIIRS CH4

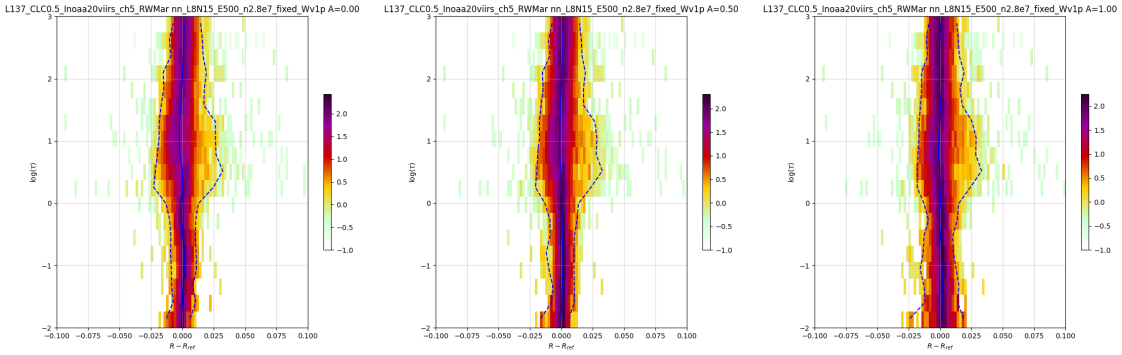

(a) (b) (c)

Figure 179: MFASIS $\Delta r_{\mathrm{MFASIS}-ref}$ as function of the cloud optical depth τ at albedo(s) of 0.00, 0.50, 1.00 (from left to right) for the instrument: NOAA 20 VIIRS CH5

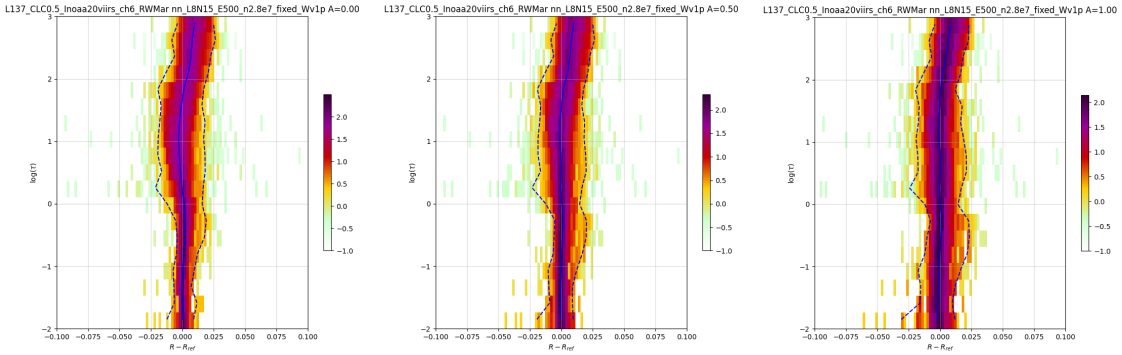

(a) (b) (c)

Figure 180: MFASIS $\Delta r_{\mathrm{MFASIS}-ref}$ as function of the cloud optical depth τ at albedo(s) of 0.00, 0.50, 1.00 (from left to right) for the instrument: NOAA 20 VIIRS CH6

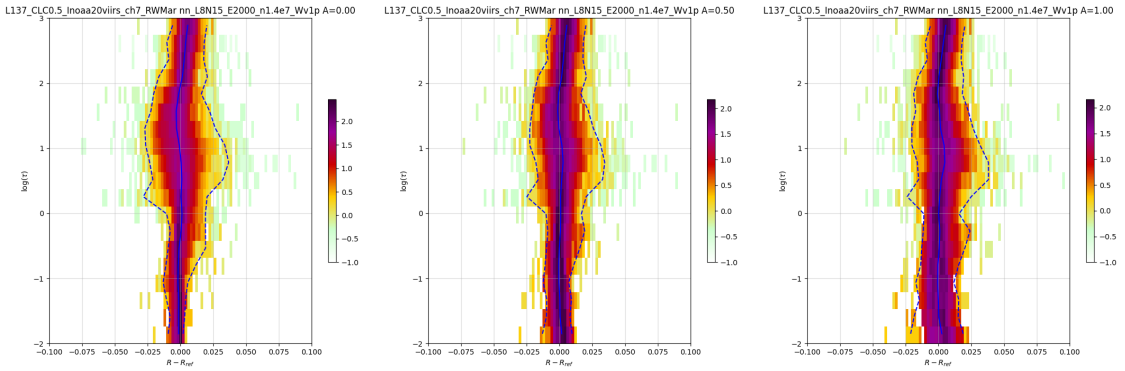

(a) (b) (c)

Figure 181: MFASIS $\Delta r_{\mathrm{MFASIS}-ref}$ as function of the cloud optical depth τ at albedo(s) of 0.00, 0.50, 1.00 (from left to right) for the instrument: NOAA 20 VIIRS CH7

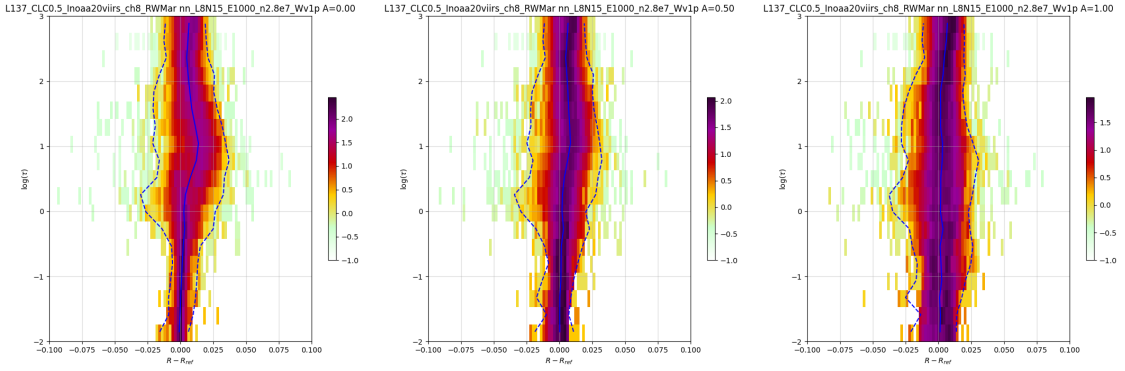

(a) (b) (c)

Figure 182: MFASIS $\Delta r_{\mathrm{MFASIS}-ref}$ as function of the cloud optical depth τ at albedo(s) of 0.00, 0.50, 1.00 (from left to right) for the instrument: NOAA 20 VIIRS CH8

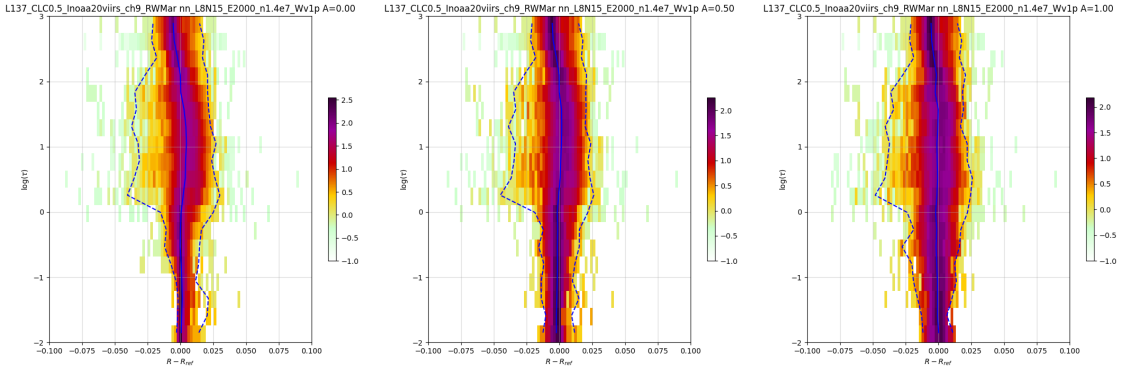

(a) (b) (c)

Figure 183: MFASIS $\Delta r_{\mathrm{MFASIS}-ref}$ as function of the cloud optical depth τ at albedo(s) of 0.00, 0.50, 1.00 (from left to right) for the instrument: NOAA 20 VIIRS CH9

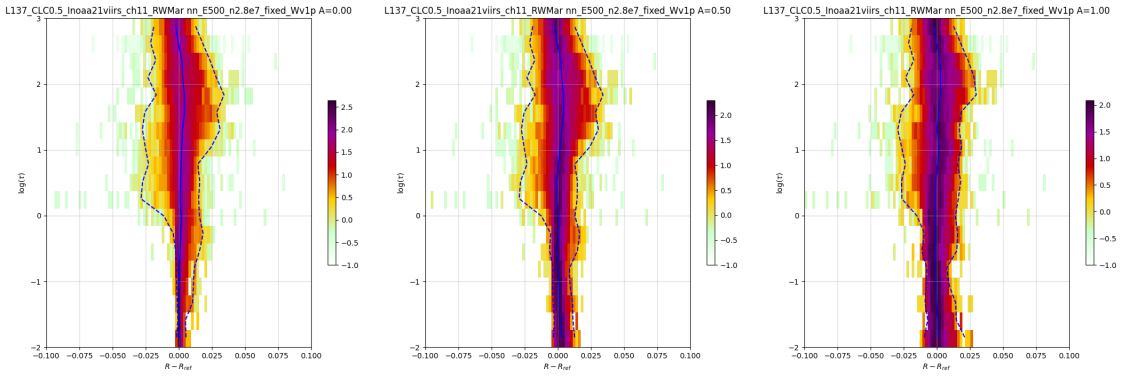

(a) (b) (c)

Figure 184: MFASIS $\Delta r_{\mathrm{MFASIS}-ref}$ as function of the cloud optical depth τ at albedo(s) of 0.00, 0.50, 1.00 (from left to right) for the instrument: NOAA 21 VIIRS CH11

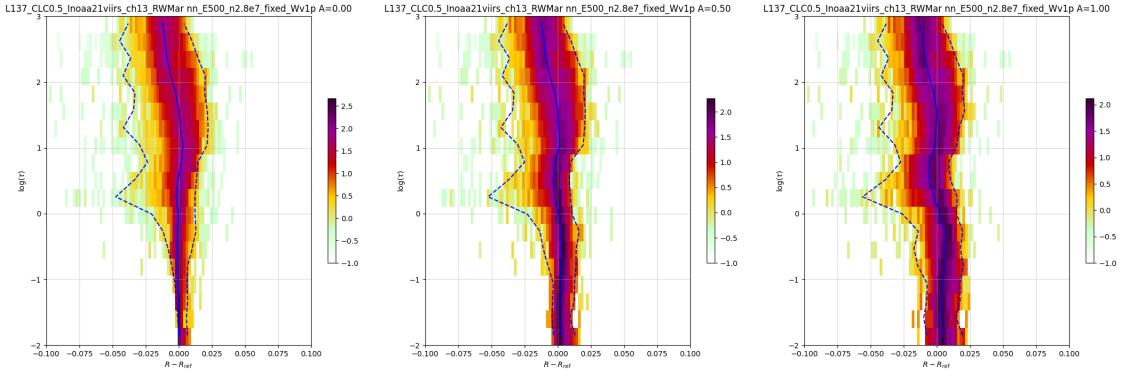

(a) (b) (c)

Figure 185: MFASIS $\Delta r_{\mathrm{MFASIS}-ref}$ as function of the cloud optical depth τ at albedo(s) of 0.00, 0.50, 1.00 (from left to right) for the instrument: NOAA 21 VIIRS CH13

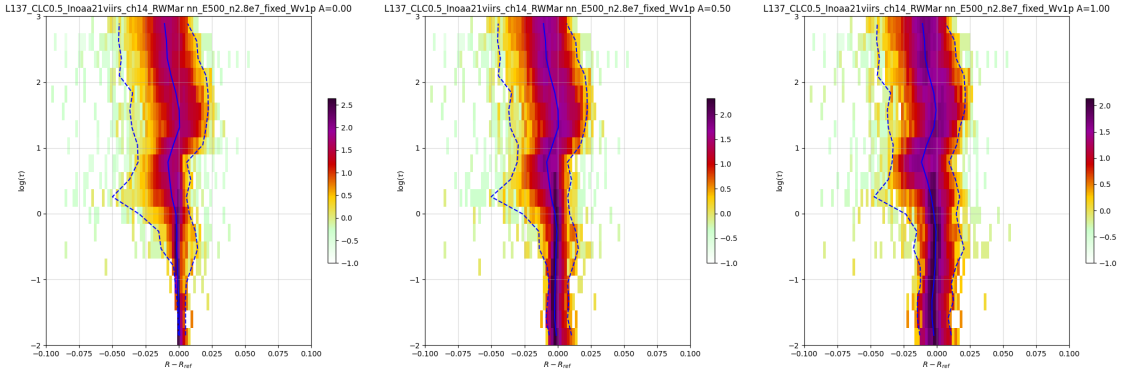

(a) (b) (c)

Figure 186: MFASIS $\Delta r_{\mathrm{MFASIS}-ref}$ as function of the cloud optical depth τ at albedo(s) of 0.00, 0.50, 1.00 (from left to right) for the instrument: NOAA 21 VIIRS CH14

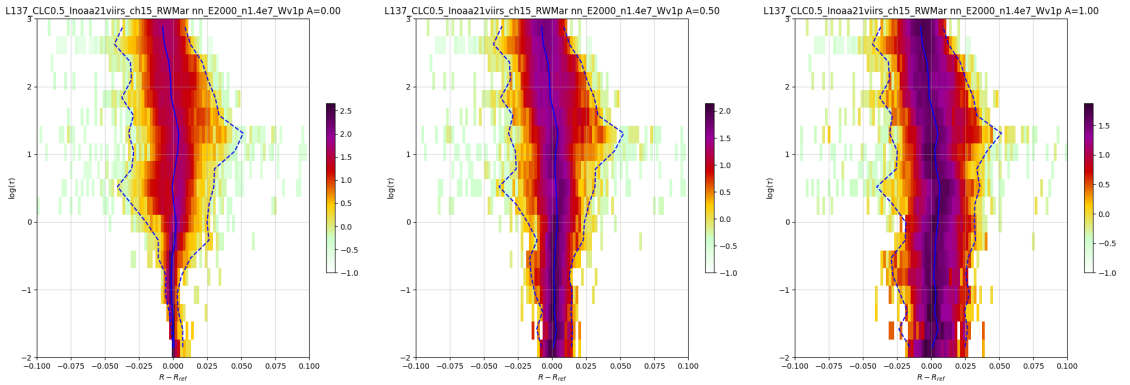

(a) (b) (c)

Figure 187: MFASIS $\Delta r_{\mathrm{MFASIS}-ref}$ as function of the cloud optical depth τ at albedo(s) of 0.00, 0.50, 1.00 (from left to right) for the instrument: NOAA 21 VIIRS CH15

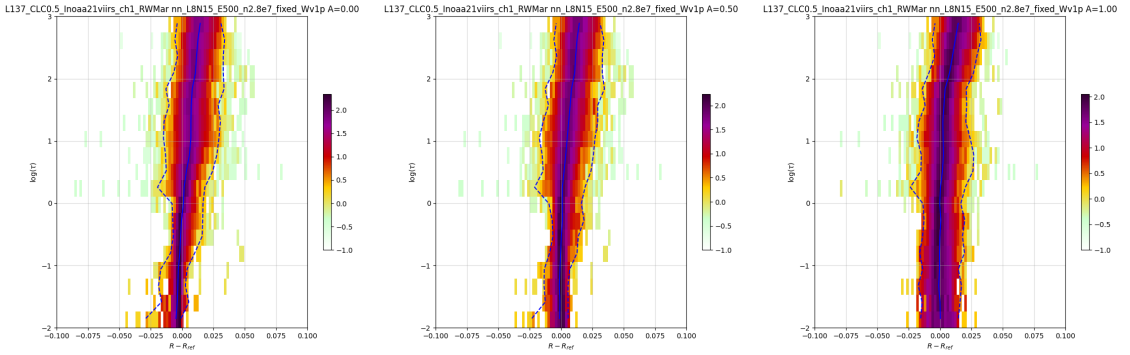

(a) (b) (c)

Figure 188: MFASIS $\Delta r_{\mathrm{MFASIS}-ref}$ as function of the cloud optical depth τ at albedo(s) of 0.00, 0.50, 1.00 (from left to right) for the instrument: NOAA 21 VIIRS CH1

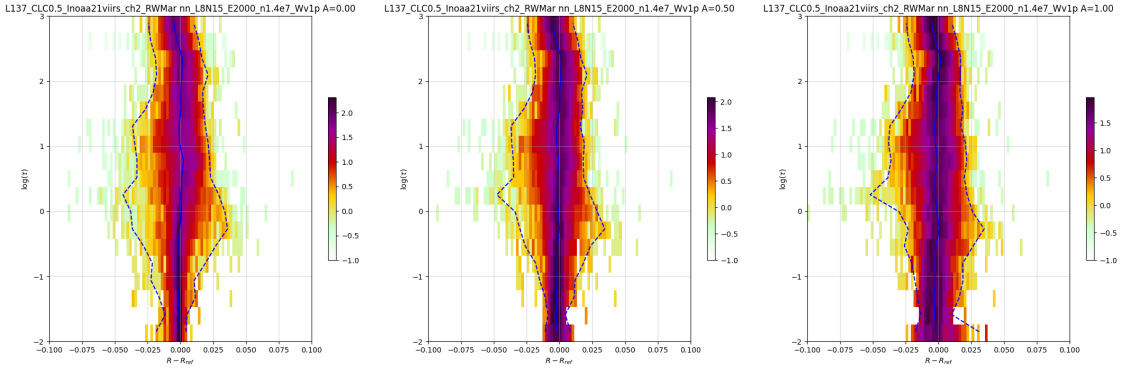

(a) (b) (c)

Figure 189: MFASIS $\Delta r_{\mathrm{MFASIS}-ref}$ as function of the cloud optical depth τ at albedo(s) of 0.00, 0.50, 1.00 (from left to right) for the instrument: NOAA 21 VIIRS CH2

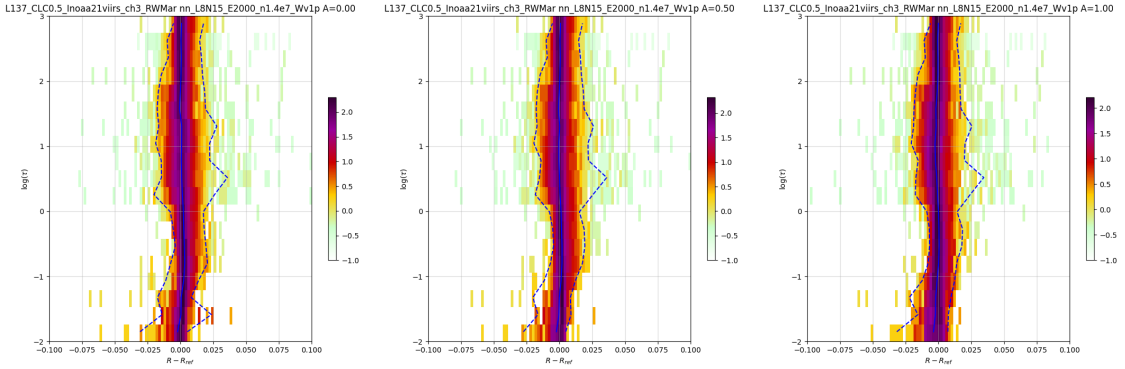

(a) (b) (c)

Figure 190: MFASIS $\Delta r_{\mathrm{MFASIS}-ref}$ as function of the cloud optical depth τ at albedo(s) of 0.00, 0.50, 1.00 (from left to right) for the instrument: NOAA 21 VIIRS CH3

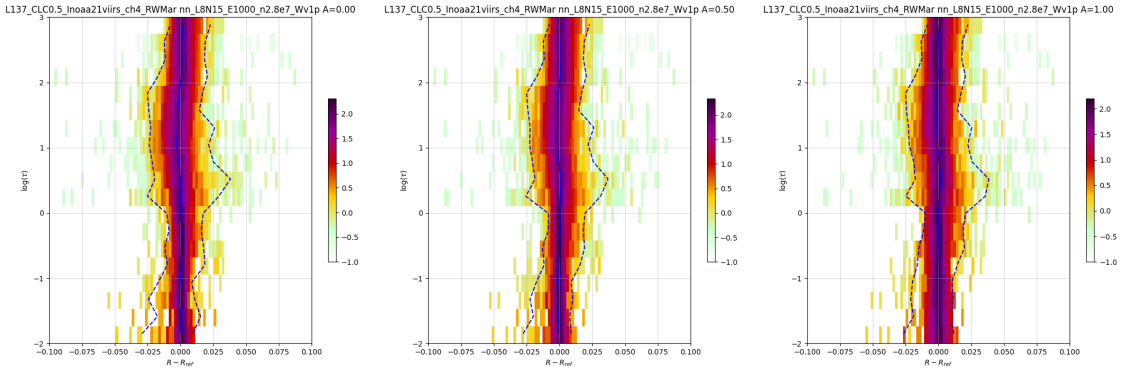

(a) (b) (c)

Figure 191: MFASIS $\Delta r_{\mathrm{MFASIS}-ref}$ as function of the cloud optical depth τ at albedo(s) of 0.00, 0.50, 1.00 (from left to right) for the instrument: NOAA 21 VIIRS CH4

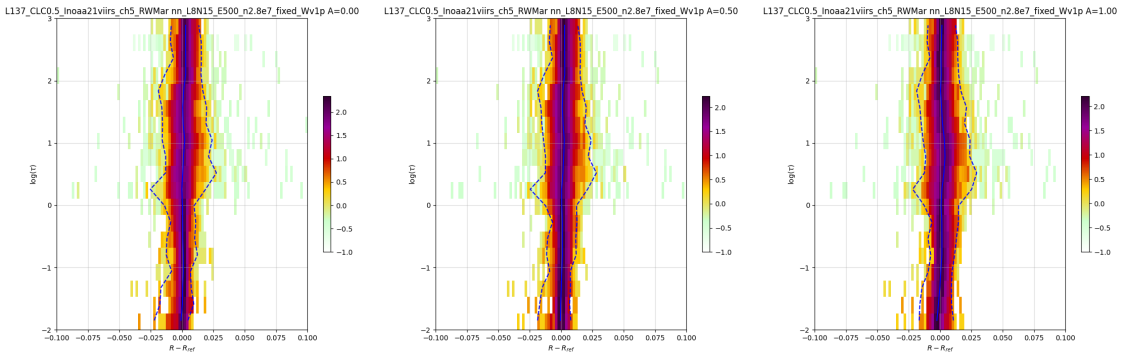

(a) (b) (c)

Figure 192: MFASIS $\Delta r_{\mathrm{MFASIS}-ref}$ as function of the cloud optical depth τ at albedo(s) of 0.00, 0.50, 1.00 (from left to right) for the instrument: NOAA 21 VIIRS CH5

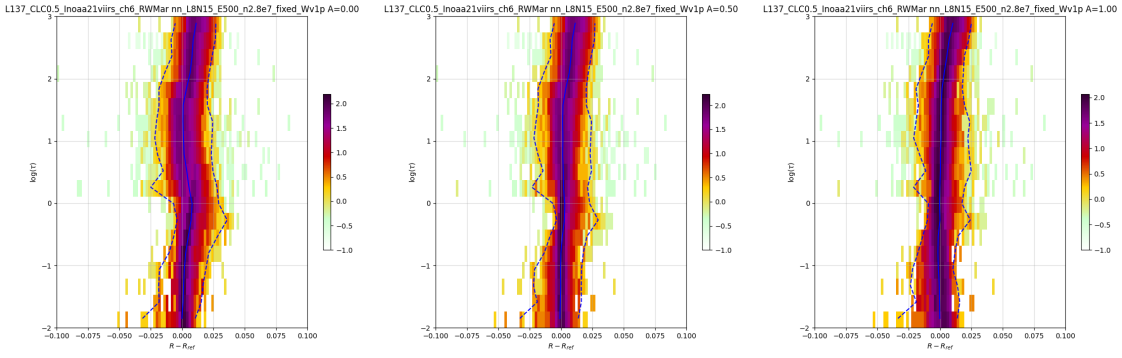

(a) (b) (c)

Figure 193: MFASIS $\Delta r_{\mathrm{MFASIS}-ref}$ as function of the cloud optical depth τ at albedo(s) of 0.00, 0.50, 1.00 (from left to right) for the instrument: NOAA 21 VIIRS CH6

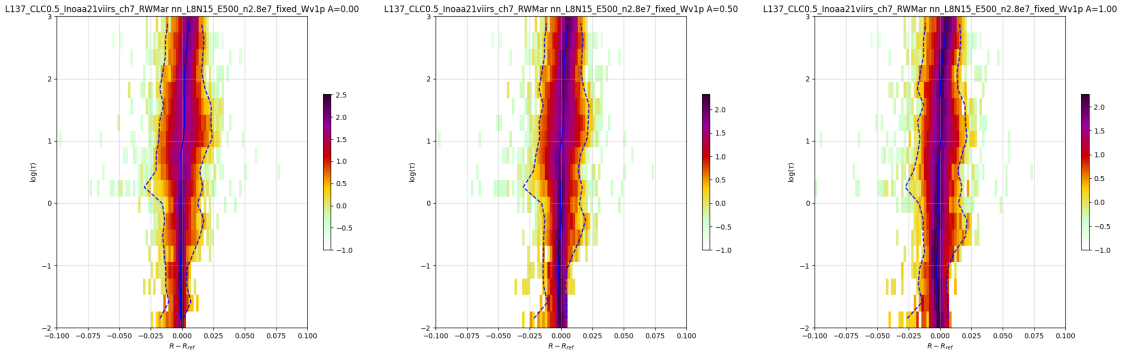

(a) (b) (c)

Figure 194: MFASIS $\Delta r_{\mathrm{MFASIS}-ref}$ as function of the cloud optical depth τ at albedo(s) of 0.00, 0.50, 1.00 (from left to right) for the instrument: NOAA 21 VIIRS CH7

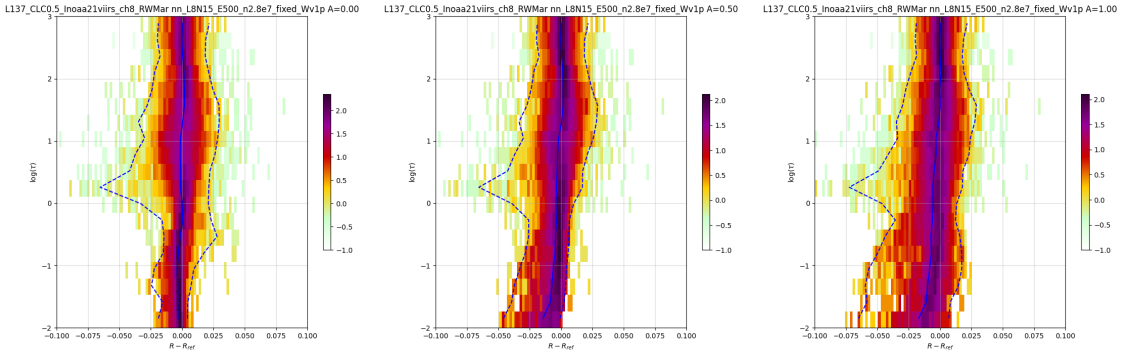

(a) (b) (c)

Figure 195: MFASIS $\Delta r_{\mathrm{MFASIS}-ref}$ as function of the cloud optical depth τ at albedo(s) of 0.00, 0.50, 1.00 (from left to right) for the instrument: NOAA 21 VIIRS CH8

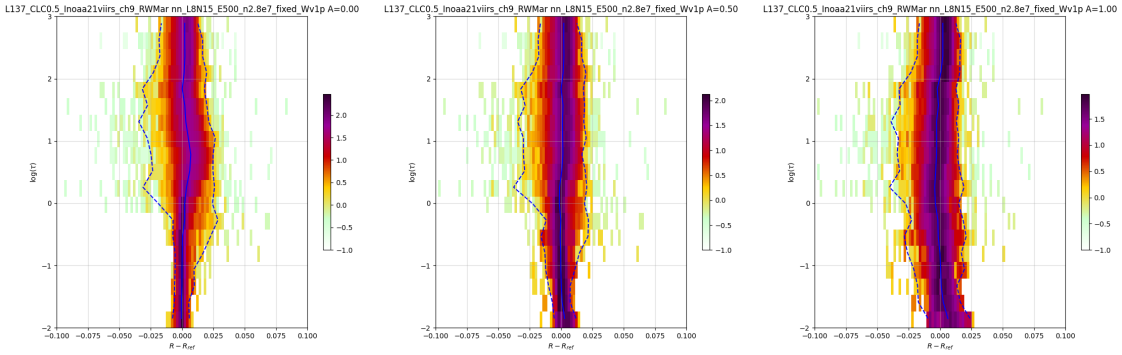

(a) (b) (c)

Figure 196: MFASIS $\Delta r_{\mathrm{MFASIS}-ref}$ as function of the cloud optical depth τ at albedo(s) of 0.00, 0.50, 1.00 (from left to right) for the instrument: NOAA 21 VIIRS CH9

List of Figures

1 Color coding for the different uncertainty values in the tables for the instruments. 3
2 MFASIS uncertainties for the instrument: DSCOVR 1 EPIC 3
3 MFASIS uncertainties for the instrument: EOS 1 MODIS 4
4 MFASIS uncertainties for the instrument: EOS 2 MODIS 5
5 MFASIS uncertainties for the instrument: FY3 3 VIRR 6
6 MFASIS uncertainties for the instrument: FY3 4 MERSI2 7
7 MFASIS uncertainties for the instrument: FY4 1 AGRI 8
8 MFASIS uncertainties for the instrument: FY4 2 AGRI 8
9 MFASIS uncertainties for the instrument: GKOMPSAT2 1 AMI . . . 8
10 MFASIS uncertainties for the instrument: GOES 13 IMAGER 9
11 MFASIS uncertainties for the instrument: GOES 14 IMAGER 9
12 MFASIS uncertainties for the instrument: GOES 15 IMAGER 9
13 MFASIS uncertainties for the instrument: GOES 16 ABI 9
14 MFASIS uncertainties for the instrument: GOES 17 ABI 10
15 MFASIS uncertainties for the instrument: GOES 18 ABI 10
16 MFASIS uncertainties for the instrument: GOES 19 ABI 11
17 MFASIS uncertainties for the instrument: HIMAWARI 8 AHI 11
18 MFASIS uncertainties for the instrument: HIMAWARI 9 AHI 12
19 MFASIS uncertainties for the instrument: JPSS 0 VIIRS 13
20 MFASIS uncertainties for the instrument: METOP 1 AVHRR 14
21 MFASIS uncertainties for the instrument: METOP 2 AVHRR 14
22 MFASIS uncertainties for the instrument: METOP 3 AVHRR 14
23 MFASIS uncertainties for the instrument: METOPSG 1 METIMAGE 15
24 MFASIS uncertainties for the instrument: MSG 1 SEVIRI 15
25 MFASIS uncertainties for the instrument: MSG 2 SEVIRI 16
26 MFASIS uncertainties for the instrument: MSG 3 SEVIRI 16
27 MFASIS uncertainties for the instrument: MSG 4 SEVIRI 16
28 MFASIS uncertainties for the instrument: MTG 1 FCI 17
29 MFASIS uncertainties for the instrument: NOAA 14 AVHRR 17
30 MFASIS uncertainties for the instrument: NOAA 20 VIIRS 18
31 MFASIS uncertainties for the instrument: NOAA 21 VIIRS 19
32 MFASIS $\Delta r_{\mathrm{MFASIS}-ref}$ as function of the cloud optical depth τ at albedo(s) of 0.00, 0.50, 1.00 (from left to right) for the instrument: DSCOVR 1 EPIC CH1 20
33 MFASIS $\Delta r_{\mathrm{MFASIS}-ref}$ as function of the cloud optical depth τ at albedo(s) of 0.00, 0.50, 1.00 (from left to right) for the instrument: DSCOVR 1 EPIC CH2 20
34 MFASIS $\Delta r_{\mathrm{MFASIS}-ref}$ as function of the cloud optical depth τ at albedo(s) of 0.00, 0.50, 1.00 (from left to right) for the instrument: DSCOVR 1 EPIC CH3 21
35 MFASIS $\Delta r_{\mathrm{MFASIS}-ref}$ as function of the cloud optical depth τ at albedo(s) of 0.00, 0.50, 1.00 (from left to right) for the instrument: DSCOVR 1 EPIC CH6 21
36 MFASIS $\Delta r_{\mathrm{MFASIS}-ref}$ as function of the cloud optical depth τ at albedo(s) of 0.00, 0.50, 1.00 (from left to right) for the instrument: EOS 1 MODIS CH10 21

37 MFASIS $\Delta r_{\mathrm{MFASIS}-ref}$ as function of the cloud optical depth τ at albedo(s) of 0.00, 0.50, 1.00 (from left to right) for the instrument: EOS 1 MODIS CH11 22
38 MFASIS $\Delta r_{\mathrm{MFASIS}-ref}$ as function of the cloud optical depth τ at albedo(s) of 0.00, 0.50, 1.00 (from left to right) for the instrument: EOS 1 MODIS CH12 22
39 MFASIS $\Delta r_{\mathrm{MFASIS}-ref}$ as function of the cloud optical depth τ at albedo(s) of 0.00, 0.50, 1.00 (from left to right) for the instrument: EOS 1 MODIS CH13 22
40 MFASIS $\Delta r_{\mathrm{MFASIS}-ref}$ as function of the cloud optical depth τ at albedo(s) of 0.00, 0.50, 1.00 (from left to right) for the instrument: EOS 1 MODIS CH14 23
41 MFASIS $\Delta r_{\mathrm{MFASIS}-ref}$ as function of the cloud optical depth τ at albedo(s) of 0.00, 0.50, 1.00 (from left to right) for the instrument: EOS 1 MODIS CH15 23
42 MFASIS $\Delta r_{\mathrm{MFASIS}-ref}$ as function of the cloud optical depth τ at albedo(s) of 0.00, 0.50, 1.00 (from left to right) for the instrument: EOS 1 MODIS CH16 23
43 MFASIS $\Delta r_{\mathrm{MFASIS}-ref}$ as function of the cloud optical depth τ at albedo(s) of 0.00, 0.50, 1.00 (from left to right) for the instrument: EOS 1 MODIS CH1 24
44 MFASIS $\Delta r_{\mathrm{MFASIS}-ref}$ as function of the cloud optical depth τ at albedo(s) of 0.00, 0.50, 1.00 (from left to right) for the instrument: EOS 1 MODIS CH2 24
45 MFASIS $\Delta r_{\mathrm{MFASIS}-ref}$ as function of the cloud optical depth τ at albedo(s) of 0.00, 0.50, 1.00 (from left to right) for the instrument: EOS 1 MODIS CH3 24
46 MFASIS $\Delta r_{\mathrm{MFASIS}-ref}$ as function of the cloud optical depth τ at albedo(s) of 0.00, 0.50, 1.00 (from left to right) for the instrument: EOS 1 MODIS CH4 25
47 MFASIS $\Delta r_{\mathrm{MFASIS}-ref}$ as function of the cloud optical depth τ at albedo(s) of 0.00, 0.50, 1.00 (from left to right) for the instrument: EOS 1 MODIS CH5 25
48 MFASIS $\Delta r_{\mathrm{MFASIS}-ref}$ as function of the cloud optical depth τ at albedo(s) of 0.00, 0.50, 1.00 (from left to right) for the instrument: EOS 1 MODIS CH6 25
49 MFASIS $\Delta r_{\mathrm{MFASIS}-ref}$ as function of the cloud optical depth τ at albedo(s) of 0.00, 0.50, 1.00 (from left to right) for the instrument: EOS 1 MODIS CH8 26
50 MFASIS $\Delta r_{\mathrm{MFASIS}-ref}$ as function of the cloud optical depth τ at albedo(s) of 0.00, 0.50, 1.00 (from left to right) for the instrument: EOS 1 MODIS CH9 26
51 MFASIS $\Delta r_{\mathrm{MFASIS}-ref}$ as function of the cloud optical depth τ at albedo(s) of 0.00, 0.50, 1.00 (from left to right) for the instrument: EOS 2 MODIS CH10 26
52 MFASIS $\Delta r_{\mathrm{MFASIS}-ref}$ as function of the cloud optical depth τ at albedo(s) of 0.00, 0.50, 1.00 (from left to right) for the instrument: EOS 2 MODIS CH11 27

53 MFASIS $\Delta r_{\mathrm{MFASIS}-ref}$ as function of the cloud optical depth τ at albedo(s) of 0.00, 0.50, 1.00 (from left to right) for the instrument: EOS 2 MODIS CH12 27
54 MFASIS $\Delta r_{\mathrm{MFASIS}-ref}$ as function of the cloud optical depth τ at albedo(s) of 0.00, 0.50, 1.00 (from left to right) for the instrument: EOS 2 MODIS CH13 27
55 MFASIS $\Delta r_{\mathrm{MFASIS}-ref}$ as function of the cloud optical depth τ at albedo(s) of 0.00, 0.50, 1.00 (from left to right) for the instrument: EOS 2 MODIS CH14 28
56 MFASIS $\Delta r_{\mathrm{MFASIS}-ref}$ as function of the cloud optical depth τ at albedo(s) of 0.00, 0.50, 1.00 (from left to right) for the instrument: EOS 2 MODIS CH15 28
57 MFASIS $\Delta r_{\mathrm{MFASIS}-ref}$ as function of the cloud optical depth τ at albedo(s) of 0.00, 0.50, 1.00 (from left to right) for the instrument: EOS 2 MODIS CH16 28
58 MFASIS $\Delta r_{\mathrm{MFASIS}-ref}$ as function of the cloud optical depth τ at albedo(s) of 0.00, 0.50, 1.00 (from left to right) for the instrument: EOS 2 MODIS CH1 29
59 MFASIS $\Delta r_{\mathrm{MFASIS}-ref}$ as function of the cloud optical depth τ at albedo(s) of 0.00, 0.50, 1.00 (from left to right) for the instrument: EOS 2 MODIS CH2 29
60 MFASIS $\Delta r_{\mathrm{MFASIS}-ref}$ as function of the cloud optical depth τ at albedo(s) of 0.00, 0.50, 1.00 (from left to right) for the instrument: EOS 2 MODIS CH3 29
61 MFASIS $\Delta r_{\mathrm{MFASIS}-ref}$ as function of the cloud optical depth τ at albedo(s) of 0.00, 0.50, 1.00 (from left to right) for the instrument: EOS 2 MODIS CH4 30
62 MFASIS $\Delta r_{\mathrm{MFASIS}-ref}$ as function of the cloud optical depth τ at albedo(s) of 0.00, 0.50, 1.00 (from left to right) for the instrument: EOS 2 MODIS CH5 30
63 MFASIS $\Delta r_{\mathrm{MFASIS}-ref}$ as function of the cloud optical depth τ at albedo(s) of 0.00, 0.50, 1.00 (from left to right) for the instrument: EOS 2 MODIS CH6 30
64 MFASIS $\Delta r_{\mathrm{MFASIS}-ref}$ as function of the cloud optical depth τ at albedo(s) of 0.00, 0.50, 1.00 (from left to right) for the instrument: EOS 2 MODIS CH8 31
65 MFASIS $\Delta r_{\mathrm{MFASIS}-ref}$ as function of the cloud optical depth τ at albedo(s) of 0.00, 0.50, 1.00 (from left to right) for the instrument: EOS 2 MODIS CH9 31
66 MFASIS $\Delta r_{\mathrm{MFASIS}-ref}$ as function of the cloud optical depth τ at albedo(s) of 0.00, 0.50, 1.00 (from left to right) for the instrument: FY3 3 VIRR CH1 31
67 MFASIS $\Delta r_{\mathrm{MFASIS}-ref}$ as function of the cloud optical depth τ at albedo(s) of 0.00, 0.50, 1.00 (from left to right) for the instrument: FY3 3 VIRR CH2 32
68 MFASIS $\Delta r_{\mathrm{MFASIS}-ref}$ as function of the cloud optical depth τ at albedo(s) of 0.00, 0.50, 1.00 (from left to right) for the instrument: FY3 3 VIRR CH3 32

69 MFASIS $\Delta r_{\mathrm{MFASIS}-ref}$ as function of the cloud optical depth τ at albedo(s) of 0.00, 0.50, 1.00 (from left to right) for the instrument: FY3 3 VIRR CH4 32
70 MFASIS $\Delta r_{\mathrm{MFASIS}-ref}$ as function of the cloud optical depth τ at albedo(s) of 0.00, 0.50, 1.00 (from left to right) for the instrument: FY3 3 VIRR CH7 33
71 MFASIS $\Delta r_{\mathrm{MFASIS}-ref}$ as function of the cloud optical depth τ at albedo(s) of 0.00, 0.50, 1.00 (from left to right) for the instrument: FY3 4 MERSI2 CH10 33
72 MFASIS $\Delta r_{\mathrm{MFASIS}-ref}$ as function of the cloud optical depth τ at albedo(s) of 0.00, 0.50, 1.00 (from left to right) for the instrument: FY3 4 MERSI2 CH11 33
73 MFASIS $\Delta r_{\mathrm{MFASIS}-ref}$ as function of the cloud optical depth τ at albedo(s) of 0.00, 0.50, 1.00 (from left to right) for the instrument: FY3 4 MERSI2 CH12 34
74 MFASIS $\Delta r_{\mathrm{MFASIS}-ref}$ as function of the cloud optical depth τ at albedo(s) of 0.00, 0.50, 1.00 (from left to right) for the instrument: FY3 4 MERSI2 CH16 34
75 MFASIS $\Delta r_{\mathrm{MFASIS}-ref}$ as function of the cloud optical depth τ at albedo(s) of 0.00, 0.50, 1.00 (from left to right) for the instrument: FY3 4 MERSI2 CH18 34
76 MFASIS $\Delta r_{\mathrm{MFASIS}-ref}$ as function of the cloud optical depth τ at albedo(s) of 0.00, 0.50, 1.00 (from left to right) for the instrument: FY3 4 MERSI2 CH1 35
77 MFASIS $\Delta r_{\mathrm{MFASIS}-ref}$ as function of the cloud optical depth τ at albedo(s) of 0.00, 0.50, 1.00 (from left to right) for the instrument: FY3 4 MERSI2 CH2 35
78 MFASIS $\Delta r_{\mathrm{MFASIS}-ref}$ as function of the cloud optical depth τ at albedo(s) of 0.00, 0.50, 1.00 (from left to right) for the instrument: FY3 4 MERSI2 CH3 35
79 MFASIS $\Delta r_{\mathrm{MFASIS}-ref}$ as function of the cloud optical depth τ at albedo(s) of 0.00, 0.50, 1.00 (from left to right) for the instrument: FY3 4 MERSI2 CH4 36
80 MFASIS $\Delta r_{\mathrm{MFASIS}-ref}$ as function of the cloud optical depth τ at albedo(s) of 0.00, 0.50, 1.00 (from left to right) for the instrument: FY3 4 MERSI2 CH5 36
81 MFASIS $\Delta r_{\mathrm{MFASIS}-ref}$ as function of the cloud optical depth τ at albedo(s) of 0.00, 0.50, 1.00 (from left to right) for the instrument: FY3 4 MERSI2 CH6 36
82 MFASIS $\Delta r_{\mathrm{MFASIS}-ref}$ as function of the cloud optical depth τ at albedo(s) of 0.00, 0.50, 1.00 (from left to right) for the instrument: FY3 4 MERSI2 CH7 37
83 MFASIS $\Delta r_{\mathrm{MFASIS}-ref}$ as function of the cloud optical depth τ at albedo(s) of 0.00, 0.50, 1.00 (from left to right) for the instrument: FY3 4 MERSI2 CH8 37
84 MFASIS $\Delta r_{\mathrm{MFASIS}-ref}$ as function of the cloud optical depth τ at albedo(s) of 0.00, 0.50, 1.00 (from left to right) for the instrument: FY4 1 AGRI CH1 37

85 MFASIS $\Delta r_{\mathrm{MFASIS}-ref}$ as function of the cloud optical depth τ at albedo(s) of 0.00, 0.50, 1.00 (from left to right) for the instrument: FY4 1 AGRI CH5 38
86 MFASIS $\Delta r_{\mathrm{MFASIS}-ref}$ as function of the cloud optical depth τ at albedo(s) of 0.00, 0.50, 1.00 (from left to right) for the instrument: FY4 2 AGRI CH1 38
87 MFASIS $\Delta r_{\mathrm{MFASIS}-ref}$ as function of the cloud optical depth τ at albedo(s) of 0.00, 0.50, 1.00 (from left to right) for the instrument: FY4 2 AGRI CH2 38
88 MFASIS $\Delta r_{\mathrm{MFASIS}-ref}$ as function of the cloud optical depth τ at albedo(s) of 0.00, 0.50, 1.00 (from left to right) for the instrument: FY4 2 AGRI CH5 39
89 MFASIS $\Delta r_{\mathrm{MFASIS}-ref}$ as function of the cloud optical depth τ at albedo(s) of 0.00, 0.50, 1.00 (from left to right) for the instrument: GKOMPSAT2 1 AMI CH1 39
90 MFASIS $\Delta r_{\mathrm{MFASIS}-ref}$ as function of the cloud optical depth τ at albedo(s) of 0.00, 0.50, 1.00 (from left to right) for the instrument: GKOMPSAT2 1 AMI CH2 39
91 MFASIS $\Delta r_{\mathrm{MFASIS}-ref}$ as function of the cloud optical depth τ at albedo(s) of 0.00, 0.50, 1.00 (from left to right) for the instrument: GKOMPSAT2 1 AMI CH3 40
92 MFASIS $\Delta r_{\mathrm{MFASIS}-ref}$ as function of the cloud optical depth τ at albedo(s) of 0.00, 0.50, 1.00 (from left to right) for the instrument: GKOMPSAT2 1 AMI CH4 40
93 MFASIS $\Delta r_{\mathrm{MFASIS}-ref}$ as function of the cloud optical depth τ at albedo(s) of 0.00, 0.50, 1.00 (from left to right) for the instrument: GKOMPSAT2 1 AMI CH6 40
94 MFASIS $\Delta r_{\mathrm{MFASIS}-ref}$ as function of the cloud optical depth τ at albedo(s) of 0.00, 0.50, 1.00 (from left to right) for the instrument: GOES 13 IMAGER CH1 41
95 MFASIS $\Delta r_{\mathrm{MFASIS}-ref}$ as function of the cloud optical depth τ at albedo(s) of 0.00, 0.50, 1.00 (from left to right) for the instrument: GOES 14 IMAGER CH1 41
96 MFASIS $\Delta r_{\mathrm{MFASIS}-ref}$ as function of the cloud optical depth τ at albedo(s) of 0.00, 0.50, 1.00 (from left to right) for the instrument: GOES 15 IMAGER CH1 41
97 MFASIS $\Delta r_{\mathrm{MFASIS}-ref}$ as function of the cloud optical depth τ at albedo(s) of 0.00, 0.50, 1.00 (from left to right) for the instrument: GOES 16 ABI CH1 42
98 MFASIS $\Delta r_{\mathrm{MFASIS}-ref}$ as function of the cloud optical depth τ at albedo(s) of 0.00, 0.50, 1.00 (from left to right) for the instrument: GOES 16 ABI CH2 42
99 MFASIS $\Delta r_{\mathrm{MFASIS}-ref}$ as function of the cloud optical depth τ at albedo(s) of 0.00, 0.50, 1.00 (from left to right) for the instrument: GOES 16 ABI CH3 42
100 MFASIS $\Delta r_{\mathrm{MFASIS}-ref}$ as function of the cloud optical depth τ at albedo(s) of 0.00, 0.50, 1.00 (from left to right) for the instrument: GOES 16 ABI CH5 43

101 MFASIS $\Delta r_{\mathrm{MFASIS}-ref}$ as function of the cloud optical depth τ at albedo(s) of 0.00, 0.50, 1.00 (from left to right) for the instrument: GOES 16 ABI CH6 43
102 MFASIS $\Delta r_{\mathrm{MFASIS}-ref}$ as function of the cloud optical depth τ at albedo(s) of 0.00, 0.50, 1.00 (from left to right) for the instrument: GOES 17 ABI CH1 43
103 MFASIS $\Delta r_{\mathrm{MFASIS}-ref}$ as function of the cloud optical depth τ at albedo(s) of 0.00, 0.50, 1.00 (from left to right) for the instrument: GOES 17 ABI CH2 44
104 MFASIS $\Delta r_{\mathrm{MFASIS}-ref}$ as function of the cloud optical depth τ at albedo(s) of 0.00, 0.50, 1.00 (from left to right) for the instrument: GOES 17 ABI CH3 44
105 MFASIS $\Delta r_{\mathrm{MFASIS}-ref}$ as function of the cloud optical depth τ at albedo(s) of 0.00, 0.50, 1.00 (from left to right) for the instrument: GOES 17 ABI CH5 44
106 MFASIS $\Delta r_{\mathrm{MFASIS}-ref}$ as function of the cloud optical depth τ at albedo(s) of 0.00, 0.50, 1.00 (from left to right) for the instrument: GOES 17 ABI CH6 45
107 MFASIS $\Delta r_{\mathrm{MFASIS}-ref}$ as function of the cloud optical depth τ at albedo(s) of 0.00, 0.50, 1.00 (from left to right) for the instrument: GOES 18 ABI CH1 45
108 MFASIS $\Delta r_{\mathrm{MFASIS}-ref}$ as function of the cloud optical depth τ at albedo(s) of 0.00, 0.50, 1.00 (from left to right) for the instrument: GOES 18 ABI CH2 45
109 MFASIS $\Delta r_{\mathrm{MFASIS}-ref}$ as function of the cloud optical depth τ at albedo(s) of 0.00, 0.50, 1.00 (from left to right) for the instrument: GOES 18 ABI CH3 46
110 MFASIS $\Delta r_{\mathrm{MFASIS}-ref}$ as function of the cloud optical depth τ at albedo(s) of 0.00, 0.50, 1.00 (from left to right) for the instrument: GOES 18 ABI CH5 46
111 MFASIS $\Delta r_{\mathrm{MFASIS}-ref}$ as function of the cloud optical depth τ at albedo(s) of 0.00, 0.50, 1.00 (from left to right) for the instrument: GOES 18 ABI CH6 46
112 MFASIS $\Delta r_{\mathrm{MFASIS}-ref}$ as function of the cloud optical depth τ at albedo(s) of 0.00, 0.50, 1.00 (from left to right) for the instrument: GOES 19 ABI CH1 47
113 MFASIS $\Delta r_{\mathrm{MFASIS}-ref}$ as function of the cloud optical depth τ at albedo(s) of 0.00, 0.50, 1.00 (from left to right) for the instrument: GOES 19 ABI CH2 47
114 MFASIS $\Delta r_{\mathrm{MFASIS}-ref}$ as function of the cloud optical depth τ at albedo(s) of 0.00, 0.50, 1.00 (from left to right) for the instrument: GOES 19 ABI CH3 47
115 MFASIS $\Delta r_{\mathrm{MFASIS}-ref}$ as function of the cloud optical depth τ at albedo(s) of 0.00, 0.50, 1.00 (from left to right) for the instrument: GOES 19 ABI CH5 48
116 MFASIS $\Delta r_{\mathrm{MFASIS}-ref}$ as function of the cloud optical depth τ at albedo(s) of 0.00, 0.50, 1.00 (from left to right) for the instrument: GOES 19 ABI CH6 48

117 MFASIS $\Delta r_{\mathrm{MFASIS}-ref}$ as function of the cloud optical depth τ at albedo(s) of 0.00, 0.50, 1.00 (from left to right) for the instrument: HIMAWARI 8 AHI CH1 48
118 MFASIS $\Delta r_{\mathrm{MFASIS}-ref}$ as function of the cloud optical depth τ at albedo(s) of 0.00, 0.50, 1.00 (from left to right) for the instrument: HIMAWARI 8 AHI CH2 49
119 MFASIS $\Delta r_{\mathrm{MFASIS}-ref}$ as function of the cloud optical depth τ at albedo(s) of 0.00, 0.50, 1.00 (from left to right) for the instrument: HIMAWARI 8 AHI CH3 49
120 MFASIS $\Delta r_{\mathrm{MFASIS}-ref}$ as function of the cloud optical depth τ at albedo(s) of 0.00, 0.50, 1.00 (from left to right) for the instrument: HIMAWARI 8 AHI CH4 49
121 MFASIS $\Delta r_{\mathrm{MFASIS}-ref}$ as function of the cloud optical depth τ at albedo(s) of 0.00, 0.50, 1.00 (from left to right) for the instrument: HIMAWARI 8 AHI CH5 50
122 MFASIS $\Delta r_{\mathrm{MFASIS}-ref}$ as function of the cloud optical depth τ at albedo(s) of 0.00, 0.50, 1.00 (from left to right) for the instrument: HIMAWARI 8 AHI CH6 50
123 MFASIS $\Delta r_{\mathrm{MFASIS}-ref}$ as function of the cloud optical depth τ at albedo(s) of 0.00, 0.50, 1.00 (from left to right) for the instrument: HIMAWARI 9 AHI CH1 50
124 MFASIS $\Delta r_{\mathrm{MFASIS}-ref}$ as function of the cloud optical depth τ at albedo(s) of 0.00, 0.50, 1.00 (from left to right) for the instrument: HIMAWARI 9 AHI CH2 51
125 MFASIS $\Delta r_{\mathrm{MFASIS}-ref}$ as function of the cloud optical depth τ at albedo(s) of 0.00, 0.50, 1.00 (from left to right) for the instrument: HIMAWARI 9 AHI CH3 51
126 MFASIS $\Delta r_{\mathrm{MFASIS}-ref}$ as function of the cloud optical depth τ at albedo(s) of 0.00, 0.50, 1.00 (from left to right) for the instrument: HIMAWARI 9 AHI CH4 51
127 MFASIS $\Delta r_{\mathrm{MFASIS}-ref}$ as function of the cloud optical depth τ at albedo(s) of 0.00, 0.50, 1.00 (from left to right) for the instrument: HIMAWARI 9 AHI CH5 52
128 MFASIS $\Delta r_{\mathrm{MFASIS}-ref}$ as function of the cloud optical depth τ at albedo(s) of 0.00, 0.50, 1.00 (from left to right) for the instrument: HIMAWARI 9 AHI CH6 52
129 MFASIS $\Delta r_{\mathrm{MFASIS}-ref}$ as function of the cloud optical depth τ at albedo(s) of 0.00, 0.50, 1.00 (from left to right) for the instrument: JPSS 0 VIIRS CH11 52
130 MFASIS $\Delta r_{\mathrm{MFASIS}-ref}$ as function of the cloud optical depth τ at albedo(s) of 0.00, 0.50, 1.00 (from left to right) for the instrument: JPSS 0 VIIRS CH13 53
131 MFASIS $\Delta r_{\mathrm{MFASIS}-ref}$ as function of the cloud optical depth τ at albedo(s) of 0.00, 0.50, 1.00 (from left to right) for the instrument: JPSS 0 VIIRS CH14 53
132 MFASIS $\Delta r_{\mathrm{MFASIS}-ref}$ as function of the cloud optical depth τ at albedo(s) of 0.00, 0.50, 1.00 (from left to right) for the instrument: JPSS 0 VIIRS CH15 53

133 MFASIS $\Delta r_{\mathrm{MFASIS}-ref}$ as function of the cloud optical depth τ at albedo(s) of 0.00, 0.50, 1.00 (from left to right) for the instrument: JPSS 0 VIIRS CH1 54
134 MFASIS $\Delta r_{\mathrm{MFASIS}-ref}$ as function of the cloud optical depth τ at albedo(s) of 0.00, 0.50, 1.00 (from left to right) for the instrument: JPSS 0 VIIRS CH2 54
135 MFASIS $\Delta r_{\mathrm{MFASIS}-ref}$ as function of the cloud optical depth τ at albedo(s) of 0.00, 0.50, 1.00 (from left to right) for the instrument: JPSS 0 VIIRS CH3 54
136 MFASIS $\Delta r_{\mathrm{MFASIS}-ref}$ as function of the cloud optical depth τ at albedo(s) of 0.00, 0.50, 1.00 (from left to right) for the instrument: JPSS 0 VIIRS CH4 55
137 MFASIS $\Delta r_{\mathrm{MFASIS}-ref}$ as function of the cloud optical depth τ at albedo(s) of 0.00, 0.50, 1.00 (from left to right) for the instrument: JPSS 0 VIIRS CH5 55
138 MFASIS $\Delta r_{\mathrm{MFASIS}-ref}$ as function of the cloud optical depth τ at albedo(s) of 0.00, 0.50, 1.00 (from left to right) for the instrument: JPSS 0 VIIRS CH6 55
139 MFASIS $\Delta r_{\mathrm{MFASIS}-ref}$ as function of the cloud optical depth τ at albedo(s) of 0.00, 0.50, 1.00 (from left to right) for the instrument: JPSS 0 VIIRS CH7 56
140 MFASIS $\Delta r_{\mathrm{MFASIS}-ref}$ as function of the cloud optical depth τ at albedo(s) of 0.00, 0.50, 1.00 (from left to right) for the instrument: JPSS 0 VIIRS CH8 56
141 MFASIS $\Delta r_{\mathrm{MFASIS}-ref}$ as function of the cloud optical depth τ at albedo(s) of 0.00, 0.50, 1.00 (from left to right) for the instrument: JPSS 0 VIIRS CH9 56
142 MFASIS $\Delta r_{\mathrm{MFASIS}-ref}$ as function of the cloud optical depth τ at albedo(s) of 0.00, 0.50, 1.00 (from left to right) for the instrument: METOP 1 AVHRR CH1 57
143 MFASIS $\Delta r_{\mathrm{MFASIS}-ref}$ as function of the cloud optical depth τ at albedo(s) of 0.00, 0.50, 1.00 (from left to right) for the instrument: METOP 1 AVHRR CH3 57
144 MFASIS $\Delta r_{\mathrm{MFASIS}-ref}$ as function of the cloud optical depth τ at albedo(s) of 0.00, 0.50, 1.00 (from left to right) for the instrument: METOP 2 AVHRR CH1 57
145 MFASIS $\Delta r_{\mathrm{MFASIS}-ref}$ as function of the cloud optical depth τ at albedo(s) of 0.00, 0.50, 1.00 (from left to right) for the instrument: METOP 2 AVHRR CH3 58
146 MFASIS $\Delta r_{\mathrm{MFASIS}-ref}$ as function of the cloud optical depth τ at albedo(s) of 0.00, 0.50, 1.00 (from left to right) for the instrument: METOP 3 AVHRR CH1 58
147 MFASIS $\Delta r_{\mathrm{MFASIS}-ref}$ as function of the cloud optical depth τ at albedo(s) of 0.00, 0.50, 1.00 (from left to right) for the instrument: METOP 3 AVHRR CH3 58
148 MFASIS $\Delta r_{\mathrm{MFASIS}-ref}$ as function of the cloud optical depth τ at albedo(s) of 0.00, 0.50, 1.00 (from left to right) for the instrument: METOPSG 1 METIMAGE CH10 59

149 MFASIS $\Delta r_{\mathrm{MFASIS}-ref}$ as function of the cloud optical depth τ at albedo(s) of 0.00, 0.50, 1.00 (from left to right) for the instrument: METOPSG 1 METIMAGE CH11 59
150 MFASIS $\Delta r_{\mathrm{MFASIS}-ref}$ as function of the cloud optical depth τ at albedo(s) of 0.00, 0.50, 1.00 (from left to right) for the instrument: METOPSG 1 METIMAGE CH1 59
151 MFASIS $\Delta r_{\mathrm{MFASIS}-ref}$ as function of the cloud optical depth τ at albedo(s) of 0.00, 0.50, 1.00 (from left to right) for the instrument: METOPSG 1 METIMAGE CH2 60
152 MFASIS $\Delta r_{\mathrm{MFASIS}-ref}$ as function of the cloud optical depth τ at albedo(s) of 0.00, 0.50, 1.00 (from left to right) for the instrument: METOPSG 1 METIMAGE CH3 60
153 MFASIS $\Delta r_{\mathrm{MFASIS}-ref}$ as function of the cloud optical depth τ at albedo(s) of 0.00, 0.50, 1.00 (from left to right) for the instrument: METOPSG 1 METIMAGE CH4 60
154 MFASIS $\Delta r_{\mathrm{MFASIS}-ref}$ as function of the cloud optical depth τ at albedo(s) of 0.00, 0.50, 1.00 (from left to right) for the instrument: METOPSG 1 METIMAGE CH6 61
155 MFASIS $\Delta r_{\mathrm{MFASIS}-ref}$ as function of the cloud optical depth τ at albedo(s) of 0.00, 0.50, 1.00 (from left to right) for the instrument: METOPSG 1 METIMAGE CH8 61
156 MFASIS $\Delta r_{\mathrm{MFASIS}-ref}$ as function of the cloud optical depth τ at albedo(s) of 0.00, 0.50, 1.00 (from left to right) for the instrument: MSG 1 SEVIRI CH1 61
157 MFASIS $\Delta r_{\mathrm{MFASIS}-ref}$ as function of the cloud optical depth τ at albedo(s) of 0.00, 0.50, 1.00 (from left to right) for the instrument: MSG 1 SEVIRI CH3 62
158 MFASIS $\Delta r_{\mathrm{MFASIS}-ref}$ as function of the cloud optical depth τ at albedo(s) of 0.00, 0.50, 1.00 (from left to right) for the instrument: MSG 2 SEVIRI CH1 62
159 MFASIS $\Delta r_{\mathrm{MFASIS}-ref}$ as function of the cloud optical depth τ at albedo(s) of 0.00, 0.50, 1.00 (from left to right) for the instrument: MSG 2 SEVIRI CH3 62
160 MFASIS $\Delta r_{\mathrm{MFASIS}-ref}$ as function of the cloud optical depth τ at albedo(s) of 0.00, 0.50, 1.00 (from left to right) for the instrument: MSG 3 SEVIRI CH1 63
161 MFASIS $\Delta r_{\mathrm{MFASIS}-ref}$ as function of the cloud optical depth τ at albedo(s) of 0.00, 0.50, 1.00 (from left to right) for the instrument: MSG 3 SEVIRI CH3 63
162 MFASIS $\Delta r_{\mathrm{MFASIS}-ref}$ as function of the cloud optical depth τ at albedo(s) of 0.00, 0.50, 1.00 (from left to right) for the instrument: MSG 4 SEVIRI CH1 63
163 MFASIS $\Delta r_{\mathrm{MFASIS}-ref}$ as function of the cloud optical depth τ at albedo(s) of 0.00, 0.50, 1.00 (from left to right) for the instrument: MSG 4 SEVIRI CH3 64
164 MFASIS $\Delta r_{\mathrm{MFASIS}-ref}$ as function of the cloud optical depth τ at albedo(s) of 0.00, 0.50, 1.00 (from left to right) for the instrument: MTG 1 FCI CH1 64

165 MFASIS $\Delta r_{\mathrm{MFASIS}-ref}$ as function of the cloud optical depth τ at albedo(s) of 0.00, 0.50, 1.00 (from left to right) for the instrument: MTG 1 FCI CH2 64
166 MFASIS $\Delta r_{\mathrm{MFASIS}-ref}$ as function of the cloud optical depth τ at albedo(s) of 0.00, 0.50, 1.00 (from left to right) for the instrument: MTG 1 FCI CH3 65
167 MFASIS $\Delta r_{\mathrm{MFASIS}-ref}$ as function of the cloud optical depth τ at albedo(s) of 0.00, 0.50, 1.00 (from left to right) for the instrument: MTG 1 FCI CH4 65
168 MFASIS $\Delta r_{\mathrm{MFASIS}-ref}$ as function of the cloud optical depth τ at albedo(s) of 0.00, 0.50, 1.00 (from left to right) for the instrument: MTG 1 FCI CH7 65
169 MFASIS $\Delta r_{\mathrm{MFASIS}-ref}$ as function of the cloud optical depth τ at albedo(s) of 0.00, 0.50, 1.00 (from left to right) for the instrument: MTG 1 FCI CH8 66
170 MFASIS $\Delta r_{\mathrm{MFASIS}-ref}$ as function of the cloud optical depth τ at albedo(s) of 0.00, 0.50, 1.00 (from left to right) for the instrument: NOAA 14 AVHRR CH1 66
171 MFASIS $\Delta r_{\mathrm{MFASIS}-ref}$ as function of the cloud optical depth τ at albedo(s) of 0.00, 0.50, 1.00 (from left to right) for the instrument: NOAA 20 VIIRS CH11 66
172 MFASIS $\Delta r_{\mathrm{MFASIS}-ref}$ as function of the cloud optical depth τ at albedo(s) of 0.00, 0.50, 1.00 (from left to right) for the instrument: NOAA 20 VIIRS CH13 67
173 MFASIS $\Delta r_{\mathrm{MFASIS}-ref}$ as function of the cloud optical depth τ at albedo(s) of 0.00, 0.50, 1.00 (from left to right) for the instrument: NOAA 20 VIIRS CH14 67
174 MFASIS $\Delta r_{\mathrm{MFASIS}-ref}$ as function of the cloud optical depth τ at albedo(s) of 0.00, 0.50, 1.00 (from left to right) for the instrument: NOAA 20 VIIRS CH15 67
175 MFASIS $\Delta r_{\mathrm{MFASIS}-ref}$ as function of the cloud optical depth τ at albedo(s) of 0.00, 0.50, 1.00 (from left to right) for the instrument: NOAA 20 VIIRS CH1 68
176 MFASIS $\Delta r_{\mathrm{MFASIS}-ref}$ as function of the cloud optical depth τ at albedo(s) of 0.00, 0.50, 1.00 (from left to right) for the instrument: NOAA 20 VIIRS CH2 68
177 MFASIS $\Delta r_{\mathrm{MFASIS}-ref}$ as function of the cloud optical depth τ at albedo(s) of 0.00, 0.50, 1.00 (from left to right) for the instrument: NOAA 20 VIIRS CH3 68
178 MFASIS $\Delta r_{\mathrm{MFASIS}-ref}$ as function of the cloud optical depth τ at albedo(s) of 0.00, 0.50, 1.00 (from left to right) for the instrument: NOAA 20 VIIRS CH4 69
179 MFASIS $\Delta r_{\mathrm{MFASIS}-ref}$ as function of the cloud optical depth τ at albedo(s) of 0.00, 0.50, 1.00 (from left to right) for the instrument: NOAA 20 VIIRS CH5 69
180 MFASIS $\Delta r_{\mathrm{MFASIS}-ref}$ as function of the cloud optical depth τ at albedo(s) of 0.00, 0.50, 1.00 (from left to right) for the instrument: NOAA 20 VIIRS CH6 69

181 MFASIS $\Delta r_{\mathrm{MFASIS}-ref}$ as function of the cloud optical depth τ at albedo(s) of 0.00, 0.50, 1.00 (from left to right) for the instrument: NOAA 20 VIIRS CH7 70
182 MFASIS $\Delta r_{\mathrm{MFASIS}-ref}$ as function of the cloud optical depth τ at albedo(s) of 0.00, 0.50, 1.00 (from left to right) for the instrument: NOAA 20 VIIRS CH8 70
183 MFASIS $\Delta r_{\mathrm{MFASIS}-ref}$ as function of the cloud optical depth τ at albedo(s) of 0.00, 0.50, 1.00 (from left to right) for the instrument: NOAA 20 VIIRS CH9 70
184 MFASIS $\Delta r_{\mathrm{MFASIS}-ref}$ as function of the cloud optical depth τ at albedo(s) of 0.00, 0.50, 1.00 (from left to right) for the instrument: NOAA 21 VIIRS CH11 71
185 MFASIS $\Delta r_{\mathrm{MFASIS}-ref}$ as function of the cloud optical depth τ at albedo(s) of 0.00, 0.50, 1.00 (from left to right) for the instrument: NOAA 21 VIIRS CH13 71
186 MFASIS $\Delta r_{\mathrm{MFASIS}-ref}$ as function of the cloud optical depth τ at albedo(s) of 0.00, 0.50, 1.00 (from left to right) for the instrument: NOAA 21 VIIRS CH14 71
187 MFASIS $\Delta r_{\mathrm{MFASIS}-ref}$ as function of the cloud optical depth τ at albedo(s) of 0.00, 0.50, 1.00 (from left to right) for the instrument: NOAA 21 VIIRS CH15 72
188 MFASIS $\Delta r_{\mathrm{MFASIS}-ref}$ as function of the cloud optical depth τ at albedo(s) of 0.00, 0.50, 1.00 (from left to right) for the instrument: NOAA 21 VIIRS CH1 72
189 MFASIS $\Delta r_{\mathrm{MFASIS}-ref}$ as function of the cloud optical depth τ at albedo(s) of 0.00, 0.50, 1.00 (from left to right) for the instrument: NOAA 21 VIIRS CH2 72
190 MFASIS $\Delta r_{\mathrm{MFASIS}-ref}$ as function of the cloud optical depth τ at albedo(s) of 0.00, 0.50, 1.00 (from left to right) for the instrument: NOAA 21 VIIRS CH3 73
191 MFASIS $\Delta r_{\mathrm{MFASIS}-ref}$ as function of the cloud optical depth τ at albedo(s) of 0.00, 0.50, 1.00 (from left to right) for the instrument: NOAA 21 VIIRS CH4 73
192 MFASIS $\Delta r_{\mathrm{MFASIS}-ref}$ as function of the cloud optical depth τ at albedo(s) of 0.00, 0.50, 1.00 (from left to right) for the instrument: NOAA 21 VIIRS CH5 73
193 MFASIS $\Delta r_{\mathrm{MFASIS}-ref}$ as function of the cloud optical depth τ at albedo(s) of 0.00, 0.50, 1.00 (from left to right) for the instrument: NOAA 21 VIIRS CH6 74
194 MFASIS $\Delta r_{\mathrm{MFASIS}-ref}$ as function of the cloud optical depth τ at albedo(s) of 0.00, 0.50, 1.00 (from left to right) for the instrument: NOAA 21 VIIRS CH7 74
195 MFASIS $\Delta r_{\mathrm{MFASIS}-ref}$ as function of the cloud optical depth τ at albedo(s) of 0.00, 0.50, 1.00 (from left to right) for the instrument: NOAA 21 VIIRS CH8 74
196 MFASIS $\Delta r_{\mathrm{MFASIS}-ref}$ as function of the cloud optical depth τ at albedo(s) of 0.00, 0.50, 1.00 (from left to right) for the instrument: NOAA 21 VIIRS CH9 75